NUMERICAL MODELLING OF LARGE SCALE TOPPLING

by

MARK ANDERSON PRITCHARD

B.A.Sc., The University of British Columbia, 1987

A THESIS SUBMITTED IN PARTIAL FULFILLMENT

OF THE REQUIREMENTS FOR THE DEGREE OF

MASTER OF APPLIED SCIENCE

in

THE FACULTY OF GRADUATE STUDIES

Department of Geological Sciences

The University of British Columbia

We accept this thesis as conforming

to the required standard

THE UNIVERSITY OF BRITISH COLUMBIA

September 1989

Department of _Geology_

The University of British Columbia
Vancouver, Canada

Date _Sept 22/89_

ABSTRACT

The principle purpose of this research is to resolve the
mode of failure of the Heather Hill landslide, one of several
well defined failures in the Beaver Valley, Glacier National
Park, British Columbia.

Field work led to the preliminary conclusion that some
type of toppling process contributed to the failure. A
literature review of toppling revealed that large scale
topples have never been quantitatively assessed, and that
currently used analytical techniques are not adequate.
Consideration of alternative numerical techniques resulted in
the distinct element method being selected as the best
technique for modelling toppling.

The Universal Distinct Element Code (UDEC) was purchased
and its suitability demonstrated by reevaluating examples of
toppling analysis reported in the literature, and evaluating a
large scale engineered slope at Brenda mine where toppling is
known to occur. UDEC is used to examine and classify the mode
of failure of the Heather Hill slide.

This research leads to very important general conclusions
on toppling and specific conclusions relating to the Heather
Hill landslide: UDEC is suitable for modelling all types of
topples. The program can be used to back analyze rock mass
strength parameters and determine the shape and location of
the final failure surface in flexural toppling. A
quantitative assessment with UDEC confirms that the base of

failure in flexural toppling may be planar or curvilinear, and that pore pressures significantly affect stability.

The Heather Hill landslide failed by flexural toppling limiting to a curvilinear failure surface, and the slope immediately north of the Heather Hill landslide is deformed by flexural toppling. The locations of landslides in the Beaver Valley correspond with the occurrence of foliated pelitic rocks in the lower slopes and the boundary between these rocks and stronger grits is the up slope limit. The kinematic test of toppling potential is violated by the Heather Hill landslide. This test is shown to only apply to small scale drained slopes.

TABLE OF CONTENTS

LIST OF TABLES

LIST OF FIGURES

ACKNOWLEDGEMENTS

"Theory and calculation are not substitutes for
judgment, but are the bases for sounder judgment. A
theoretical framework into which the known empirical
observations and facts can be accommodated permits us to
extrapolate to new conditions with far greater
confidence than we could justify by empiricism alone".

R. Peck, 1969

1.0 Introduction

1.1 Rationale for Research

The research described in this thesis was undertaken to investigate large scale natural slope movements in the Beaver Valley, Glacier National Park, British Columbia. The Beaver Valley forms the eastern part of a major transportation corridor that traverses the Selkirk Mountains at Rogers Pass. This corridor is utilized by the Trans Canada Highway and a twinned section of the CP Rail main line.

Although the economic importance of the Beaver River Valley as the eastern approach to the Rogers Pass route has long been recognized, the distribution of large mass movement hazards along the valley slopes has only recently been documented (Pritchard et.al., 1988).

The Heather Hill landslide, one of several well defined failures in the valley, is selected as a representative example for detailed study. The primary objective is to determine the mode of failure of this landslide. This knowledge will enable others to more effectively assess risks associated with it and other mass movements.

1.2 Research Procedure

Field work at the Heather Hill landslide was undertaken during the summer of 1988. This led to the preliminary conclusion that a toppling process (Goodman and Bray, 1976) contributed to the failure at Heather Hill and adjacent areas of deep-seated instability. Moreover, the same process appears to be affecting other slopes nearby which presently show no indication of deep-seated failure. This preliminary conclusion meant that any technique of stability analysis used to examine the Heather Hill failure must be able to model large scale toppling in natural slopes, but should not be unduly biased towards a toppling mode of failure.

The literature survey of toppling reported in Chapter 2 was undertaken at this point. This review reveals that very little is known about toppling in large natural slopes, and that currently used analytical techniques are inadequate for these slopes. To explain the mechanism of the Heather Hill failure a method of analysis capable of modelling toppling, but not restricted to this mode of failure, is required. A conclusion of the literature review is that a numerical package known as the Universal Distinct Element Code (UDEC) is the most suitable program.

The suitability of UDEC for analysis of all types of topples is demonstrated. The program is then used to examine and

classify the mode of failure of the Heather Hill landslide,
illustrating the ability of the distinct element method to
model rock mass deformation in the slopes of the Beaver
Valley. This analysis also demonstrates that UDEC provides an
important framework for engineering design and for explaining
the geomorphic features associated with the evolution of
natural slopes.

1.3 Thesis Structure

This research is reported in three parts.

Part I contains this introductory chapter, and the literature
review (Chapter 2).

Part II is concerned with the description and use of UDEC.
Chapter 3 introduces the program, outlining the theory of the
distinct element method and the capabilities and limitations
of UDEC. Chapter 4 demonstrates that the distinct element
method can be used to model all types of toppling failures.
This is done by using UDEC to reevaluate examples of toppling
analysis reported in the literature or known to the author.

In Part III the mechanism of failure of the Heather Hill
landslide is evaluated. Chapter 5 is a characterization of
the study area. This chapter includes the regional geology

and geomorphic development of the Beaver Valley, previous work on the slope movements, and the results of the 1988 field program. In Chapter 6 the Heather Hill landslide development is modelled using UDEC.

Chapter 7 contains the conclusions of this research, and gives recommendations for further work.

2. Literature Review

2.1 Introduction

The aims of this review are to summarize the state-of-the-art in toppling and to identify deficiencies. Toppling is defined and an historical review is provided in the first section. In subsequent sections the history of toppling research is outlined, the development and capabilities of physical and numerical models of toppling are reviewed, and some of the physical and mechanical parameters that influence toppling are discussed. A summary of gaps in the understanding of toppling and suggestions for further research are included at the end of the review.

2.2 General Definition and Historical Perspective

Toppling failure is generally defined as the down-slope overturning, either through rotation or flexure, of interacting columns or blocks of rock (Goodman and Bray, 1976). This mode of failure can develop in slopes which contain well developed discontinuities or a pervasive foliation dipping steeply into the slope. In addition, the discontinuities or foliation should strike parallel or subparallel (plus or minus 20 degrees) to the slope crest, and

lateral release should be possible due to the topography of the slope or down-slope trending discontinuities.

Toppling failures have only been described in literature within the last twenty five years, and attempts to model toppling have only been undertaken in the last twenty years. As a result of the brief period that this mechanism of failure has been recognized, references on toppling are sparse.

One of the first references describing the motion of this type of failure as toppling is Muller (1968). Physical model studies were carried out under Muller's direction by Hofmann (1972).

Significant studies on the mechanics of toppling were undertaken from 1970 to 1974 at Imperial College by Ashby (1971) and Cundall (1971). Ashby provided a comprehensive analysis of the sliding and overturning components of toppling. His work, which explained the kinematics of toppling and examined the influence of physical and mechanical parameters, later became the foundation for limit equilibrium methods of toppling analysis (Sec. 2.4.3). Cundall (1971) made one of the earliest attempts to study toppling numerically using the distinct element method (Sec. 2.4.5).

During the same period, researchers at James Cook University made significant contributions to the understanding of

toppling in jointed rock mass behaviour. Burman (1974) introduced rotation into numerical simulations of block rock systems, and discussed the influence of block rotation on planar failures.

One of the first qualitative papers describing field examples of toppling failures was published by de Frietas and Watters (1973). This paper is particularly significant as it convincingly demonstrates that toppling failure " ... requires neither unusual geological conditions, nor unusual geological materials in order to develop; in fact the reverse would seem to be true." As well, their paper provided much needed field evidence of toppling failures and demonstrated that topples occur at all scales and in contrasting structural settings. Their work was pivotal in persuading the geotechnical community to accept toppling as a significant and distinct mode of failure.

With the recognition of toppling came the development of techniques to assess the stability of slopes prone to toppling. The best known technique for analyzing toppling stability is the limit equilibrium method (Goodman and Bray, 1976). This method is based on an evaluation of static forces and moments of a system of blocks representing the slope. Goodman and Bray also defined the various types of topples and their occurrence, and proposed a kinematic test of the potential for toppling (Secs. 2.3, 2.4.2). Both the kinematic

test and the limit equilibrium analysis have become accepted techniques for predicting and analyzing block toppling failures (Choquet and Tanon, 1985).

Simultaneously, but primarily separately, finite element modelling of jointed rock mass was developing (Sec. 2.4.4). Many finite element programs described in the literature owe their origins to work by Duncan and Goodman (1968) who outlined a finite element technique for jointed rock. Kalkani (1977) and Hittinger (1978) completed important finite element studies of jointed rock; Kalkani with well jointed rock slopes and Hittinger with toppling.

Also simultaneously, Cundall was continuing analytical work on the deformation of jointed rock using the distinct element method. Cundall et al. (1978) modelled an example of toppling published by Goodman and Bray (1976) as a validation of the method.

From the late seventies to present work on toppling has dealt mainly with case histories, using both the limit equilibrium (Wyllie, 1980; Piteau and Martin, 1981; Piteau et al., 1981), and the finite element (Brown et al., 1980; Brown , 1982; Evans et al., 1981) methods of analysis. One post-1980 publication uses the distinct element method to analyze a toppling slope (Ishida et al., 1987). Many papers since the late seventies discuss refinements to the limit equilibrium

technique, or provide nomograms to facilitate use of the limit equilibrium method (Piteau and Martin, 1981; Piteau et al., 1981; Teme and West, 1983; Zanbak, 1983; Choquet and Tanon, 1985; Sagaseta, 1986).

2.3 Types of Topples

The generally accepted definitions of the process and types of toppling are given by Goodman and Bray (1976) and Hoek and Bray (1977). Toppling failure as defined by Goodman and Bray (1976) can be comprised of three types of motion:

Flexural Toppling:

    Continuous columns of rock bend down-slope, eventually breaking in tension at depth. Prior to fracture, displacement is accommodated by internal deformation of the intact rock columns and flexural slip along the separations between columns (Fig. 2.1a)

Block Toppling:

    Columns of rock, divided by cross joints, overturn down-slope. The failure surface steps as required along joints, but no sliding occurs on cross joints. (Fig. 2.1b).

Block/Flexural Toppling:

Columns of rock overturn down-slope by rotation and sliding on cross joints. The motion is similar to block toppling, but unlike block toppling sliding on cross joints is significant (Fig. 2.1c).

These definitions accurately describe the types of deformation behaviour that can occur during toppling. However, the mode of toppling that occurs in real slopes is often a complicated mix of the modes defined above.

2.4 Methods of Analysis

2.4.1 Physical Models

Some of the earliest modelling attempts utilized the friction table or tilt table. Ashby (1971), Soto (1974), and Whyte (1973) examined block and block/flexural toppling, Kuykendall (1975), experimented with flexural toppling models, and Hofman (1973) considered mixed modes of block/flexure and flexural toppling. The limit equilibrium method and numerical methods quickly became more popular primarily due to their flexibility.
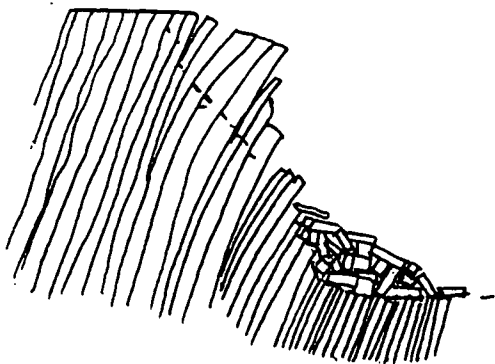
Figure 2.1a   Flexural Toppling
              (after Goodman and Bray, 1976)
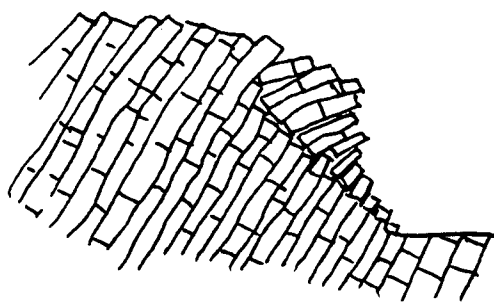
Figure 2.1b   Block Toppling
              (after Goodman and Bray, 1976)
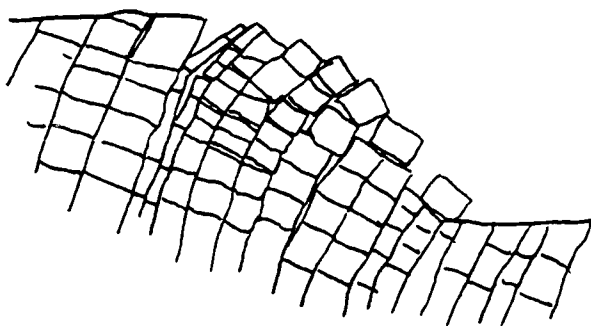
Figure 2.1c   Block/Flexural Toppling
              (after Goodman and Bray, 1976)

11

2.4.2 Kinematic Analysis

Prediction of toppling potential using a kinematic analysis was proposed by Goodman and Bray (1976). For toppling to be possible the pole to the regular discontinuity set dipping into the slope must lie outside a great circle whose dip is the slope face angle plus the friction angle of the discontinuity. This test can be quickly done using a stereonet plot (Fig. 2.2a).

The test is based on two limiting stress conditions of toppling at the point where flexural slip along discontinuities occurs. The first condition results from stress equilibrium requirements and applies at the free surface of the slope (slope face). Along the slope face the maximum ($\sigma 1$) and median ($\sigma 2$) stress directions must lie in the plane of the slope. The minimum stress ($\sigma 3$) is oriented normal to the slope face and has zero magnitude. It is assumed that the median stress acts parallel to the trend of the slope and the maximum perpendicular (Fig 2.2b).

The second condition comes from the requirements for shear along the discontinuities near the slope face. Given that $\sigma 3$ is zero, for shear (in the $\sigma 1$, $\sigma 3$ plane) to be possible along the discontinuity the maximum principal stress must act at an angle to the pole of the discontinuity equal or greater than the friction angle of the discontinuity. Using these two

failure criteria, that the maximum principal stress direction is aligned with the slope face (θ) and must be inclined by at least the friction angle (ϕ) to the discontinuity, it is possible to determine the limiting conditions for stability; that $\theta \leq (\phi + \alpha)$ (Goodman and Bray, 1976) (Fig. 2.2c).

This test has gained acceptance since it was proposed. However, it can only predict whether toppling failure is kinematically possible; it cannot predict whether or not a given slope will topple. Choquet and Tanon (1985) suggest a minor alteration of this test to include a limiting condition of toppling that occurs when the failure plane becomes so steep that the columns will fail purely by sliding along joints.

2.4.3 Limit Equilibrium Method

By far the most popular analytical technique to predict whether a slope will topple is the limit equilibrium method developed by Goodman and Bray (1976). This technique is based on the kinematics developed by Ashby (1971) and can be used to calculate a factor of safety for a slope prone to toppling. As the technique is described in detail by Hoek and Bray (1977) and by Goodman and Bray (1976), this review will provide only a brief summary of the method concentrating on the capabilities and limitations of the technique.

Toppling possible for poles lying within ruled region.
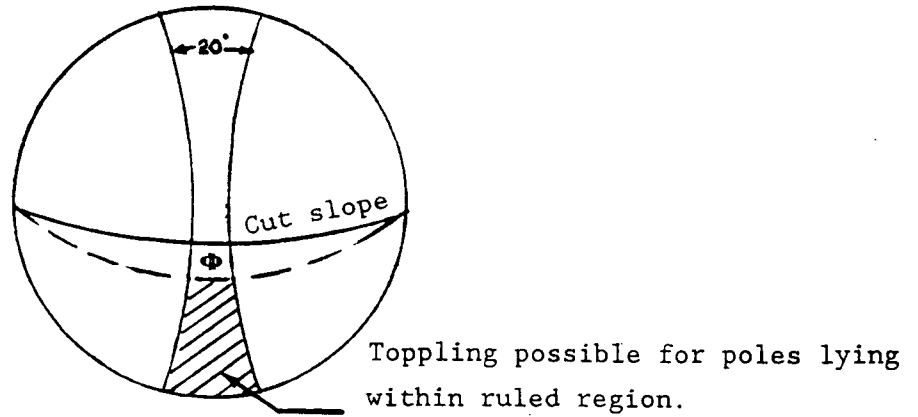
Figure 2.2a   Kinematic Test of Toppling Potential using Stereoplot. (after Goodman and Bray, 1976)
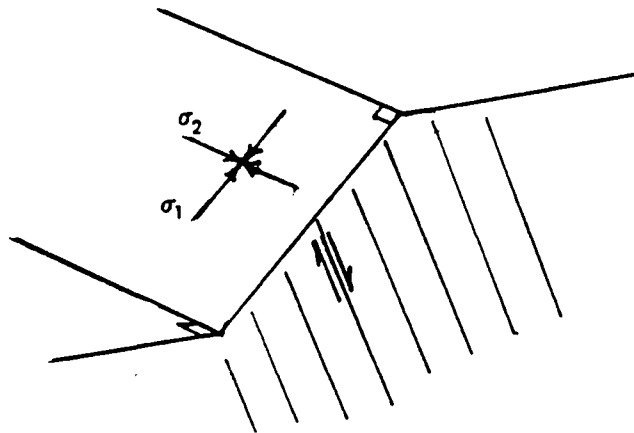
Figure 2.2b   Stress Orientations on Slope and Direction of Shear on Discontinuities (after Goodman and Bray, 1976).
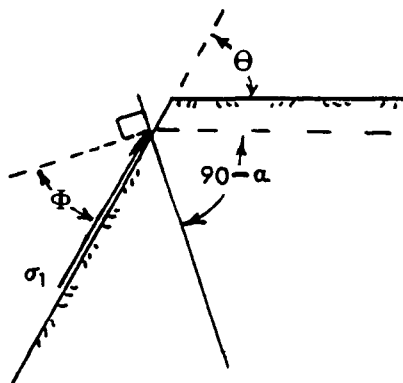
Figure 2.2c   Condition for Interlayer Slip (after Goodman and Bray, 1976).

14

The limit equilibrium solution is formed by approximating the slope as a series of columns resting on a stepped base (Fig. 2.3). The solution begins by resolving the forces acting on the uppermost column in the slope into forces normal (y') and parallel (x') to the base of the block. The failure mode for the block is determined by solving two statics problems, one assuming block sliding and one assuming block toppling. The resultant x' forces from each potential mode of failure are compared, and the solution producing the largest resultant in the x' direction is taken to be the mode of failure of the block. This resultant x' force is then applied to the next block in the slope and the analysis is repeated. The analysis progresses from block to block down the slope to the toe block. The final resultant force at the toe block is the force required to maintain the stability of the slope. A Factor of safety can be calculated from the ratio of the coefficient of friction of the last block without support to the coefficient of friction with support.

There are several limiting assumptions to this analysis.

1. No block can be both toppling and sliding.

2. The method only applies to block toppling of continuous columns. Columns may be jointed, but slip on joints or overturning of individual blocks defined by joints within a column is not allowed.
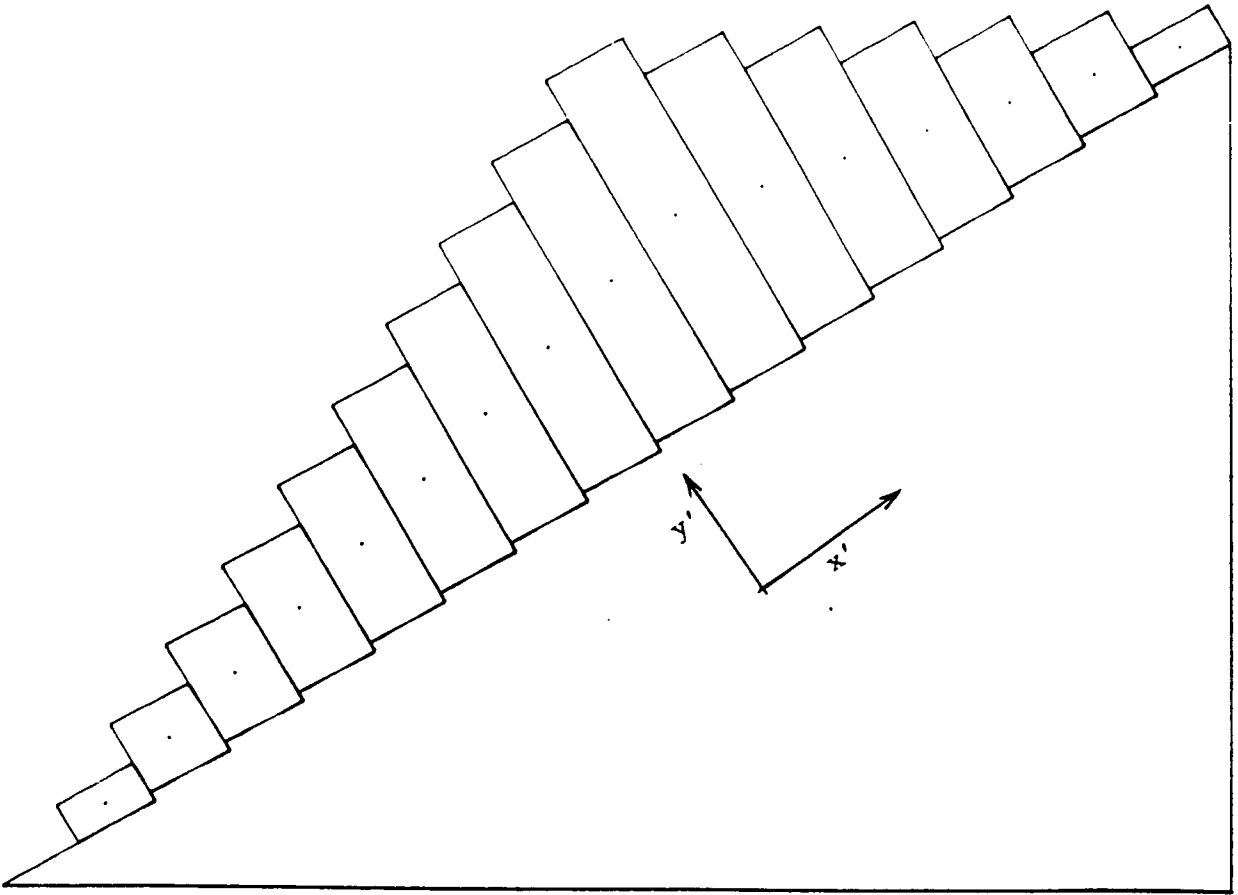
Figure 2.3   Typical Slope Configuration Assumed in Limit
Equilibrium Method of Analysis.
(after Goodman and Bray, 1976)

3. The columns are rigid. The technique cannot accurately analyze toppling with large internal column deformations.

4. The location and inclination of the stepped failure plane must be assumed.

5. The analysis is by definition a static balance of forces. Toppling failure of a slope is a dynamic process, and deformation affects strength parameters. A limit equilibrium analysis of toppling does not allow evaluation of mobilized strength of joints, which depends not only on normal stress, but also on tangential displacement. In other words, the analysis cannot incorporate non-linear stress-displacements joint relationships.

6. Current programs restrict the slope geometry to a uniform step and block width.

Even with these limitations, the limit equilibrium method has proven useful for examining toppling. The simplicity of the solution and the output of required retaining force or factor of safety have lead to the successful use of the technique for engineering design (Piteau et al., 1981).

2.4.4 Finite Element Method

The finite element method has been used with moderate success to model toppling slopes as a discretized continuum containing joint elements. This section will give a brief history of the application of the finite element method to toppling failures followed by the capabilities and limitations of the technique and its use in practice.

Finite element models owe their development to many workers who each improved the technique for modelling jointed rock mass (Duncan and Goodman, 1968; Goodman et al., 1968; Goodman and Dubois, 1971; Burman, 1974). Although finite element methods for jointed rock have been used extensively in all areas of rock mechanics, there are few applications of the method to toppling (Burman et al., 1975; Kalkani and Piteau, 1976; and Hittinger, 1978).

Finite element methods are capable of modelling topples more realistically than the limit equilibrium method. The constitutive relationships of the intact rock mass and the joints can be more realistically modelled, pore pressures can be introduced, and any geometry, geology, and loading histories can be used.

However, the finite element method is not without problems. It has a limited ability to model jointed rock mass because of

its continuum formulation. To obtain the approximate solution of displacements and stresses in the problem domain, large matrices must be formulated and solved from the governing equations at the grid points. Whenever significant displacement occurs at a grid point this global stiffness matrix must be reformed. Thus, problems with large displacements are time consuming and difficult to solve. The method is also not a dynamic technique. It can predict stresses and displacements, but if a slope is unstable it cannot be used to study how a failure progresses.

The state-of-the-art in finite element analysis of toppling appears to be the program developed by Hittinger (Hittinger, 1978). A case history by Brown et al. (1980) applies this program to analyze a real slope. Evans et al. (1981) reports what appears to be the most recent attempt to apply finite element analysis to toppling.

The lack of use of the finite element method in toppling analysis is likely a result of the complexity of the technique. Except for large problems that justify the time involved in a more detailed analysis, practitioners prefer the simpler limit equilibrium technique.

2.4.5 Distinct Element Method

The distinct element method has a much more clearly defined history than the finite element method. The finite element method applied to jointed rock and specifically to topples owes its development to a large number of researchers, but the development of the distinct element method can be traced to one researcher, Dr. P.A. Cundall. The original paper describing the method was published in 1971 (Cundall, 1971). Since this publication, Cundall, and others have continued to develop the method. This section provides a brief history of the development of the distinct element method as it relates to toppling failure. The capabilities and limitations of the method along with its use in practice will be discussed.

The technique applies an explicit, finite difference method of solution to model large displacements and rotations of block systems. The rock mass is represented by an assemblage of blocks, and the discontinuities dividing the blocks act as boundary interactions with a prescribed joint behaviour.

Since it was first described in 1971, the method has evolved into a highly flexible computer package. The original program considered the blocks to be rigid and applied a simplistic joint relationship. By the mid eighties the original program had been modified into several versions that included such capabilities as block deformation and splitting (Cundall et

al., 1978; Cundall and Marti, 1979), a joint generator capable of creating discontinuous joints by sets (Cundall, 1983), transient fluid pressure and flow utilizing joint permeability linked to mechanical deformation, and various joint constitutive models (Cundall, 1985; Cundall and Lemos, 1988). In addition the distinct element method has been linked to a boundary element code allowing significant reduction of the computational size of some problems (Lemos and Brady, 1983). By 1985 these and other features had been unified into a two dimensional program known as the universal distinct element code (UDEC). A three dimensional version of this program is known as 3DEC.

All the advantages noted in Section 2.4.4 for the finite element method also apply to the distinct element method, however the distinct element method has additional advantages over the finite element method. A particular advantage of the finite difference technique is its computational simplicity. Because the method is an explicit finite difference approach, solved using dynamic relaxation, it does not form large matrices and makes limited demands on computer memory requirements. The formulation of the problem as a collection of interacting blocks also has advantages over the continuum method used by finite element techniques. The making and breaking of contacts between blocks and large displacements and rotations of blocks are more easily accommodated.

Disadvantages of the method include the often small time step, and corresponding long run time, required to ensure numerical stability. This disadvantage has become much less significant in the last few years as desk top computers have become cheaper and more powerful.

2.4.6   Comparative Assessment of Analytical Methods

By far the most popular method reported in the literature to model toppling is the limit equilibrium method. However, the method cannot accurately predict the stability of topples that undergo internal deformation (flexure) prior to failure, or when the constitutive relationships of the intact rock or joints vary in a non-linear manner with stress level or displacement. Although serious, these problems are often overshadowed by problems with the fundamental assumptions of the method listed in Section 2.4.3.

As discussed in Section 2.4.4, finite element methods overcome most of the limitations of the limit equilibrium method, but they have been used much less frequently to model toppling. Most of the finite element work with toppling slopes is restricted to hard, stiff rock. This is done either to facilitate comparison of finite element results to real rock slopes (Brown et al., 1980; Kalkani and Piteau, 1976; Evans et al., 1981), the limit equilibrium method, or physical models (Hittinger, 1978). When hard rock is modelled it deforms

little, and most of the stress dependent deformation is derived from the joints. The preference for hard rock topples is partially a result of research being directed toward small scale topples where low in situ stress conditions support rigid block behaviour. As a result of this preference for small slopes with rigid column behaviour, large slopes with higher in situ stresses and corresponding larger column deformations, have not been studied.

Distinct element methods have been applied to block topples both as a validation of the distinct element method and as a modelling technique for examining block toppling. Cundall (1971), Cundall et al. (1977), and Cundall et al. (1978) all use block toppling examples to validate the distinct element method. Aside from these brief uses of toppling as examples of distinct element method validation, there are very few examples in the literature of the distinct element method being used to model either hypothetical or real toppling slopes.

Hocking (1978) used a rigid block distinct element program to examine toppling sliding failure modes of hypothetical blocky slopes. More recently Ishida et al. (1987) applied a rigid block version of the distinct element method to a real example of block toppling. The version of the distinct element method used by Ishida et al. (1987) is, however, outdated compared to other available programs. The distinct element method does not

appear to have been used to model the more complex flexural and composite modes of toppling.

In summary, toppling research has been largely directed towards the limit equilibrium method. This method cannot realistically be used when rock or joint strengths vary non-linearly with stress or in any manner with displacement. Finite element methods can predict toppling slope deformation more accurately than the limit equilibrium method, but have not been used as extensively. Also, the finite element method is formulated as a continuum and cannot accommodate large displacements as well as the distinct element method. The distinct element method is designed to model large deformations, but its formulation requires long computer runs. There are very few applications of the distinct element method to block toppling, and none to flexural toppling.

2.5   Parameters Controlling Toppling: Discussion

2.5.1   Influence of Structure and Rock Type

All rock types are susceptible to toppling if the requisite geometry and structure are present (de Frietas and Watters, 1973; Goodman and Bray, 1976). Structure provides distinct planes of weakness within the rock mass, and lithology

controls the strength and deformation characteristics of the intact rock.

The influence of jointing is fundamental, as evident in the definitions of topple types. Flexural toppling occurs in columns with no cross-fractures, block toppling occurs by separation along pre-existing joints, and block-flexural toppling requires a pervasive cross-jointing.

The primary strength characteristics of intact rock that influence toppling slope failures are shear and tensile strength, stress-strain relationships, and, perhaps, rheology. These properties are dependent on rock type. At low to moderate confining pressures, strong rock will have a high elastic modulus and exhibit low strain to a brittle failure. Weak rock will have an lower elastic modulus and a non-linear stress strain relationship allowing large deformations for stress levels close to ultimate failure.

There is nothing quantitative in the literature concerning the influence of these rock strength characteristics on topples. This seems to be an inadvertent result of the direction toppling research has taken. Research has concentrated on the limit equilibrium method, with a small amount of work on the finite element method. The limit equilibrium method has inherent restrictions on the deformation behaviour of intact rock and joints. The finite element method does not have

these restrictions, but it has also been used very little for modelling toppling.

2.5.2   Shear Strength of Discontinuities.

It is important to note that toppling failure is often controlled by the behaviour of discontinuities, not by the stress-strain properties of intact rock. This is especially true in small scale topples where low in situ stresses cause little deformation to intact rock. The intact rock is essentially rigid and the mechanical behaviour of discontinuities is of paramount importance.

Discontinuities provide a defined surface of failure in the rock mass, and can have complicated non-linear stress-displacement behaviour that includes peak and/or residual strength, creep deformation properties, cohesion, and separation in tension.

Shear strength of a discontinuity depends on the normal stress, the inclination and strength of irregularities on the surface (Patton, 1966; Ladanyi and Archambault, 1969), and on displacement. Surface irregularities cause a discontinuity to dilate when tested under constant normal stress. If a dilative discontinuity is confined during shear the normal stress on the discontinuity will increase, increasing the shear strength. Consequently, in a real slope with dilative

26

joints finite or distinct element models will be simulating conservative behaviour if dilation is not included in the joint behaviour of the model (Barton, 1986).

Dilation of joints is limited by the shear strength of asperities on the joint surface. Ladanyi and Archambault (1969) observed the stress level at which shearing of asperities occurs to be approximately $9.5 \times 10^6 N/m2$. Above this level, dilation of joints will not occur. Depending on the rock density and stress history, this is roughly equivalent to the stress level at a 300 to 450m depth. Theoretically all but the largest slopes should display some degree of dilatant joint behaviour.

The above discussion on deformation characteristics of intact rock and joints leads into a discussion of scale influences on topples. The most fundamental difference between a small slope (<100m high) and a large slope is the in situ stress condition. As described above, this confinement acts to increase the strength of dilative joints undergoing shear. Hence, the shear strength of dilative discontinuities will increase with confinement in higher slopes. Bovis (1982), suggested dilation of discontinuities could explain the arrested development of some toppling failures.

2.5.3 Groundwater

Few researchers have given more than simplistic treatment to
the influence of groundwater on toppling. Like the influence
of rock strength characteristics discussed earlier, this is a
result of the direction toppling research has taken. Much of
the research that has been done is aimed at solving
engineering problems related to mining or slope excavation.
Because of the small scale of these failures and the dilated
nature of the rock, the slopes are often assumed to be drained
with no pore pressure (Choquet and Tanon, 1985). Even when
pore pressures are included in the analysis, the assumptions
used for the water table and flow are often simplistic
(Hittinger, 1978; Piteau et al., 1981; Brown, 1982). The most
common assumption for the water table is a straight line from
the toe of the slope up to a point directly below the crest of
the slope. From this point the water table is assumed to be
horizontal back into the slope.

The assumption of no pore pressures or an approximate water
table may be adequate for the analysis of road cuts and pit
slopes, but topples in larger slopes may require a more
accurate consideration of pore pressure. Larger slopes are
part of a regional flow system and, except in the most arid
regions, will have a water table. In order for the influence
of pore pressures to be correctly modelled, the

groundwater flow system in the slope must be accurately quantified.

2.6   Summary of Areas Needing Further Work

2.6.1   Failure Plane Prediction

One of the problems with the commonly used limit equilibrium method for toppling analysis developed by Goodman and Bray (1976) is that it cannot predict the shape and location of the failure plane. The user must apply a trial and error approach, selecting different planar failure surfaces to determine the surface with the lowest factor of safety. Also, this limit equilibrium method assumes that the failure surface is planar, but it is not known if this is always true.

Further research into the formation and shape of the failure surface in all types of topples is required. The distinct element method is capable of predicting a failure surface configuration by modelling both intact rock and joint deformations using realistic constitutive relationships. Using this method to model toppling deformation of hypothetical slopes having variable material properties and geometry should lead to a better understanding of the development and geometry of flexural toppling failures.

2.6.2 Influence of Confining Stress

The influence of in situ stresses on rock strength is well
understood and can be incorporated in the constitutive stress-
strain laws for intact rock and joints. One of the flaws of
the limit equilibrium approach to toppling analysis is that it
does not incorporate realistic in situ stresses. Although
both the finite element and finite difference methods utilize
more realistic stresses, neither has been used to investigate
the influence of stress conditions on toppling slopes. This
can be done with the distinct element method using large scale
slopes and deformable blocks.

2.6.3 Toppling in Mixed Rock Types

No attempt has been made to numerically model toppling slopes
of mixed rock types. Large slopes consisting of layered hard
and soft units (ie: sandstone and shale, or quartzite and
phyllite) that undergo significant overturning and flexure
prior to failure cannot be accurately modelled with the limit
equilibrium method.

A research program could use the distinct element method to
compare the behaviour of mixed rock type slopes to slopes of
one material. The primary goal would be to numerically
reproduce the deformation observed in these slopes.

2.6.4 Time Dependent Deformation

Most of the research on toppling in the literature concentrates on small rapidly excavated slopes. Creep deformations in these slopes are likely insignificant compared to deformations from stress changes. In larger natural slopes excavated by fluvial and/or glacial erosion or oversteepened by mass wasting or tectonic uplift, creep influences may be much more significant. It may be possible to use finite difference techniques applied to a discretized continuum (such as the program FLAC, described by Cundall and Board, 1988), or finite element techniques to model this type of deformation.

2.6.5 Large Slopes and Weak Rock

Most toppling research has dealt with engineering or mining excavations. At the scale of these small excavations, deformation of the intact rock is much less significant than deformation along discontinuities in the rock.

In large slopes, the strength and deformation characteristics of both the rock material and rock mass will contribute to stability. In addition, increased confining stresses will increase the strength of dilative joints. Although there are several qualitative descriptions of large scale topples in the literature (Tabor, 1971; de Frietas and Watters, 1973; Bovis, 1982; Holmes and Jarvis, 1985; Evans, 1987; Pritchard et.al.,

1988), no analysis of these slopes that incorporates the influence of the rock material or rock mass strength has yet been attempted.

2.6.6 Groundwater

To date, no researcher working on toppling slopes has considered the heterogeneous, anisotropic nature of hydraulic conductivity in bedded deposits. A more detailed treatment of the groundwater flow may not be necessary in smaller toppling slopes, but it may be required for realistic modelling of larger mountain scale topples.

3. Distinct Element Method

3.1 Introduction: UDEC

The universal distinct element code (UDEC) marketed by Itasca Consultants was purchased for this research program. The historic development and capabilities of this program and its particular advantages for modelling jointed rock systems are reviewed in section 2.4.5. The remainder of this chapter discusses the theory, features, and limitations of the program. UDEC is a very comprehensive modelling package with many features. Only the features used in this research program are discussed in this chapter. Readers interested in a more complete general description of the program are referred to Lemos et al. (1985). The general references used in the following discussion are: Cundall (1987), Itasca (1989), Lorig (1984), and Cundall et al. (1978).

UDEC is written in FORTRAN77 and is available in source code or executable form. This research uses UDEC version 1.5 released March, 1989. It is compiled for operation on an 80386-based microcomputer running DOS3.x, using SVS FORTRAN 386, the PHARLAP linker, and ICG X-AM DOS extender (Itasca, 1989). Screen graphics support is handled through a FORTRAN-linkable library (SCITECH plotting package) (Itasca, 1989). The version used for this research was compiled to utilize approximately four megabytes of RAM, and a math coprocessor.

With this amount of memory a problem size of approximately
2500 rigid blocks or 1000 fully deformable blocks can be used.

3.2   Theory of Distinct Element Method

The distinct element method is based on a discontinuum
approach to rock mass modelling that allows a jointed rock
mass to be represented by distinct blocks that interact along
their boundaries. In addition to the discontinuum modelling
of the block interaction, each block can be allowed to deform
as a continuum modelled by finite differences (Fig. 3.1a).

3.2.1   Explicit Solution Procedure

Deformation is determined by using an explicit solution
procedure time stepping algorithm. In an explicit method, all
quantities on one side of all equations are known and a simple
calculation produces the quantity at the next time step. In
UDEC the quantities calculated are incremental displacements
or strains. The technique relies on the fact that it takes a
finite time for a displacement to pass through the system of
blocks. If the time step is small enough such that a
displacement cannot propagate from one block to an adjacent
block in one time step, then the equations of motion for all
blocks become uncoupled and the numerical procedure is stable.
When continuum finite difference zones are applied within the

Distinct Element Model

Continuum
Elements

Discontinuum Elements
(Joints)
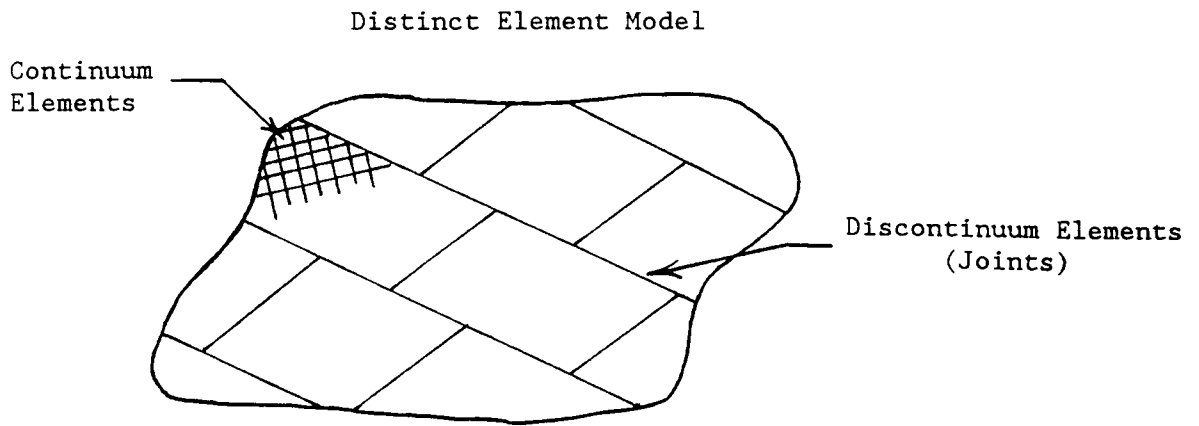
Figure 3.1a   Nature of Distinct Element Model
(after Itasca, 1989)

Constitutive
Relation

Stress

Displacement
or Strain

Law of Motion

$$\ddot{u} = \frac{Force}{Mass}$$

$\ddot{u}$ integrated twice
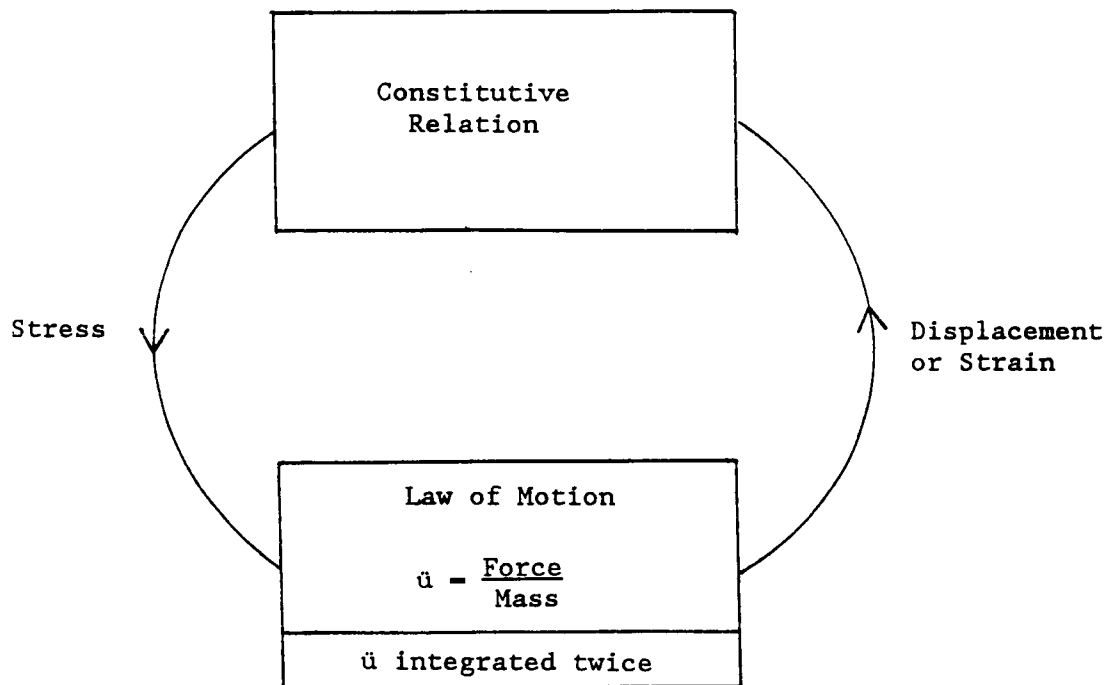
Figure 3.1b   Distinct Element Model Calculation Cycle
(after Cundall et.al., 1977)

blocks, the time step also becomes dependent on the propagation of information between adjacent zones within the block. Determination of the required time step is based on the mass and material stiffness of blocks or zones. The main disadvantage of this method of solution is the small time step required.

The program iterates by using force displacement laws to determine the net force on each block resulting from the influence of surrounding blocks and a blocks own weight. It then uses these forces and the time step to determine block accelerations and displacements. The cycle repeats itself when the increment of displacement is used to reevaluate the forces on each block. This procedure is diagrammatically illustrated in Figure 3.1b. The user is responsible for determining when the problem either stabilizes or fails. This is achieved by monitoring time histories of displacements, velocities, or any of several other parameters selected by the user within the problem.

3.2.2 Equations of Motion and System Damping

The solution process described in the previous section is known as dynamic relaxation and was first described by Otter el.al. (1966). In dynamic relaxation the blocks are moved according to Newton's second law of motion, which is justified

on physical grounds (Cundall, 1987). This law can be written
in the form:

$$\frac{\partial \dot{u}}{\partial t} = \frac{F}{m} \qquad [1]$$

where   F= force

     m= mass

     $\dot{u}$= velocity

     t= time

Using central difference theory we can write the above
equation as:

$$\dot{u}^{(t + \Delta t/2)} = \dot{u}^{(t - \Delta t/2)} + \frac{F^{(t)}}{m} \Delta t \qquad [2]$$

Written for a block with gravity (g_i) included this equation
becomes:

$$\dot{u}_i^{(t + \Delta t/2)} = \dot{u}_i^{(t - \Delta t/2)} + (\frac{\Sigma F_i^{(t)}}{m} + g_i) \Delta t \qquad [3]$$

where i denotes a directional index

     $\dot{u}_i$= the velocity of the center of mass and

     g_x= 0

Note that this central difference integration assumes that
acceleration is constant over a time increment from $(t - \Delta t/2)$
to $(t + \Delta t/2)$.

By integrating the expression for velocity at the half time
step over the interval (t) to $(t + \Delta t)$, incremental

displacement (u_i) of the block is determined. This is then used to obtain the new block location (x_i):

$$x_i(t + \Delta t) = x_i(t) + \dot{u}_i(t + \Delta t/2) \, \Delta t \qquad [4]$$

The development is similar for rotational motions of the blocks. Rotational velocities at the half timestep are given by:

$$\dot{\theta}(t + \Delta t/2) = \dot{\theta}(t - \Delta t/2) + \frac{\Sigma M(t)}{I} \Delta t \qquad [5]$$

where $\dot{\theta}$ = angular velocity of block about its centroid

I = moment of inertia of block about its centroid

ΣM = sum of the moments about the block centroid

Rotational displacements are given by:

$$\theta_i(t + \Delta t) = \theta_i(t) + \dot{\theta}_i(t + \Delta t/2) \, \Delta t \qquad [6]$$

For static solutions, some form of energy dissipation or damping must be included to prevent the system from oscillating indefinitely. UDEC uses either mass proportional or stiffness proportional damping. Each of these simulate viscous dashpots attached to the system. Mass proportional dampens the system to an absolute frame of reference, and is akin to immersing the whole system in a viscous fluid. Stiffness proportional damping is a relative damping technique that applies dashpots only across contacts between blocks. Only mass proportional damping is used in this research program.

In mass proportional damping, the dashpots generate a force
that opposes the blocks velocity and is proportional to the
block velocity and mass. The equation of motion is modified
as follows to include viscous damping.

$$\frac{\partial \dot{u}}{\partial t} = \frac{F}{m} - \alpha \dot{u} + g \qquad [7]$$

where α is the damping factor

In finite difference notation centered at time t velocity at
the half time step becomes:

$$\dot{u}^{(t + \Delta t/2)} = \{\dot{u}^{(t - \Delta t/2)}(1 - \frac{\alpha \Delta t}{2}) + (\frac{F}{m} + g)\Delta t\}/(1 + \alpha \Delta t/2) \qquad [8]$$

Rotations are damped in a similar manner (Itasca, 1989).

This scheme of damping is not without difficulties. Applying
velocity proportional damping to blocks that are moving at a
constant velocity generates erroneous body forces opposing the
direction of motion of the block. These spurious body forces
may affect the solution (Cundall, 1987).

UDEC partially overcomes this problem by adjusting the damping
factor based on the sum of the change in kinetic energy in the
system in a time step. The damping factor is adjusted each
time step to maintain a prescribed ratio (R) of power adsorbed
by damping in the system to total change in kinetic energy in
the system. As the acceleration of a system of blocks reduces

39

to zero, the damping factor also reduces to zero. Experience

has shown that adjusting the damping factor to maintain R at

approximately 0.5 produces a damping effect that approaches

critical damping (Lorig, 1984).

In practice this is only a partial solution. In systems with

a significant variation in block size or motion, large

accelerating blocks will have a disproportionate affect on the

sum of the kinetic energy term, and the damping factor will be

weighted to these blocks. In such a system, small blocks

moving at a constant velocity will still experience spurious

body forces.

Manual damping is also available for dynamic simulations. A

description of how the damping factor can be determined

manually for mass or stiffness proportional damping is given

by Cundall et al. (1978) and Lorig (1984).

3.3   Features of UDEC

3.3.1   Block Interface Constitutive Relations

UDEC has two built in interface, or joint constitutive

relationships. The original joint relationship is linear

elastic-plastic. A continuously yielding joint model that is

capable of modelling progressive damage of the joint due to

shearing has also been incorporated in the program (Cundall

and Lemos, 1988). Only the original joint relationship is used in this research.

In the original joint relationship, the deformability and frictional characteristics of block interfaces are represented by spring - slider systems located at the contact points between blocks. Incremental normal and shear forces (ΔF_n, ΔF_s) are related to the incremental relative displacement (Δu_n, Δu_s) using linear force displacement laws:

$$\Delta F_n = K_n \; \Delta u_n \qquad\qquad [9]$$
$$\Delta F_s = K_s \; \Delta u_s \qquad\qquad [10]$$

where K_n and K_s are the contact normal and shear stiffnesses. A mechanical representation of this model is shown in Figure 3.2a.

Edge to edge joint contacts are represented by two corner to edge contacts, with the force applied at each corner distributed over a contact length L as shown in Figures 3.2b and 3.2c. The normal and shear stress across each contact ($\Delta\sigma_n$, $\Delta\sigma_s$) are related to displacement in the same manner as force across a single contact above:

$$\Delta\sigma_n = k_n \; \Delta u_n \qquad\qquad [11]$$
$$\Delta\sigma_s = k_s \; \Delta u_s \qquad\qquad [12]$$

where k_n and k_s are the normal and shear stiffnesses expressed in stress/length rather than force/length.
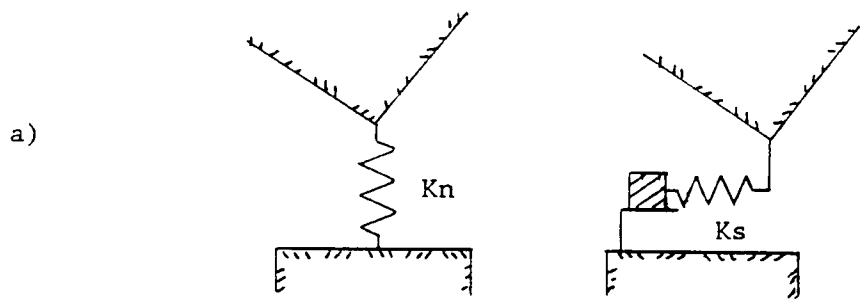
a) Normal Interaction   Shear Interaction

b)

c)
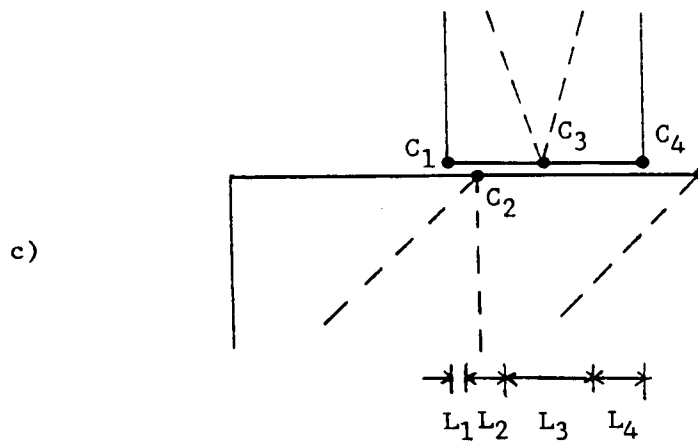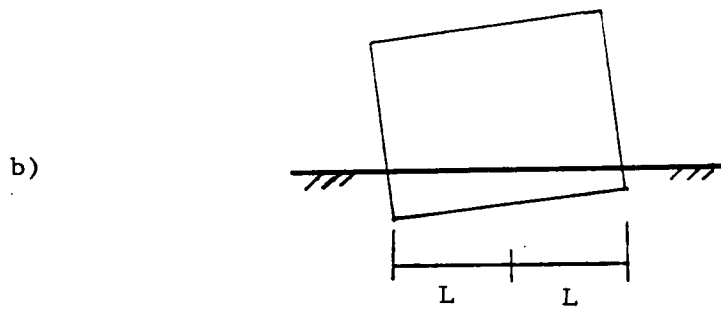
Figure 3.2a) Mechanical Representation of Interfaces in Distinct Element Model
b) Edge to Edge Contact
c) Contact Length for Fully Deformable Blocks
(after Itasca, 1989)

Figure 3.2c also illustrates how exterior grid points on blocks resulting from internal discretization are modelled. These grid points are treated as new corners, and the expressions discussed above are applied.

Mechanically, the overlap of two blocks is proportional to the normal force or stress on the contact. In the iterative cycle of the program, a change in overlap is used to update the contact forces or stresses, which are then used to determine new block accelerations.

The main difference between normal and shear behaviour of the joints is the incorporation of a peak elastic strength in shear. The peak strength of the joint is limited by a Mohr-Coulomb friction law:

$$|\sigma_s| \leq c + \sigma_n \tan \phi \qquad\qquad [13]$$

where c and ϕ are the joint cohesion and friction angle.

Tensile strength normal to the joint can be included, and dilation can be added as an increment to the joint friction angle.

The bilinear elastic-plastic model behaviour described above is a simplification of real joint behaviour and has limitations. In reality both shear and normal stiffness increase with the confining stress on a joint, and real joints usually do not display instantaneous plastic shear at the peak

strength. In real joints, plastic displacement begins to accumulate before the peak shear strength is reached, and the shear stress required for continuous plastic shear is often considerably less than the peak shear strength. Figures 3.3a and 3.3b illustrate how the model differs from real joint behaviour.

The continuously yielding joint model mentioned at the beginning of this section is designed to more realistically model joint behaviour. Like the original model, normal and shear stresses are related through joint stiffnesses to displacements. In the continuously yielding model the normal and shear stiffnesses increase with confining stress, and the continuous accumulation of plastic shear begins before the peak shear strength is reached. The model also allows the shear stress in the post peak plastic region to drop below the peak shear stress. (Cundall et al., 1978; Cundall and Hart, 1984; Cundall and Lemos, 1988; and Itasca, 1989)

3.3.2 Block Deformability and Constitutive Relations

Three types of block deformability are available in UDEC: rigid, simply deformable, and fully deformable.

In a system comprised of rigid blocks, all the deformation is accommodated by normal and shear displacement on the joints. The blocks have two translational and one rotational degrees of freedom, but the geometry of the blocks does not change.

a)   Shear
      Stress

Elastic

Shear Displacement

b)   Shear
      Stress

Elastic

Shear Displacement
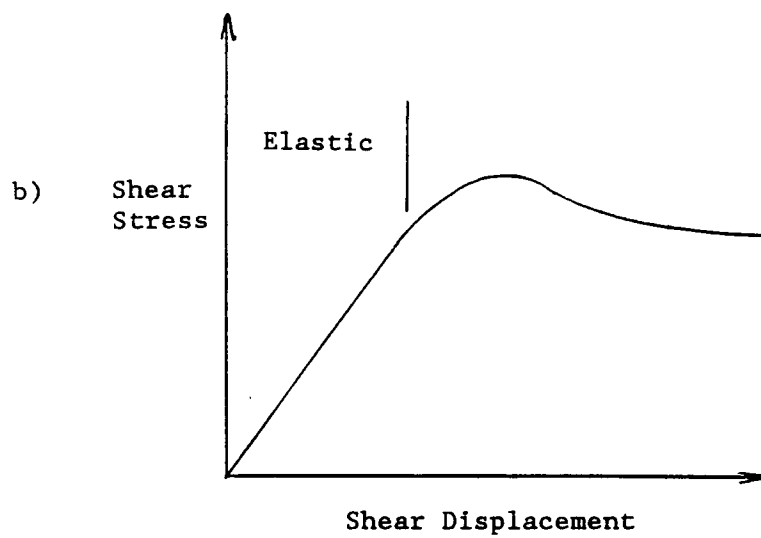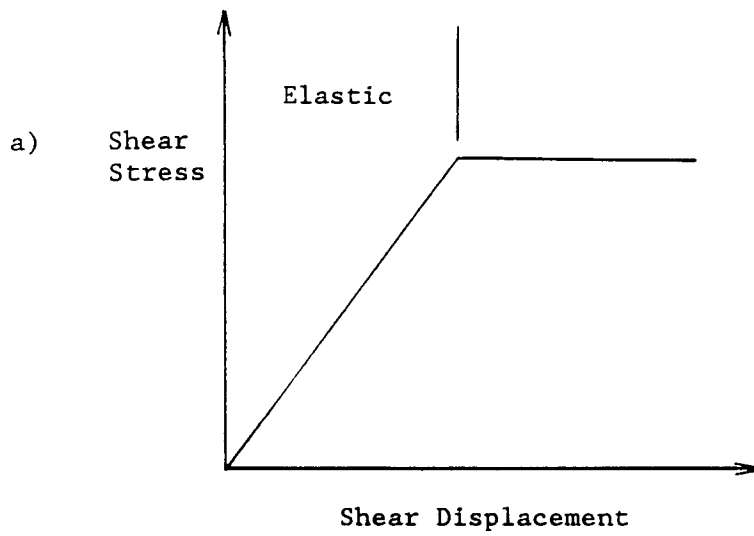
Figure 3.3a)   Elastic-Plastic Joint Model
        b)   Typical Joint Behaviour

This type of analysis is appropriate when the intact rocks elastic deformation is negligible compared to deformation on discontinuities.

Simply deformable blocks add three more internal degrees of freedom corresponding to three strains in two dimensions (ε_{xx}, ε_{yy}, $\varepsilon_{xy}+\varepsilon_{yx}$), and incorporate the ability to fracture based on Griffith's theory (Cundall et al., 1978; Cundall and Marti, 1979; and Williams and Mustoe, 1987). The aim of this formulation is to incorporate block deformation, but avoid computer intensive fully deformable blocks. Because this type of block is constrained to the combined degrees of freedom outlined above, they are not as accurate as fully deformable blocks and are not used in this research.

Fully deformable blocks are appropriate when confining stresses or transient loads are high enough that internal block deformation is significant relative to block displacements and joint deformations. In this formulation individual blocks are discretized into triangular finite difference zones and modelled as a continuum. The solution method is explicit, differences are centered in time and space, and plane strain conditions are assumed (Cundall et al., 1978).

The general solution sequence for a grid point formed by the triangular zoning is as follows. In each time step, stresses

are integrated about the grid point to determine a resultant
force from surrounding zones. To this is added the total of
any external forces from block contacts or otherwise. Net
acceleration is obtained by dividing the net force by the
lumped mass at the grid point and adding gravitational
acceleration. The equation of motion can be written as
follows:

$$\frac{\partial \dot{u}_i}{\partial t} = \frac{\int_s \sigma_{ij} \, n_j \, ds + F_i}{m} + g_i \qquad [14]$$

where   s = the surface enclosing the mass m lumped at a
         gridpoint

n_j = the unit normal to s,

F_i = the resultant of all external forces applied to
        the gridpoint

g_i = gravitational acceleration, and

i and j are directional indices.

In a similar manner to the equation of motion for blocks,
central differences are applied to the accelerations of grid
points to determine velocities and relative displacements.
The basic definitions of two dimensional strain are used to
relate zone strains and rotations to nodal displacements as
follows:

$$\dot{\varepsilon}_{ij} = \frac{1}{2} (\dot{u}_{i,j} + \dot{u}_{j,i}) \qquad [15]$$

$$\dot{\theta}_{ij} = \frac{1}{2} (\dot{u}_{i,j} - \dot{u}_{j,i}) \qquad [16]$$

where u= relative displacement

i and j are directional indices

comma i or j (ie: ,i or ,j) denotes a partial

derivative with respect to i or j, and the dots are

time derivatives.

A detailed description of how the strain components for the
constant strain elements are determined from the displacement
of the surrounding nodes is given by Cundall et al. (1978).

The strain components in a zone are used to determine zone
stresses by the block constitutive relations. The standard
stress-strain formulation for a linear homogeneous isotropic
material is used. The relationship is used in an incremental
form and restricted to plane strain conditions. The equation
is:

$$\Delta \tau_{ij}^{e} = \lambda \Delta \varepsilon_v \delta_{ij} + 2\mu \Delta \varepsilon_{ij} \qquad [17]$$

where λ, μ are the Lame constants,

$\Delta \tau_{ij}^{e}$ are the elastic increments of the stress tensor,

$\Delta \varepsilon_{ij}$ are the incremental strains,

$\Delta \varepsilon_v$ = the increment of volumetric strain ($\Delta \varepsilon_{11} + \Delta \varepsilon_{22}$)

δ_{ij} = Kronecker delta function.

In UDEC, two constitutive relationships for fully deformable
blocks are available. Both use the above stress-strain
relationship, but one incorporates strength limits in the rock
defined by a Mohr-Coulomb envelope. With this formulation,

48

the rock deforms elastically up to the strength limit and plastically past this point. The user defines the envelope by selecting the rock internal friction angle, cohesion, tensile strength, and dilation angle.

The stress increments determined in Eq. [17] are used to update stresses in the elements, and the cycle repeats itself when these element stresses are used in Eq. [14] to determine nodal accelerations.

3.4 Limitations of UDEC

There are a few limitations built into the relationships used in UDEC.

At the moment the constitutive relationship for the intact rock is limited to a linear elastic-plastic analysis of homogeneous isotropic blocks.

In models with large and small blocks undergoing different accelerations, the velocity proportional damping used in UDEC can create spurious forces in the system (Sec. 3.2.2). These artificial forces can affect the solution of the problem in some systems.

With very large problems execution time is still a limiting factor. The size of problem that can be run is not limited by computer memory as much as by computational speed.

Probably the two factors that have the most impact on the effectiveness of UDEC are the accuracy of input parameters, and the users' ability to interpret the results of the analysis.

Using the full capabilities of UDEC to accurately solve a rock mechanics problem often requires complete knowledge of the rock and joint strengths and elastic properties. With most engineering problems, economics preclude the site characterization required to accurately determine these parameters.

UDEC is an interactive program that relies on the user to assess the performance of the model. It is deceptively easy to use, but the well developed interactive graphics and program output can instill a false sense of confidence in an unskilled user. The user must be familiar with rock mechanics, elastic theory, and the capabilities and limitations of the distinct element method to correctly assess the performance of a model. Without a thorough understanding of all of these areas, it is possible to seriously misinterpret the program output.

4.0 Modelling Toppling with UDEC

4.1 Introduction

The literature review in chapter 2 shows that a distinct element program such as UDEC has been used to model block toppling, and concludes that it should be able to model both block and flexural modes of toppling. The unique combination of discontinuum and continuum methods of solution in UDEC should make the program well suited for modelling flexural modes of toppling.

The theoretical basis of UDEC has been thoroughly validated against exact analytical solutions by earlier researchers (Cundall, 1971; Cundall et al., 1978; Cundall, 1983; Cundall, 1985; Cundall and Lemos, 1988). The aim of this chapter is to demonstrate that UDEC can be used to accurately model both block and flexural types of toppling affecting engineered slopes.

Block toppling is modelled by repeating an example of the limit equilibrium method of analysis first reported in Goodman and Bray (1976). This example has also been evaluated using a predecessor of UDEC (Cundall et al., 1978). UDEC is applied to this example and the results compared with the earlier analyses.

Examples of flexural toppling are not as common as block toppling in the literature. The few examples reported either involve undesirable complications, or do not report the rock strength or geometric parameters necessary to accurately formulate the problem in a distinct element model. For these reasons the examples selected and modelled with UDEC in Section 4.3 are not definitive.

These models demonstrate that UDEC is able to reproduce the deformations observed in the example slopes using reasonable estimates of mechanical and geometric parameters. This verification is necessary before proceeding with the analysis of toppling in natural slopes where measurement of mechanical properties of rock material and rock mass, and the ability to observe deformation patterns are necessarily compromised.

4.2 Rigid Block/Flexural Toppling Example

A simple, hypothetical example of block/flexural toppling was reported Goodman and Bray (1976) who also analyzed it using the limit equilibrium method. Cundall et al. (1978), used a predecessor of UDEC to analyze the same model. These studies report the friction angle along the sides and base of the blocks necessary to maintain stability. This section compares

these values with the limiting friction angle for stability determined with UDEC.

The model geometry and scale are shown in Figure 4.1. The simplifications and restrictions that apply in the limit equilibrium method are simulated with this UDEC model. The rigid block model and the original joint model (Sec. 3.3.1) are used. The joints are assumed to have no cohesion or tensile strength.

Gravity is applied to the blocks while the toe block is held fixed. Once the slope is stable under gravity, the toe block is removed. The friction angle on the joints is then changed in an iterative manner to identify the value at which the slope becomes unstable. Stability of the slope is assessed by monitoring mechanical time histories of the velocities and displacements of the blocks.

Figures 4.2a and 4.2b are history plots of mechanical time versus horizontal velocity for the block corner labelled H1 in Figure 4.1. Note that the ordinate scale in Figure 4.2b is different than in Figure 4.2a.

Figure 4.2a is for a trial that did not fail. Characteristics of the history include initial movement due to toe block excavation, and stability shown by velocities returning to

H_1

Toe Block
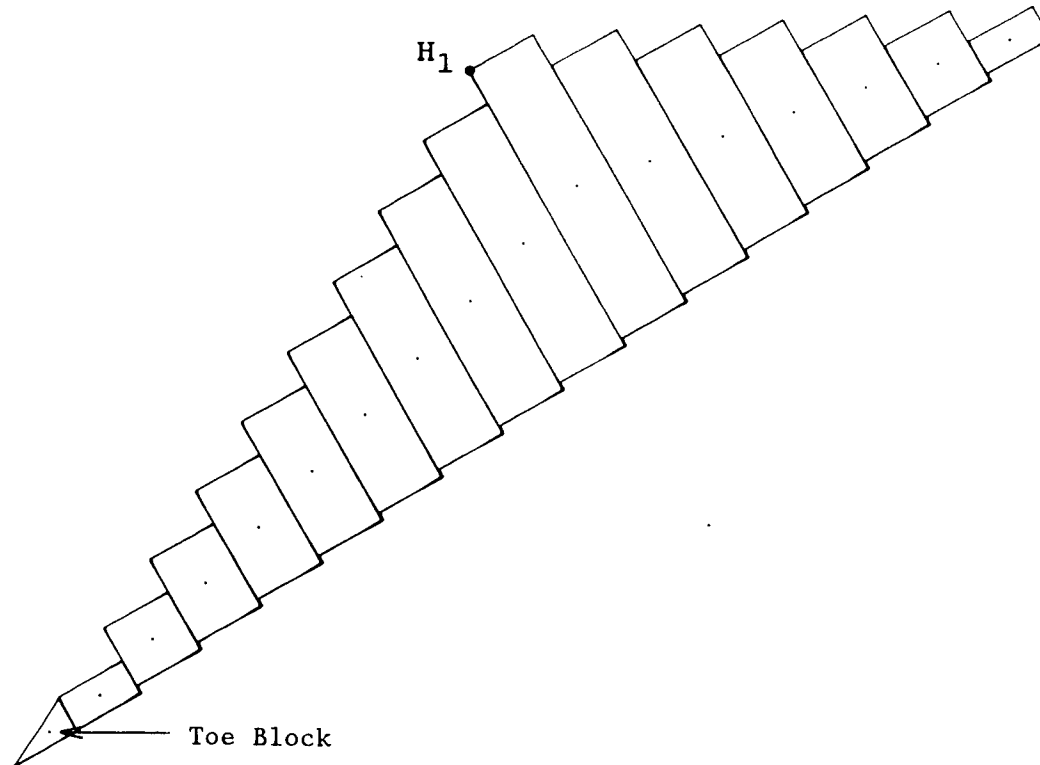
Figure 4.1 Geometry of UDEC model for Block Toppling

UDEC (Version 1.50)

legend

31/05/1989 16: 11
cycle   4000

−5.33E−03 <hist 1> 1.01E−05

(*10**−3)

Toe Excavation   Stability

.0

−1.0

−2.0

−3.0

−4.0

−5.0

.5   .6   .7   .8   .9

Univ. of British Columbia   .
Dept. of Geological Science .
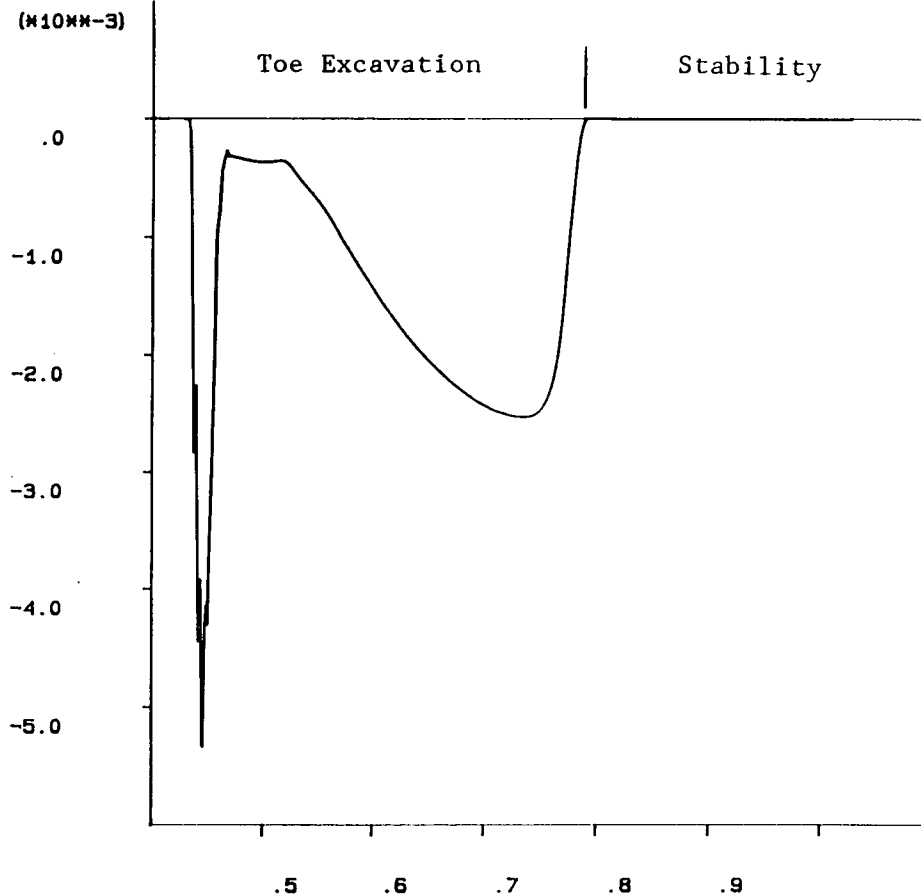
Figure 4.2a   Horizontal Velocity vs. Mechanical Time at H_1,
Stable Slope

(*10** 0)

55

UDEC (Version 1.50)

legend

31/05/1989   16: 50
cycle   17010

-4.76E-01 <hist 1> 3.80E-05

Univ. of British Columbia
Dept. of Geological Science

Toe Excavation

(*10**-1)

Failing Slope

.0

-.5

-1.0

-1.5

-2.0

-2.5

-3.0

-3.5

-4.0

-4.5

1.0   2.0   3.0   4.0   5.0
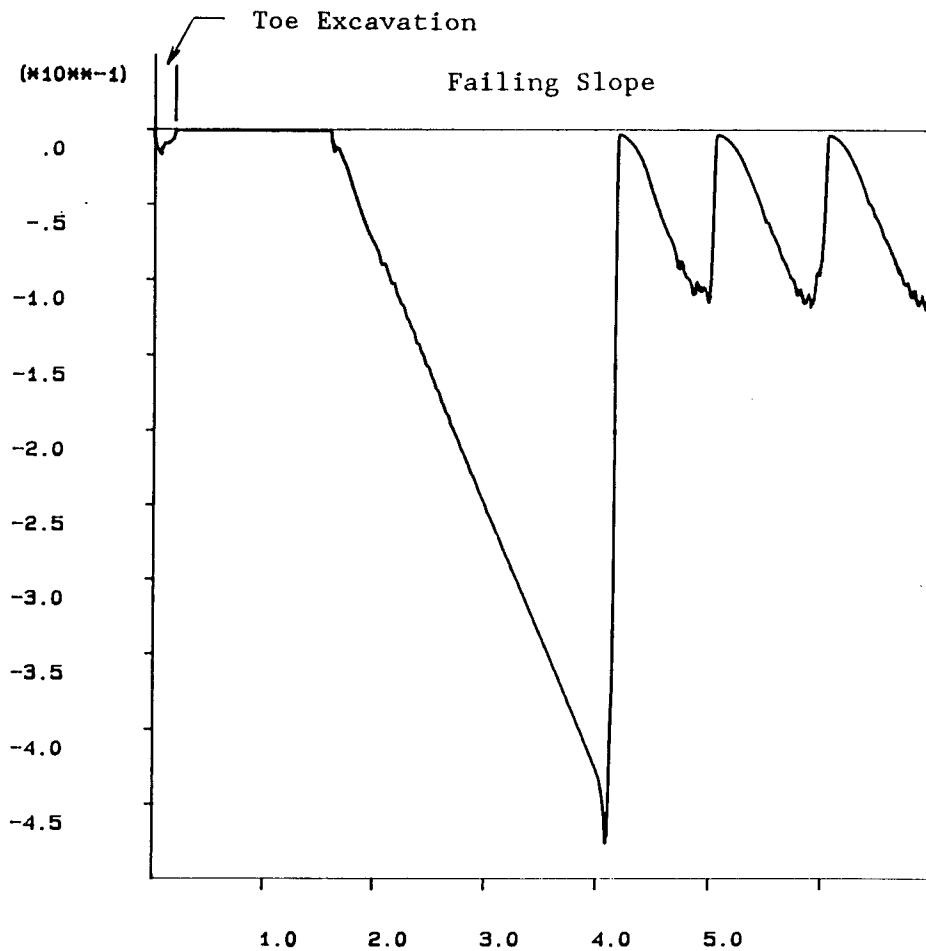
Figure 4.2b   Horizontal Velocity vs. Mechanical Time at H_1,
Failing Slope   (*10** 0)

zero. Initial movement while the problem was loaded under gravity with the toe block is not included.

Figure 4.2b is for a trial that did fail. Note that the velocities do not return to zero, but continue to oscillate indefinitely. This type of oscillation is a typical indication of failure for these trials.

Figure 4.3 demonstrates the deformation of a failing slope at a much later stage.

Table 4.1 lists the limiting range of values for joint friction angle determined with UDEC, by Goodman and Bray (1976) and by Cundall et al. (1978). Note that the limit equilibrium analysis produces one friction value, but due to the nature of the solution procedure, the distinct element method produces a range of values. This range can be narrowed by further iteration. In these trials the range of limiting friction angle reported was iterated to within 0.05 degrees. When rounded to the first decimal place this range can be expressed as a single value (Table 4.1).

The friction angle values determined with UDEC lie within the range determined by Cundall et al. (1978), but do not correspond exactly to the value determined with the limit equilibrium analysis. One reason for this slight difference is the block geometry used in the UDEC analysis.

UDEC (Version 1.50)

legend

7/06/1989   13: 27
cycle 127030
-1.565E+01 < x <   1.381E+02
-1.292E+02 < y <   3.051E+01

block plot
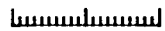
|......|......|
0   2e 1

velocity vectors
        maximum -   9.458E-02

L_I_I_I_I_I
0   5e -1

Univ. of British Columbia
Dept. of Geological Science
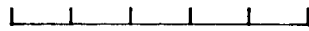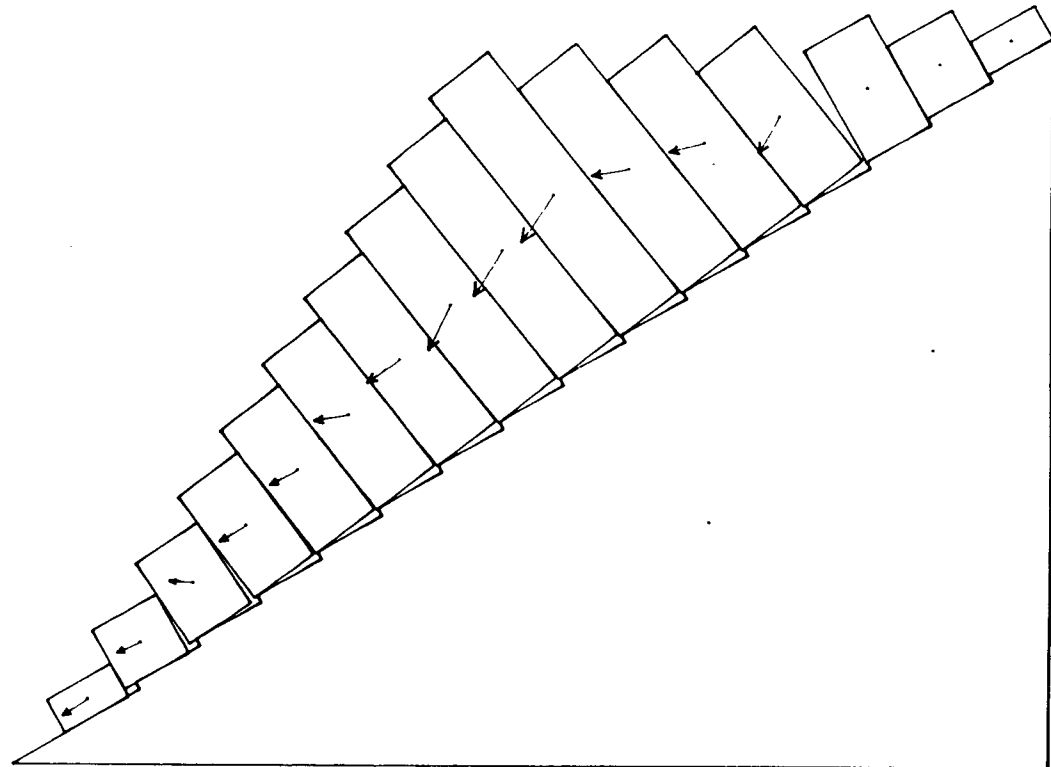
Figure 4.3   Pattern of Deformation for Failing Slope

In UDEC the corners of blocks are rounded to facilitate the analysis of block interaction mechanics. The block corners are rounded with a circle tangent to each side of the corner, and the user selects the radius of the circle to be used.

Rounding the block corners effectively reduces the width of the blocks where they are in contact with the failure plane. This increases the overturning moment, decreasing the stability of the block. As a result, somewhat higher friction angles are required along the sides of the block to maintain stability.

The results from two sets of trials with UDEC using a rounding radius of 0.1m and 0.01m are reported in Table 4.1. A comparison of the limiting friction angle for each rounding length verifies that when a smaller rounding length is used the blocks are stable at a lower friction angle. As a result of the influence of rounded corners, the limiting friction angle for stability determined with UDEC is slightly more conservative than the friction angle determined with the limit equilibrium method.

Table 4.1: Range of Limiting Friction Angle for Block Toppling.	
	Friction angle range (deg.)
Goodman and Bray (1976)	38.2
Cundall et al. (1978)	37.6 to 38.7
UDEC (Round=.1m)	38.4
UDEC (Round=.01m)	38.3
The UDEC input file used to create this model is given in Appendix 1.	

4.3 Flexural Toppling Examples

Available examples of flexural toppling are not well enough defined to be used for a definitive analysis. For this reason, the examples used in this section are only intended as a demonstration of the ability of UDEC to model flexural topples.

The examples were chosen for their relative simplicity. Both are examples of purely flexural toppling using a simple slope profile, one rock type, and columns of a uniform width.

4.3.1 Base Friction Model

This example of flexural toppling is taken from a series of model studies with a base friction table reported in Kuykendall (1975) and Hittinger (1978). The base friction table is comprised of a continuous sand paper belt driven at a

constant velocity. The model rests on this belt and is constrained from moving with the belt by a fixed barrier. When the belt is in motion, friction between the model and the sandpaper simulates body forces in the model.

For the series of studies reported in Kuykendall (1975) and Hittinger (1978) a thin slab of a sand, oil, and flour mixture was spread on the base friction table to form the model. An initially larger, rectangular model was formed and "consolidated" by turning on the machine. The machine was turned off while the slope and discontinuities were cut, and turned back on for the test (Hittinger, 1978).

The model selected for evaluation with UDEC is shown in Figure 4.4. This particular model was selected for study with UDEC because it failed along a well developed failure surface with significant block rotation.

The geometry of this model could not be reproduced at the same scale with UDEC due to problems with decimal precision when designating the block rounding length. The model created with UDEC is 100 times larger than the base friction model, but with the same geometry (Fig. 4.4). The dimensions of the base friction model and the UDEC model are defined in Table 4.2.

UDEC (Version 1.50)

legend

14/06/1989 15: 16
cycle   2000
-3.810E+00 < x <   8.001E+01
-6.015E+01 < y <   2.367E+01

block plot

0   2e   1

Univ. of British Columbia   .
Dept. of Geological Science   .

H

α

w

θ
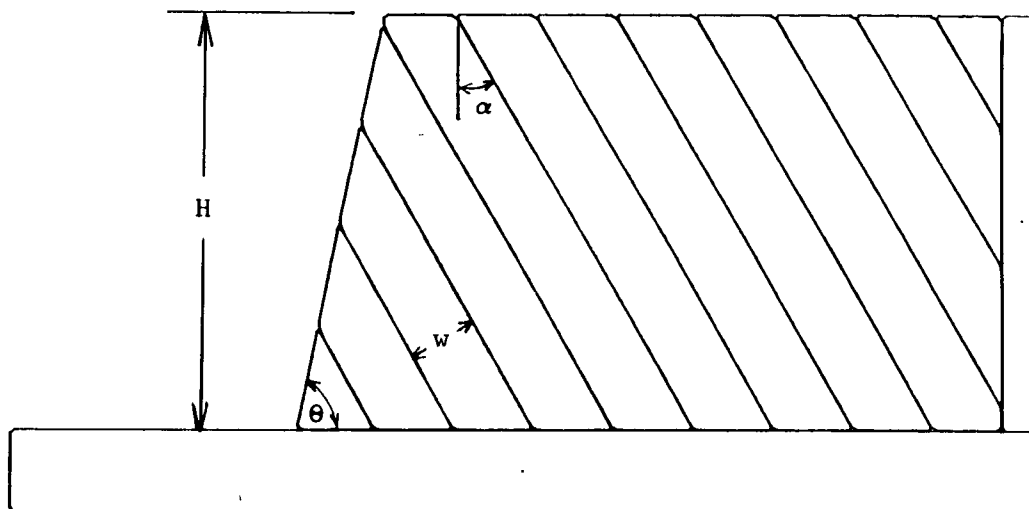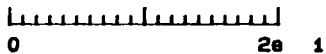
Figure 4.4   Geometry of Base Friction Model and UDEC Model

Table 4.2: Geometry of Base Friction Model and UDEC Model		
Parameter	Base Friction Model	UDEC Model
Slope Height (H)	12 inches	30.5 m
Slope Face Angle (θ)	78 degrees	78 degrees
Joint Inclination (from vertical) (α)	30 degrees	30 degrees
Column Width (w)	2 inches	5.08 m

The modelling procedure is as follows. A rectangular block
bounded by fixed support blocks is created. This center block
is then divided by the 60 degree dipping joint set and by a
crack that is used to simulate the slope face. The angled
blocks that form the slope are divided into finite difference
zones, and material properties are applied to the zoned blocks
and the joints. Initial in situ stresses at $K_0=1.0$ are
applied in the fully deformable blocks, and the system is
allowed to come to equilibrium under gravity. The slope is
then excavated, and gravity is applied until stability or
failure is achieved.

The only physical property of the model material reported in
Hittinger (1978) is the friction angle of a cohesionless
joint, which is 39 degrees. This joint friction angle is used
in the UDEC model. It is assumed that the joints have no
cohesion, tensile strength, or dilation.

All other required parameters in the UDEC model are assumed. The elastic parameters used are in the range of a typical sandstone (Hunt, 1986). Initially the intact rock friction angle, cohesion and tensile strength are set large enough that the excavated slope will be stable. The cohesion and tensile strength are then progressively lowered to determine the limiting values for stability. The internal friction angle is fixed at 39 degrees and dilation equals zero.

The range of values that will produce the approximate failure geometry of the base friction model is reported in Table 4.3. At a cohesion of 0.09 MPa and a tensile strength of 0.10 MPa the slope becomes unstable. At these values the failure surface exits just above the toe block and is slightly steeper than in the base friction model. When cohesion and tensile strength are reduced further to 0.06 and 0.075 MPa respectively, the failure surface moves lower in the slope and better approximates the base friction model failure.

Table 4.3: Values of UDEC Parameters for Base Friction Model.		
Material Number	Parameter	Value
Block Mat 1	Density (kg/m^3)	2600
	Bulk Modulus (MPa)	10500
	Shear Modulus (MPa)	10000
	Cohesion (MPa)	0.09
	Tensile Strength (MPa)	0.10
	Friction Angle (deg.)	39
	Dilation (deg.)	0
Joint Mat 1	Friction Angle (deg.)	39
	Cohesion (MPa)	0
	Tensile Strength (MPa)	0
	Dilation (deg.)	0
	Normal Stiffness (MPa/m)	15000
	Shear Stiffness (MPa/m)	10000

Figures 4.5a and 4.5b compare the base friction model deformation to the deformation produced by UDEC using the physical parameters listed in Table 4.3 (cohesion and tensile strength reduced to 0.06 and 0.075 MPa, respectively). The magnitude and pattern of deformation in the UDEC model are illustrated in Figure 4.5b by contours of horizontal displacement. Rotation is accommodated at the locations where the columns fail forming a failure plane that has nearly the same angle and position as the failure plane in the physical model.

The failure condition in the UDEC model is inferred from time histories of velocities at several locations along the slope face, from the pattern and magnitude of velocities in the model, and from the actual deformation of the model.
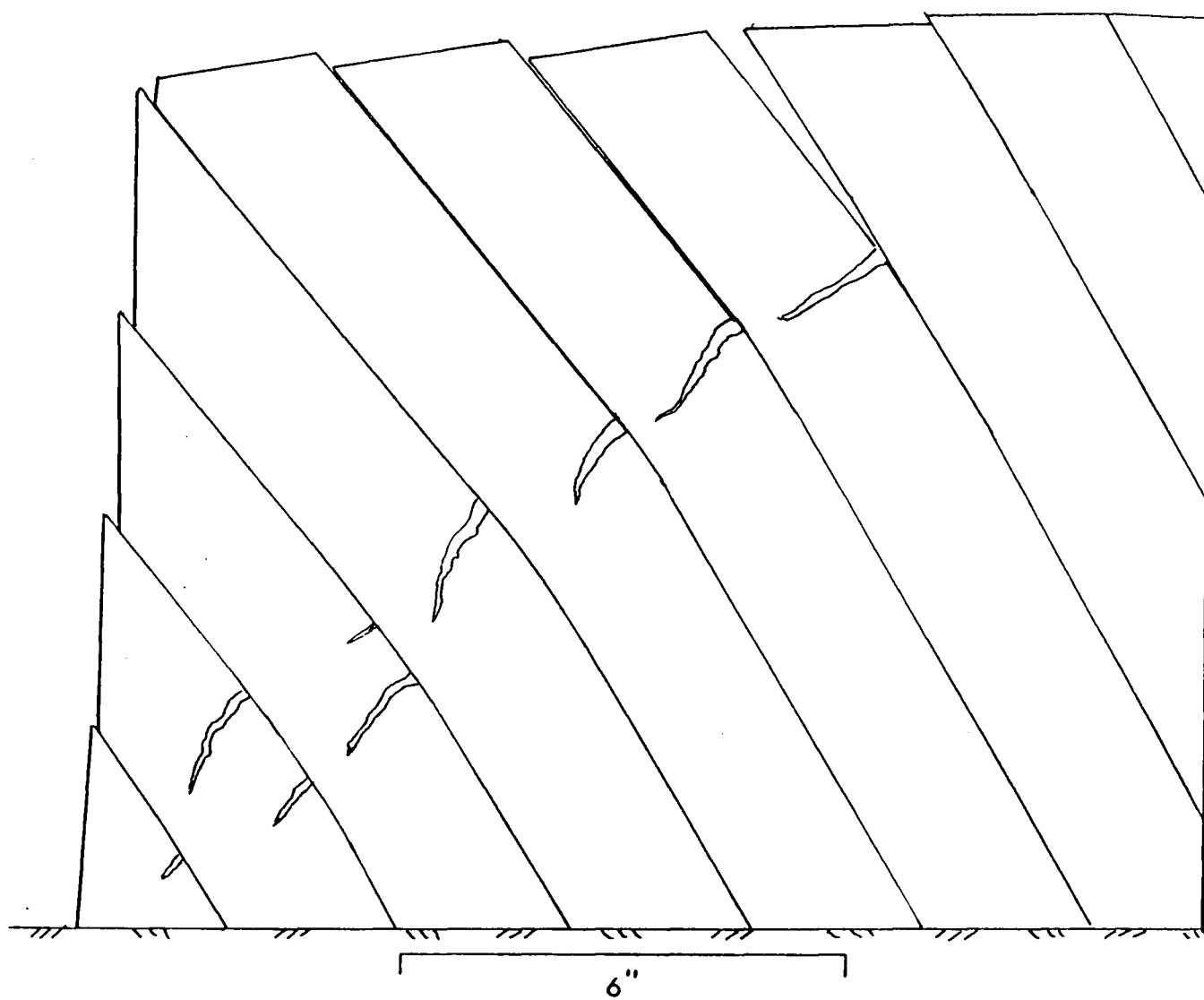
Figure 4.5a   Base Friction Model Deformation
(from Hittinger, 1978; Figure 4-13)
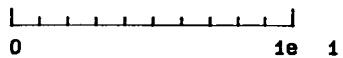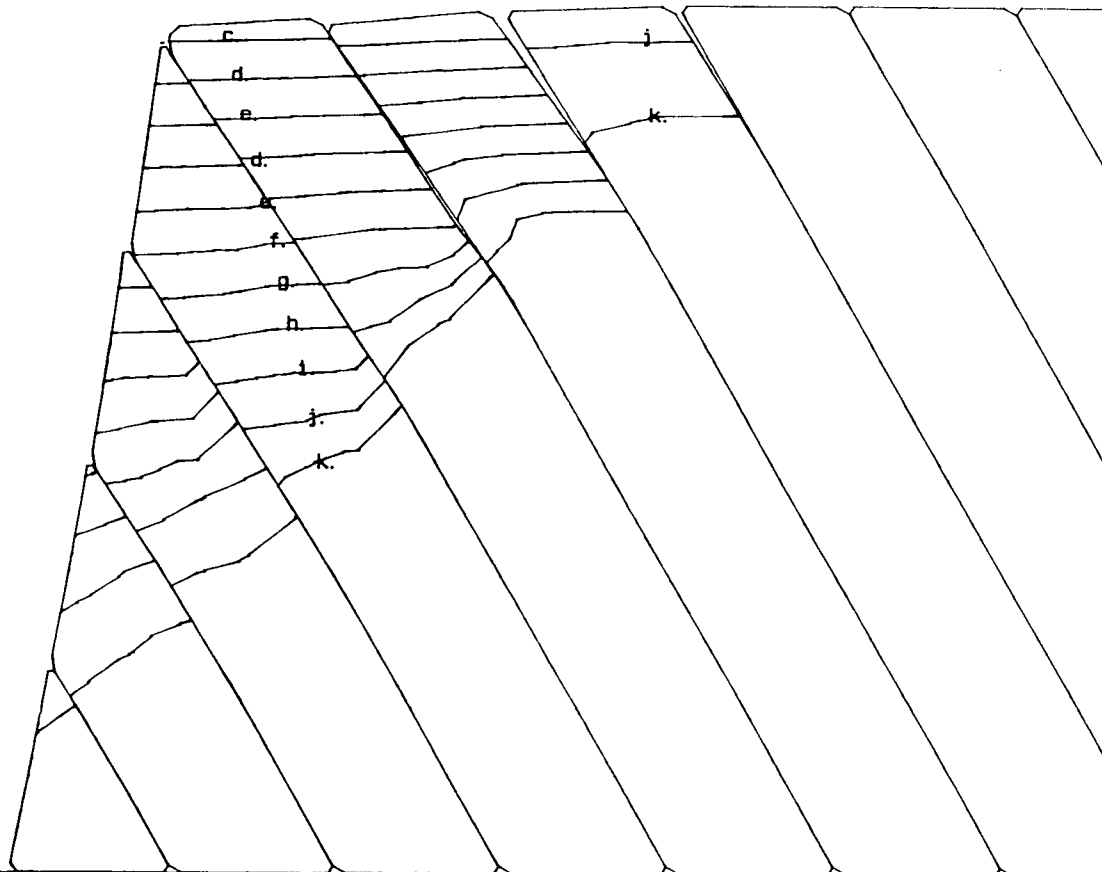
Figure 4.5b   UDEC Simulation of Base Friction Model
Deformation

4.3.2 Brenda Mine

The previous example demonstrates the ability of UDEC to reproduce the geometry of failure seen in a base friction model of flexural toppling. In this section a larger, engineered slope that is known to be susceptible to toppling is modelled using UDEC.

The purpose of this model is to demonstrate that UDEC can simulate flexural toppling in a real slope using reasonable rock and joint strength parameters, and to illustrate that larger scale topples behave differently than smaller topples.

The slope chosen for this study is the east/west trending south wall of the Brenda Mine in Peachland, British Columbia. The original slope experienced significant toppling deformation when mined at 40 degrees to a depth of approximately 200 meters. Water pressure is considered to be a significant factor in the stability of this slope (Piteau and Assoc., 1988). This slope is currently being depressurized, set back and re-benched at an overall slope angle of 45 degrees.

The rock forming the slope is hard, fractured quartz diorite with three major discontinuity sets. Set A discontinuities are continuous gouge filled faults that trend approximately

east/west, dip from 70 to 80 degrees south, and have an estimated spacing of 15 to 27 meters in the vicinity of the south wall. Set B consists of joints and faults which strike approximately north/south and dip moderately to steeply to the northeast. Set C are east/west trending joints that dip from 23 to 50 degrees to the north (Piteau and Assoc., 1988)

Toppling motion of the original wall is accommodated by flexural slip along the gouge filled, east-west trending faults of Set A. It is also believed that these faults act as low permeability barriers to groundwater (Piteau and Assoc., 1988).

The UDEC simulation considers the stability of the new 45 degree slope. It is assumed that the Set A faults divide the slope into inclined columns (Piteau and Assoc., 1988). Although a real slope is used, all of the rock and joint strength parameters in this analysis are initially unknown.

The procedure is similar to that used for the physical model in the previous section. The model is created by dividing a large rectangular domain into inclined blocks, defined by the Set A faults. A dip of 80 degrees and spacing of 27 meters are chosen for these faults. These blocks are further divided for later excavation of the slope face. The blocks are zoned and material properties are applied to the zoned blocks and joints. The boundaries of the domain are fixed and gravity is

applied to stress the domain. Once the stresses in the domain have come to equilibrium, the slope is excavated two benches at a time to the final depth. The stresses in the slope are allowed to come to equilibrium between excavations.

Initially the joint friction angle is set at a value that ensures the slope will be stable at the final excavation level. Once at the final excavation level, the joint friction angle is iterated to determine the limiting value. The UDEC input file for this model is given in Appendix 1.

The zoned block geometry prior to failure is shown in Figure 4.6a. Note that the inclined joint deep in the slope is created to facilitate the finite difference zoning. This joint is fixed and does not influence the model.

To study the influence of groundwater an analysis is done using a bilinear water table that approximates the conditions in the real slope (Fig. 4.6b). This analysis applies pore pressures along the faults based on this water table.

Two modes of toppling failure are identified for this slope. The first mode of failure is a purely flexural topple and the second mode is a more complicated movement herein referred to as a "graben" topple.

UDEC (Version 1.50)

legend

14/06/1989 15: 23
cycle 31000
-4.000E+01 < x <   8.400E+02
-5.900E+02 < y <   2.900E+02

zones plotted in fdef blocks
block plot

0   2e   2

Univ. of British Columbia   .
Dept. of Geological Science .
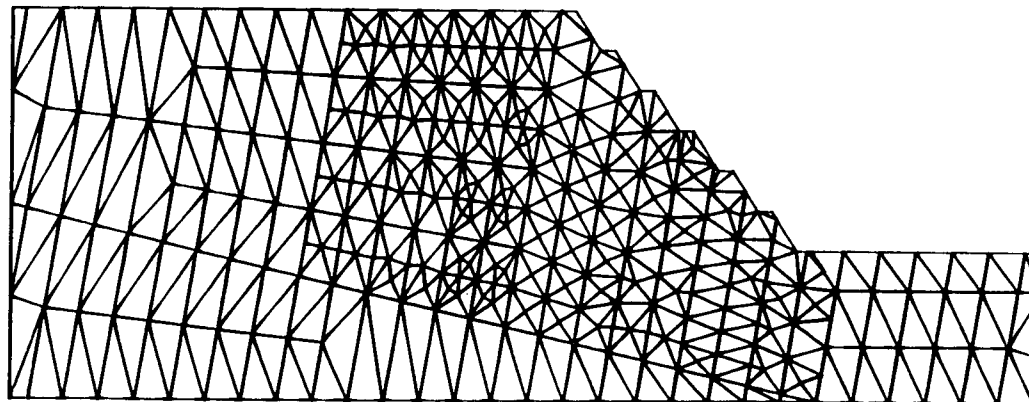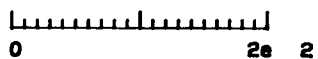
Figure 4.6a   Brenda Mine: Zoned Block Geometry
                             Prior to Failure

UDEC (Version 1.50)

legend

14/08/1989 15:29
cycle 31000   8.400E+02
-4.000E+01 < x <   2.900E+02
-5.900E+02 < y <

block plot

0   2e 2

Univ. of British Columbia
Dept. of Geological Science
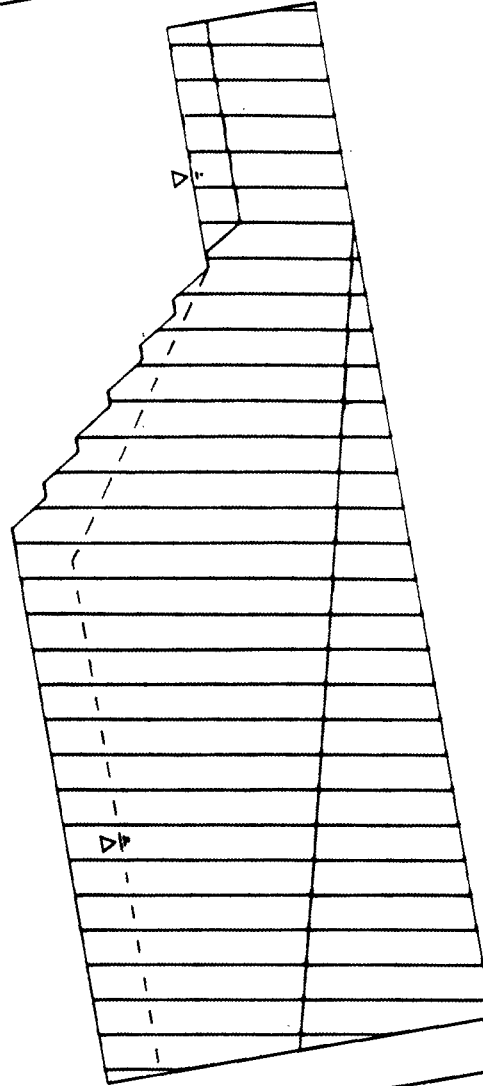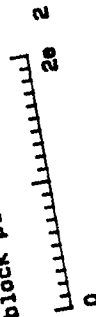
Figure 4.6b Brenda Mine: Block Geometry and Water Table Used
                          in UDEC Model

The limiting joint friction angle and other fixed parameter values for pure flexural toppling are given in Table 4.4. The initial value and limiting range of joint friction are given for both the dry and saturated trials. Note that Table 4.4 reports only the limiting friction angle for the particular rock strengths used. It is expected that there are many combinations of rock and joint parameters that will allow flexural toppling in this model.

Table 4.4: UDEC Parameters for Brenda Mine Model: Pure Flexural Toppling.		
Material Number	Parameter	Value
Block Mat 1	Density (kg/m^3)	2700
	Bulk Modulus (MPa)	33333
	Shear Modulus (MPa)	20000
	Cohesion (MPa)	0.15
	Tensile Strength (MPa)	0.21
	Friction Angle (deg.)	35
	Dilation (deg.)	0
Joint Mat 1 Initial	Friction Angle (deg.)	25
Limiting Range Dry	Friction Angle (deg.)	18.75 to 20.0
Limiting Range Wet	Friction Angle (deg.)	21.25 to 23.75
	Cohesion (MPa)	0
	Tensile Strength (MPa)	0
	Dilation (deg.)	0
	Normal Stiffness (MPa/m)	40000
	Shear Stiffness (MPa/m)	20000

Figures 4.7a and 4.7b illustrate the deformation that results for the dry slope. Figure 4.7a illustrates the deformation of the blocks and velocity of the grid points during failure. Figure 4.7b illustrates the deformation of the blocks giving

UDEC (Version 1.50)

legend

15/06/1989 09:52
cycle 97000
  2.250E+02 < x <   6.750E+02
 -3.750E+02 < y <   7.500E+01

block plot

|_____| 1e 2
0
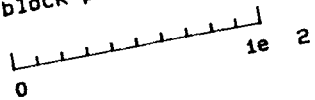
velocity vectors
      maximum =   2.644E+00

|_____| 1e 1
0

Univ. of British Columbia
Dept. of Geological Science
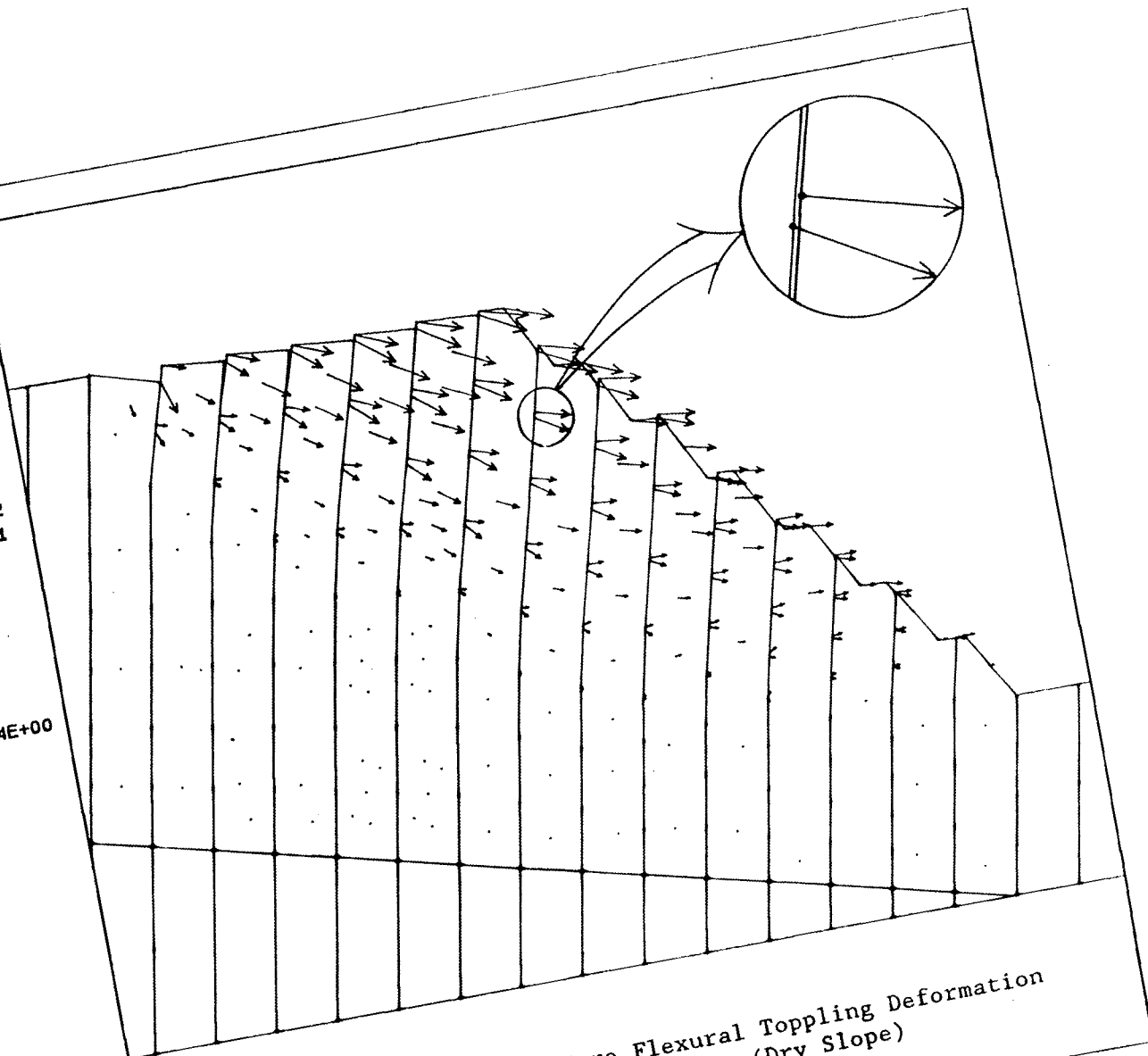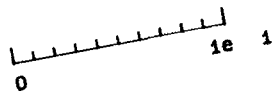
Figure 4.7a Brenda Mine: Pure Flexural Toppling Deformation
with Grid Point Velocities (Dry Slope)

UDEC (version 1.50)

legend

14/06/1989 16:04
cycle 97000   6.750E+02
2.250E+02 < x <   7.500E+01
-3.750E+02 < y <

block plot

0   1e   2
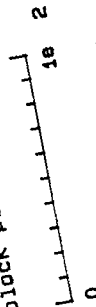
x-disp contours= 1.000E+00
contour interval= 1.000E+00
number of contours/color= 2
min= 0.000E+00 max= 1.000E+01

0.000E+00 1.000E+00
2.000E+00 3.000E+00
4.000E+00 5.000E+00
6.000E+00 7.000E+00
8.000E+00 9.000E+00
1.000E+01 1.000E+01

a: 0.000E+00
k: 1.000E+01

Univ. of British Columbia
Dept. of Geological Science
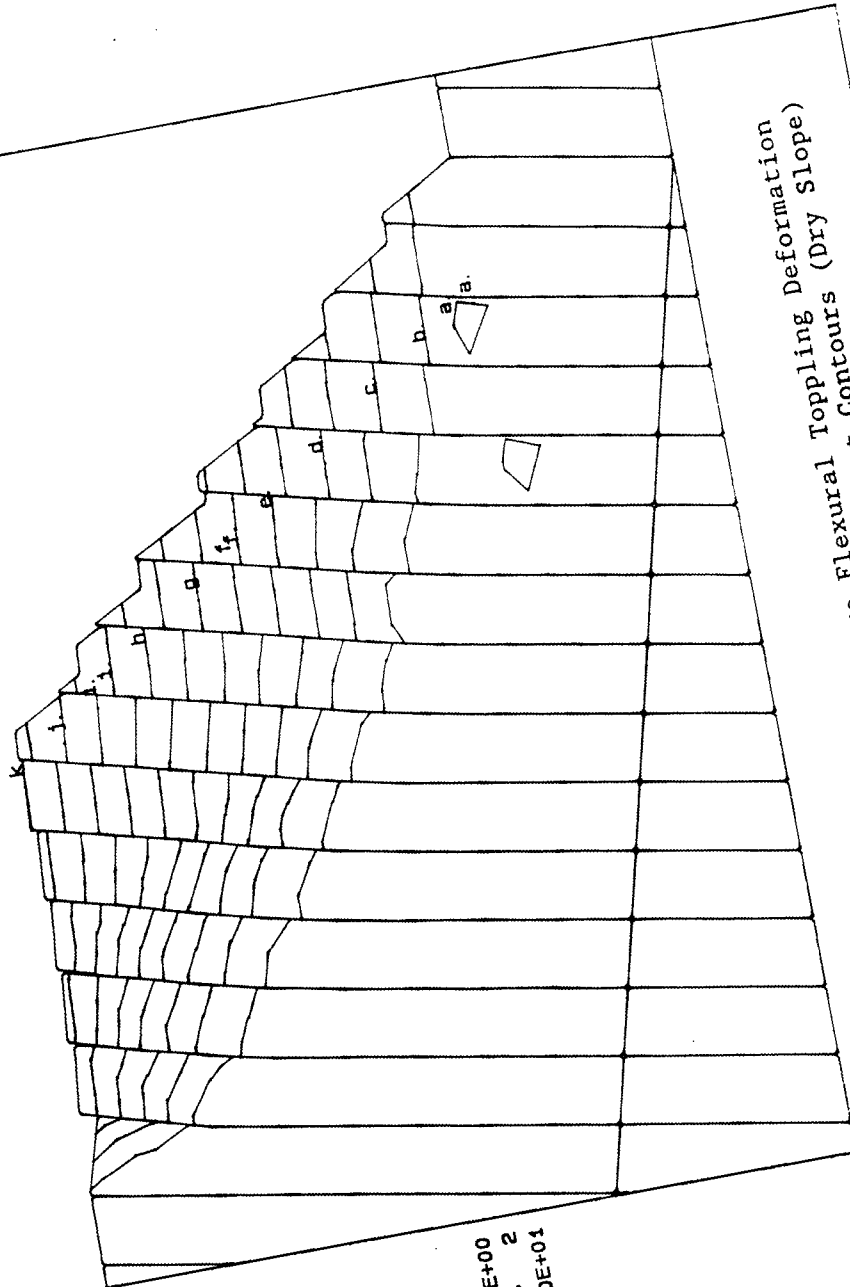
Figure 4.7b Brenda Mine: Pure Flexural Toppling Deformation
with Horizontal Displacement Contours (Dry Slope)

contours of horizontal displacement of the grid points. Note
that shear along the Set A faults is indicated by different
grid point velocity directions on opposite sides of the
faults, and that grid point velocities attenuate with depth as
expected in toppling. The geometry of the failure indicates
that overturning is being accommodated at a defined depth in
each block.

One of the most significant characteristics of this simulation
is the circular nature of the failure surface defined by the
block overturning. This is most clearly illustrated by the
horizontal displacement contours in Figure 4.7b.

The addition of pore pressures as defined in Figure 4.6b does
not affect the shape of the failure surface. The limiting
joint friction angle range with these buoyant forces is given
in Table 4.4.

A second model of failure, referred to as a "graben" topple,
is also identified. This mode of failure is shown in Figures
4.8a and 4.8b and is characterized by a wedge shaped block
dropping down behind the top of the slope while the lower
portion of the slope fails by flexural toppling.

The physical parameters in this example are similar to those
that produced pure flexural toppling (Table 4.5). The
difference is a small increase in the block internal friction

UDEC (Version 1.50)

legend

14/06/1989   16:16
cycle   40500
2.250E+02 < x <   6.750E+02
-3.750E+02 < y <   7.500E+01

block plot

0   1e 2

velocity vectors
           maximum =   1.702E+00

0   5e   0
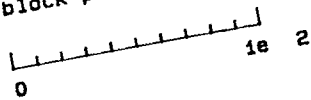
Univ. of British Columbia
Dept. of Geological Science
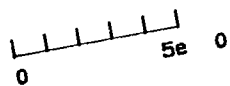
"Graben" block

No shear on Fault

Figure 4.8a   Brenda Mine: "Graben" Toppling Deformation
with Grid Point Velocities (Dry Slope)

77

UDEC (Version 1.50)

legend

14/06/1989   16: 27
cycle   40500
2.250E+02 < x <   6.750E+02
-3.750E+02 < y <   7.500E+01

block plot

0   1e   2
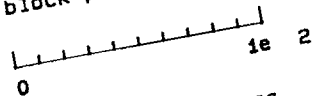
    x-disp   contours
contour interval=   2.500E-01
number of contours/color=   2
min= 2.500E-01 max= 3.000E+00
  2.500E-01   5.000E-01
  7.500E-01   1.000E+00
  1.250E+00   1.500E+00
  1.750E+00   2.000E+00
  2.250E+00   2.500E+00
  2.750E+00   3.000E+00
a: 2.500E-01
k: 2.750E+00

Univ. of British Columbia
Dept. of Geological Science
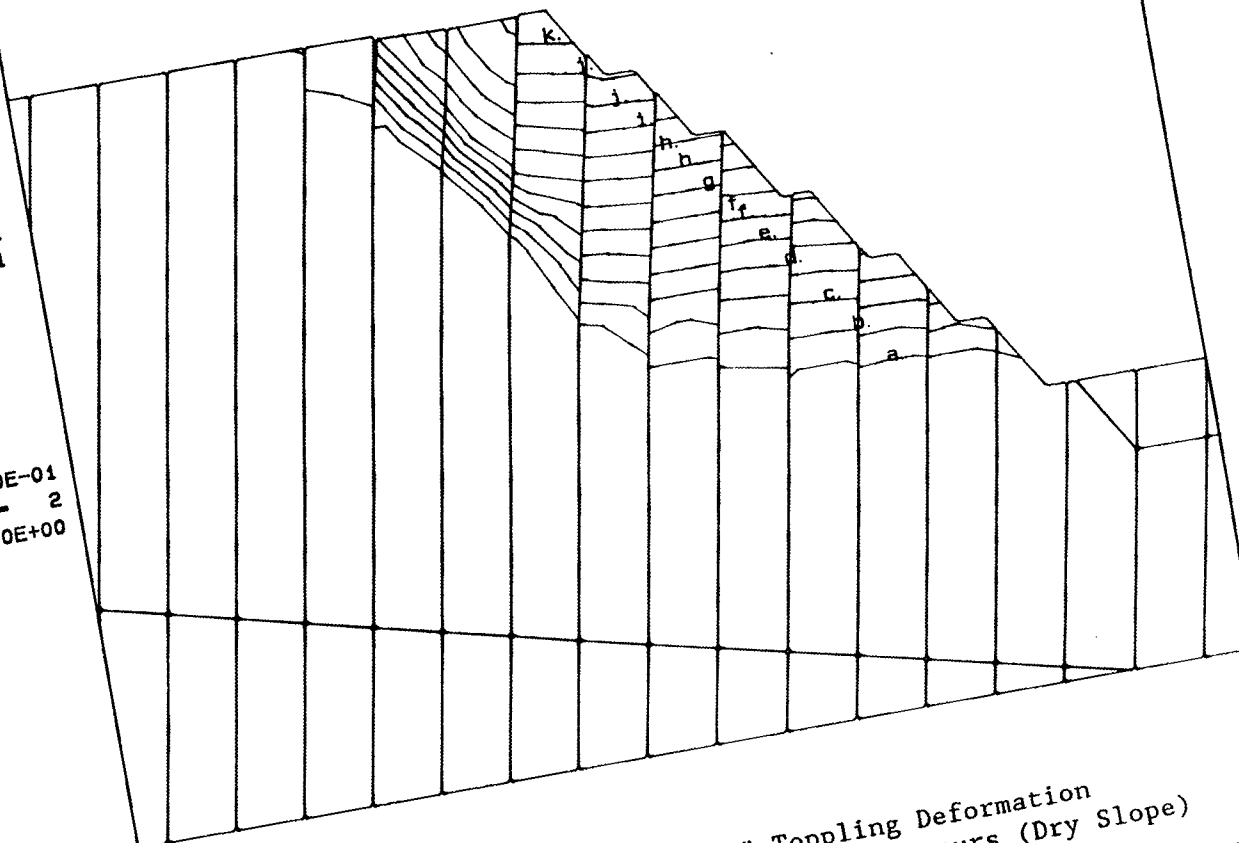
Figure 4.8b   Brenda Mine: "Graben" Toppling Deformation
              with Horizontal Displacement Contours (Dry Slope)

78

angle, and a decrease in cohesion and tensile strength by two thirds. The procedure is the same as for the previous example. The block friction angle, cohesion and tensile strength are fixed, and trials with different joint friction angles are run to determine the limiting value for stability. This analysis is not done with pore pressures.

Table 4.5: UDEC Parameters for Brenda Mine Model: "Graben" Topple		
Material Number	Parameter	Value
Block Mat 1	Density (kg/m^3)	2700
	Bulk Modulus (MPa)	33333
	Shear Modulus (MPa)	20000
	Cohesion (MPa)	0.05
	Tensile Strength (MPa)	0.05
	Friction Angle (deg.)	40
	Dilation (deg.)	0
Joint Mat 1 Initial.....	Friction Angle (deg.)	25
Flexural Toppling Begins (Dry).......	Friction Angle (deg.)	21.25 to 22.5
"Graben" Toppling Begins (Dry).......	Friction Angle (deg.)	18.75 to 20.0
	Cohesion (MPa)	0
	Tensile Strength (MPa)	0
	Dilation (deg.)	0
	Normal Stiffness (MPa/m)	40000
	Shear Stiffness (MPa/m)	20000

When the joint friction angle is lowered to between 21.25 and 22.5 degrees, pure flexural toppling develops. The geometry of this failure is similar to the failure shown in Figure 4.7, but only involves the slope down to the top of the fifth bench. When the friction angle is lowered further to between

18.75 and 20 degrees the "graben" topple shown in Figure 4.8 develops.

Initially this "graben" topple is a pure flexural topple. After some rotation, the blocks that form the "graben" stop failing by overturning and begin to fail by sliding. The sliding surface develops through the point of bending in each column formed by the initial toppling. The velocity vectors in Figure 4.9a show that within the "graben", blocks on either side of a fault are moving in the same direction. This indicates that shear is no longer occurring along the fault. The lower part of the slope continues to fail by flexural toppling.

This mode of failure is very similar to a failure described as a type of moment driven deformation by Nieto (1987). In this example, Nieto describes a mine slope that is failing by moment driven deformation (flexural toppling) and active and passive wedges (Fig. 4.9a). In this example, favorably oriented joint sets allow the upper, active, and lower, passive, wedges to form while the middle portion of the slope fails by block toppling. The passive wedge is driven by the combined loading of the overturning portion of the slope and the active wedge.

The "graben" topple demonstrated by UDEC has many of the same characteristics as this example of moment driven deformation

Active
Wedge

Toppling Section

Base of Toppling
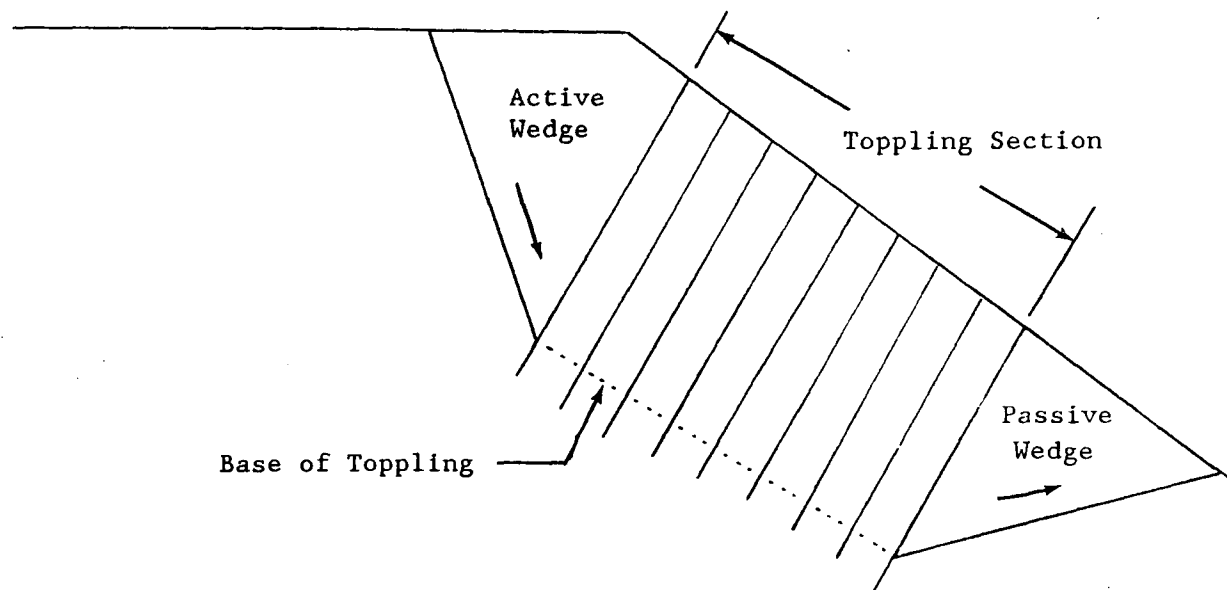
Passive
Wedge

Figure 4.9a   Moment Driven Deformation with Active
and Passive Wedges   (after Nieto, 1987)

described by Nieto (Fig. 4.9b). The "graben" is an active wedge that loads the toppling blocks below, and the geometry of the toppling blocks in the lower part of the slope is similar to the passive wedge in Figure 4.9a.

4.4 Conclusions

The block toppling simulation verifies that UDEC can be used to model block toppling, but because of the influence of block rounding is slightly more conservative.

Although the flexural toppling examples reported in this section are intended as demonstrations, several conclusions can be drawn from them.

In both examples, flexural toppling failure occurs using reasonable estimates of rock and joint properties. This confirms that UDEC can simulate flexural types of toppling failure.

In the simulation of the base friction model, the rock strength parameters are adjusted to find the values that produce the base friction model failure geometry. This simulation demonstrates that UDEC can be used to back analyze a flexural toppling failure to obtain strength values at failure.

UDEC (Version 1.50)

legend

14/06/1989 16:16
cycle 40500   6.750E+02
2.250E+02 < x <   7.500E+01
-3.750E+02 < y <

block plot

$\vdash$ 0   5e 1e 2

velocity vectors
maximum =   1.702E+00

$\vdash$ 0   5e 0

"Active" Wedge

Toppling Region
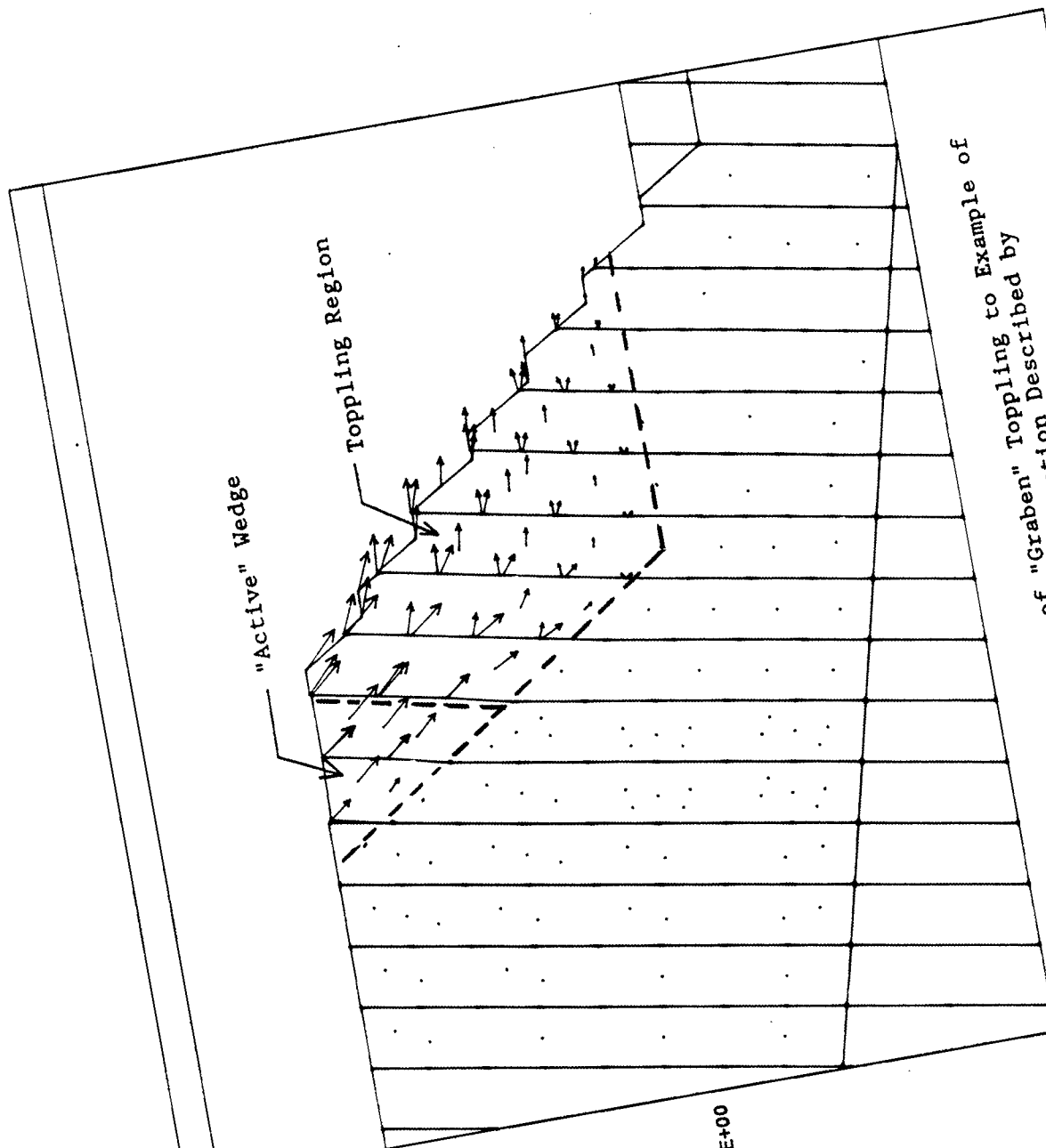
Figure 4.9b   Similarity of "Graben" Toppling to Example of
Moment Driven Deformation Described by
Nieto, 1987 (Figure 4.9a)

Univ. of British Columbia
Dept. of Geological Science

83

Flexural toppling research using physical or finite element models has only produced planar failure surfaces. The simulations in this section indicate that the failure surface generated in flexural toppling may be planar or curvilinear. In the UDEC simulation of the base friction model with a slope height of approximately 30 meters, the failure surface is planar, but in the 180 meter high Brenda Mine slope the failure surface is curvilinear. It is suspected that the transition from a planar to a curvilinear failure surface is in part controlled by the size of the slope, the density of back dipping discontinuities, and is also dependent on the values of block cohesion and tensile strength.

The geometry and location of the failure surface in larger slopes is dependent on the combination of block cohesion, block tensile strength, and the joint friction angle. When cohesion and tensile strength are set at .15 MPa in the Brenda Mine slope, only pure flexural toppling with a curvilinear failure surface occurs for the range of joint friction angle tested (25 to 15 degrees). When cohesion and tensile strength are set at .05 MPa, both curvilinear, flexural toppling and "graben" toppling can occur depending on the joint friction angle.

The UDEC "graben" toppling simulation demonstrates that flexural toppling can result in deformation similar to the

mode of moment driven deformation described by Nieto (1987).
In addition, the UDEC simulation suggests that the
characteristic active and passive wedges formed in this mode
of failure do not necessarily require favorably oriented joint
sets to occur.

Pore pressure significantly affects the stability of slopes
susceptible to flexural toppling. Including pore pressures in
the Brenda Mine model (Fig. 4.6b) requires an increase in the
joint friction angle of 13 to 26 percent (2.5 to 5 degrees) to
maintain stability (Table 4.4).

4.4.1 Recommendations for Slope Design with UDEC

It is possible to use UDEC to design slopes in a rock mass
susceptible to toppling. However, the accuracy of the design
is dependent on the accuracy of the rock mass strength
parameters used in the model. The best way to determine these
parameters is by back analysis of a large number of known
toppling failures in similar rock types, which has not yet
been done.

Even without accurate knowledge of rock mass strength
parameters, it is still possible to apply UDEC to examine the
mode of toppling possible in a slope and to develop a
conservative design. This can be done by fixing the rock and
joint strength parameters, the water table, and the joint

inclination and spacing at conservative values, and varying the slope face angle and height. Such an analysis allows the designer to determine the maximum slope height and face angle for large slopes susceptible to toppling. In addition, the analysis yields the potential failure geometry, and can be used to assess the effect of different dewatering schemes and other stabilization methods.

5.0 Site Characterization

5.1 Introduction

The Beaver River Valley is situated in Glacier National Park between Golden and Revelstoke, British Columbia (Fig. 5.1), and forms the eastern part of a narrow transportation corridor which traverses the rugged Purcell and Selkirk Mountains. The route was first discovered and utilized by the Canadian Pacific Railway (now CP Rail) in the late 19th century. The Trans Canada Highway was constructed along the corridor in the early 1960's and a second CP Rail line has recently been completed.

Both CP Rail alignments enter the northern end of the Beaver Valley along the valley bottom and climb the western slopes. The highway also enters from the north, but high on the eastern slope. It then descends to the valley floor, crosses the Beaver River, and climbs again along the western slope (Fig. 5.1).

Although the economic importance of the Beaver River Valley as the eastern approach to the Rogers Pass route has long been recognized, large, deep-seated mass movement hazards along the valley slopes have only recently been documented (Pritchard et al., 1988).

LEGEND

LANDSLIDES

Scarp – defined

Scarp – estimated

Scarp – suspected

OTHER

Glacier National Park Boundary (GNP)

CP Rail

Trans Canada Hwy.

Contour interval 400m

Topography from:
Energy Mines and Resources
Canada Map, MCR 219

117° 30'

100km

51° 20' GNP

ALBERTA

Lake Louise

Revelstoke

Banff

CALGARY

B.C.

CANADA

U.S.A.

1000m

N

Cupola Ck.

(Ck. A)

Heather Mt.
2405m

(Ck. B)

Heather Hill Landslide

(Ck. C)

Study area

Griffith Landslide

Purcell Mountains

Unnamed Landslides

Cedar Ck.

Prairie Hills

Sturdee Ck.

(Raspberry Ck.)

Cut Ck.

(Suprise Ck.)

CP old

CP new

Stoney Ck.

Hermit Range

Beaver R.

Selkirk Mountains

Tupper Ck.

Mt. Tupper
2728m

Connaught Tunnel

Mt. Macdonald Tunnel

Figure 5.1 Topographic map of the Beaver River Valley Showing Locations of Deep Seated Landslides (from Pritchard et.al., 1988)

Field work during the summer of 1988 concentrated on an area

of the east slope of the Beaver River Valley including the

Heather Hill landslide and adjacent slopes to the north (Fig.

5.1). This site was selected for detailed study because it

contains a well developed and well defined, deep-seated

landslide, and the opportunity to study slopes immediately

adjacent which show lesser degrees of deformation and no

apparent deep-seated instability.

The regional geology and slope deformation in the Beaver

Valley, and the geology of the Heather Hill study area are

discussed in this chapter.

5.2 Regional Geology

5.2.1 Bedrock Geology

The Beaver Valley is situated in the Omineca Tectonic Belt of

British Columbia. The northwest trending valley is flanked on

the east by the Prairie Hills of the Purcell Mountains and on

the west by the Hermit and Sir Donald Ranges of the Selkirk

Mountains.

The regional geology is shown in Figure 5.2, and Figure 5.3.

The valley is formed in rocks of two groups: the Hadrynian
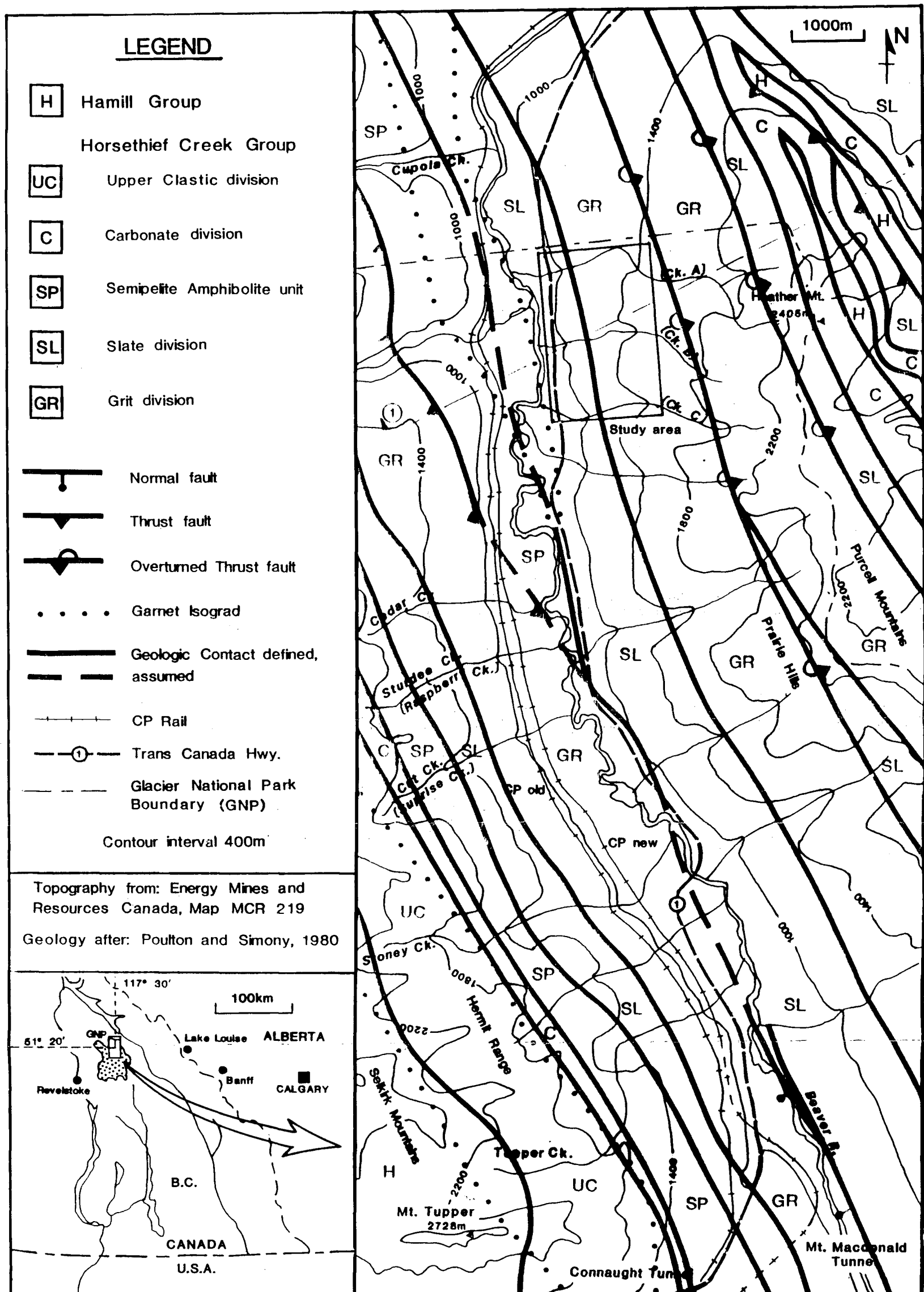
Figure 5.2 Regional Geology map of the Beaver River Valley
(after Poulton and Simony, 1980)

Cross-Section 1

No V.E.

Elevation (m)

3000

2000

1000

0

Beaver Valley

Heather Mt.

Garnet Isograd

GR

GR

GR

GR

SP

SL

SL

C

H

C

SL

H

C

SL

Dogtooth Fault
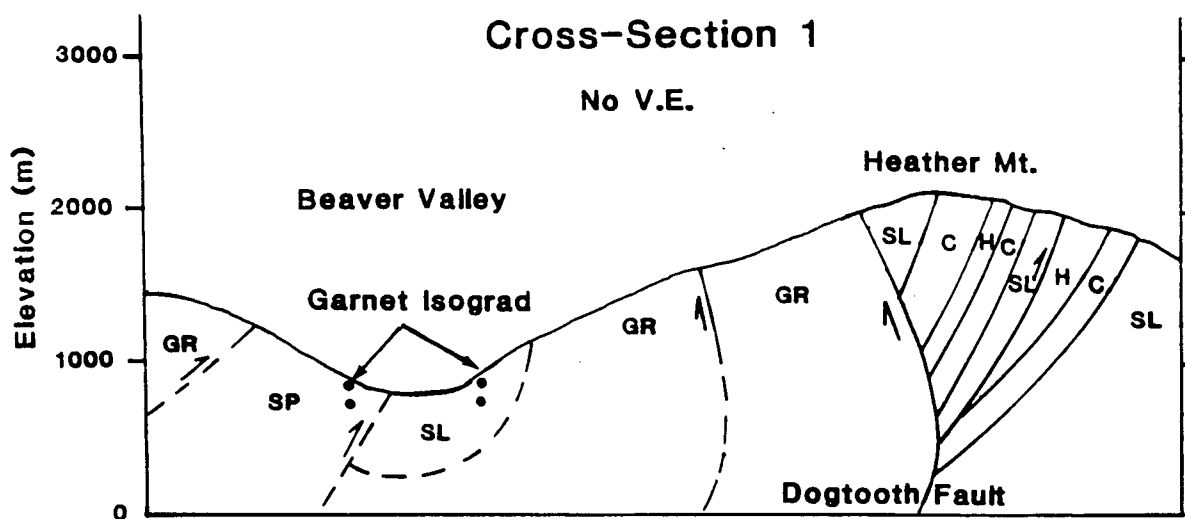
Figure 5.3 Geological Cross Section Number 1, Beaver River
Valley. See Legend Fig. 5.2. (after Simony and
Wind, 1970; Poulton and Simony 1980)

(Late Precambrian) Horsethief Creek Group, and the Lower

Cambrian Hamill Group (Wheeler, 1963; Simony and Wind, 1970).

The Horsethief Creek Group includes a lower grit division

successively overlain by a slate division, a carbonate

division, and an upper clastic division. The slate division

is further divided into a semipelite amphibolite unit in the

Beaver Valley. The Hamill Group consists of Upper, Middle and

Lower Members of which only the dominantly quartzite Lower

Member is present in the Beaver Valley (Simony and Wind,

1970).

The east slope of the Beaver Valley consists of a series of

imbricate thrust sheets, with the slopes formed primarily in

the overturned grit and slate divisions of the Horsethief

Creek Group. On the west valley slopes, only one west-dipping

thrust fault interrupts the upright stratigraphic sequence of

grit through upper clastic divisions, overlain by Lower Hamill

quartzites (Poulton and Simony, 1980).

In the Beaver Valley, the rocks are complexly folded

exhibiting planar bedding (S0) on the scale of outcrop.

Penetrative foliation (S1) that is axial planar to the first

phase of folding is virtually obliterated on both sides of the

Beaver River by intense crenulation cleavage (S2) (Rickard,

1961; Simony and Wind, 1970). The S0 bedding trends

dominantly northwestward throughout the area, dipping steeply

east on the east side of the valley and steeply west on the
opposite side (Simony and Wind, 1970).

5.2.2 Geomorphic Development of Beaver Valley

The geomorphic development of the Beaver Valley is dominated
by several periods of glacial advance and retreat. These
glacial periods have been tentatively grouped into three
events (VanBuskirk, 1987).

The first glacial event reached an elevation of at least 2950
meters (Thurber Consultants Ltd., 1983a) and created the broad
U-shaped Beaver Valley with a slope angle of between 20 and 25
degrees. The second glacial event reached an elevation of
approximately 1100 meters and oversteepened the lower valley
slopes. This oversteepening is evidenced by truncated spurs
and steeper slope angles of 30 to 45 degrees. These glacial
events were probably complete by approximately 9000 years
B.P., but a minor readvance occurred prior to approximately
7500 years B.P. (Thurber Consultants Ltd., 1983a). During
this third event ice readvanced down the Beaver Valley to
approximately the location of the east portal of the Mt.
Macdonald tunnel. Drainage of the Beaver Valley was
periodically blocked during this time by a concurrent
readvance down the Cupola Creek Valley[1]. This blockage formed
a lake to an approximate elevation of 990 meters in the valley

---

[1]Cupola Creek Valley is just off the north edge of Figure 5.1,
on the west side of the Beaver Valley

causing deltas to develop at the mouths of major tributary streams (Thurber Consultants Ltd., 1983a).

Since the third glacial event, the sediment supply resulting from the reworking of these deltas into modern alluvial fans, and the addition of sediment to the alluvial fans resulting from debris torrents has created a series of local base levels along the Beaver River, causing the floodplain to aggrade.

5.3 Characteristics of Beaver Valley Slope Movements

The large landslides shown in Figure 5.1 are located on the lower valley slopes in the grit and slate divisions of the Horsethief Creek Group. The lower grit division consists mainly of coarse and fine-grained gritty, feldspathic and micaceous sandstone with slate interbeds (Simony and Wind, 1970); planar bedding and graded beds on the scale of outcrop are common (Poulton and Simony, 1980). The slate division consists of pelitic rocks, with minor coarser clastic and carbonate interbeds transitional with adjacent units.

The exact age of the failures is unknown. It is believed that the initial Griffith slide (Fig. 5.1) predates the last glaciation (Thurber Consultants Ltd., 1979), and that all show evidence of post glacial movement.

The elevation of the floor of the valley at the end of the final period of glaciation is unknown. However, drill investigations of the valley floor for the new CP Rail line went to an elevation of 755 meters and did not encounter bedrock (Thurber Consultants Ltd., 1983b).

Natural slope angles in the valley vary from 20 to 45 degrees. The height of the landslides, measured from the level of the floodplain (approximate elevation of 825 meters) to the top of the headscarps, varies from 450 to 1250 meters. The volume of the slope movements varies from approximately 5 to 30 $x10^6m^3$. It is possible that these failures extend below the current floodplain level. For this reason, the estimated maximum relief and volume of these failures may be conservative.

Progressive deformations have been measured at the Griffith slide (Fig. 5.1) where continuous movement of the debris has caused displacement of the current CP Rail line throughout its life, necessitating detailed geotechnical studies and mitigative works. Monitoring of slope indicators shows deformations of up to approximately 30 mm over a one month monitoring period (Thurber Consultants Ltd., 1979). Whether or not other deep seated mass movements are moving, and their rate of movement are not yet known.

5.4 Previous Landslide Studies in the Beaver Valley

Previous unpublished work describes and quantifies the mode of failure of the slopes. In a report to CP Rail, EBA Engineering Consultants Ltd. (1976) outlined the location of many slope movements in the valley. Based on the geometry of the bedrock slide scarps and rubble, EBA suggested that the modes of the failure are circular. In a later report for Environment Canada Parks, EBA Engineering Consultants Ltd. (1978) evaluated the stability of the Heather Hill landslide as a deep-seated rotational failure. Piteau and Associates Ltd. (1982), in work for CP Rail on the west valley slope near the entrance to Rogers Pass, observed several localities where preexisting toppling failures (Goodman and Bray, 1976) are exposed by railway or creek cuts. Rapp (1987), using the nomograms developed by Brown (1982), confirmed that large scale toppling failure is possible in the valley slopes; furthermore, Rapp postulated that slides such as the Griffith and Unnamed slide represent the final stages of earlier massive toppling failures.

5.5 Field Program

5.5.1 Introduction

Field investigation of the study area shown in Figure 5.1 was
undertaken during the summer of 1988. This work involved
structural mapping along the creek gullies and the highway
back slope. Temporary benchmarks were established along the
highway and at the base of each creek using an AGA model 14A
Electronic Distance Meter (EDM) and a Wild T2 theodolite.
Traverses were started from these benchmarks and carried up
the creeks and around the slide headscarp using a hip chain
and hand held clinometer for control. These traverses were
later transferred to a 1 to 2500 scale 5 meter contour
interval topographic map of the study area (Maps 1A and 1B,
Map Pocket).

5.5.2 Local Geology

The geology of the study area consists of the lower grit and
slate divisions of the Horsethief Creek Group (Fig. 5.2).
Pelitic rocks of the slate division occupy the base of the
slope, and traverses upslope perpendicular to the strike of
the S0 bedding encounter a gradational change to grit division
rocks. S0 bedding thickness varies from millimeters to tens
of meters, but the most common thickness is in the range of
0.1m to 3m.

Analysis of the field data indicates several dominant
structural features: S0 planar bedding foliation, S2
crenulation cleavage, and at least two joint sets (J1, J2).
S1 axial planar foliation exists, and appears to be
subparallel to the S0 foliation, however the orientation of S1
foliation is difficult to quantify due to the effect of S2
crenulation cleavage. The J1 joint set trends northwesterly,
sub-parallel to the S0 foliation, but dips downslope
perpendicular to it. The J2 joint set is oriented
perpendicular to both the S0 foliation and the J1 set. These
joint sets occur most commonly in the more competent gritty
beds, and combine with the S0 foliation to break the rock mass
into large blocky fragments. Slaty beds contain very few of
the J1 or J2 joints but display intense crenulation cleavage.

Structural data were obtained from traverses up the three
creek gullies, around the base of the Heather Hill landslide
headscarp, and along the highway cut.

Equal area stereonet plots of the structure in each creek are
given in Appendix 2. Three plots are shown for each traverse;
the poles to the S0 and S2 discontinuities, a contour plot of
the S0 and S2 poles, and a plot of the poles to all joints.
In addition, a plot of poles to all the joints measured in the
creeks and a contour plot of these poles are given.

The average orientation for the S0 and S2 discontinuity sets from each traverse and the estimated average joint orientations for all the creeks in the study area are summarized in Table 5.1 and plotted in Figure 5.4. The creek traverses are used to categorize the structure along the slope. The average structural orientations from the traverse around the base of the Heather Hill landslide headscarp are also shown in Figure 5.4 to illustrate the toppling of the rock mass.

Table 5.1: Structural Data Summary in Study Area				
Traverse	S0 Bedding	S2 Cleavage	J1 Joint	J2 Joint
Creek A	333\66	005\62	N\A[2]	N\A[2]
Creek B	338\47	023\56	N\A[2]	N\A[2]
Creek C	338\46	024\51	N\A[2]	N\A[2]
All Creek Data	N\A[2]	N\A[2]	140\33 to 204\54	247\90
HeadScarp	346\21	043\42	163\73 to 212\79	N\A[2]

The structural relationship between the S0 bedding and the S2 cleavage is consistent in the study area, but the S0 and S2

---

[2]For the creek traverses, N\A indicates that the data cannot be correlated as one data set. For the joint data, N\A indicates that the data did not correlate well enough to make an estimate of average orientation for the creek or headscarp traverses.
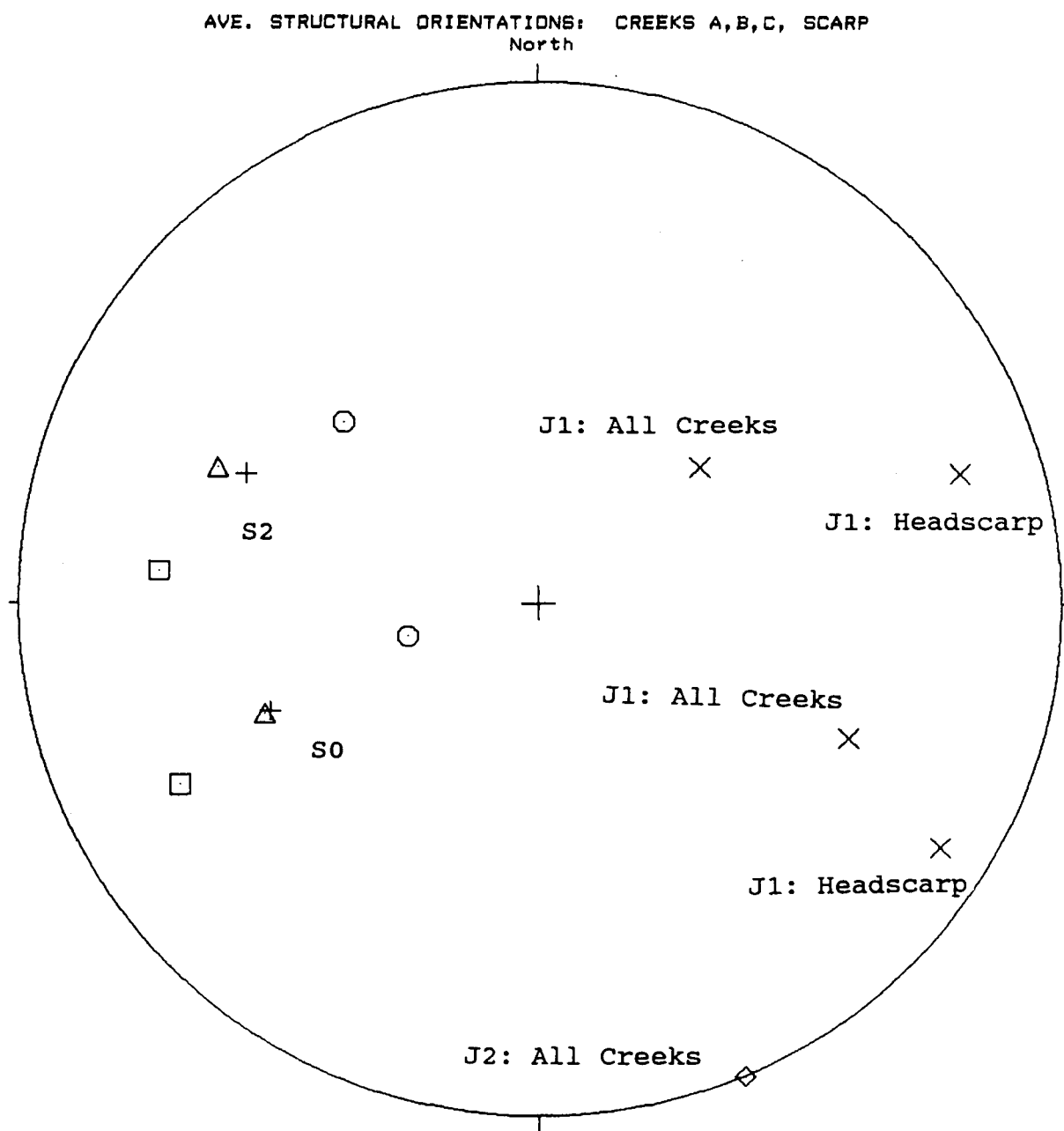
AVE. STRUCTURAL ORIENTATIONS: CREEKS A,B,C, SCARP

Figure 5.4 Structural Geology Summary for Study Area

orientations vary slightly as indicated in Figure 5.4. The
strikes of these structures do not vary significantly, but the
dips of both S0 and S2 are greater in Creek A than in Creeks B
and C.

The joint data from each creek is much more scattered than the
S0 or S2 data, and no statistical averages of the joint
orientations could be determined. However, the contour plot
of the data in Appendix 2 illustrates the dominant J1 and J2
joint sets and is used to estimate the average orientation of
these joint sets in the study area (Table 5.1).

5.5.3 Evidence of Deformation

The decrease in the dip of S0 and S2 from north to south in
the study area is indicated by comparing the dip shown from
Creek A with Creek B, and Creek B with Creek C in Figure 5.4.
This can be explained as a natural structural variation, or as
an increase in the degree of toppling in the southern and
middle part of the study area. There is evidence that
suggests the decrease is at least partially a result of
toppling. Toppling of S0 bedding is visible in the high, near
vertical cuts (60m) of the creek valleys. In these creek cuts
toppling and dilation are seen to increase updip.
Investigation of the slope just to the north of Creek B
upslope of a cut backslope along Highway 1 revealed obsequent
scarps with torn surficial soil and roots and relief of up to

1.5 meters (Map 1A). Obsequent scarps are generally viewed as an indication of toppling (Goodman and Bray, 1976).

The traverse around the base of the headscarp supports the visible evidence of toppling cited above. The average structural orientations from this traverse indicate the toppled nature of the rock mass in the headscarp relative to that of the creek traverses. The data from this traverse are believed to be from disturbed zones of rock and not representative of the intact structure. It is believed that the rock above the headscarp, which has an average bedding foliation dip approximately 5 degrees lower than in Creek C, is more representative of the extent of toppling prior to dep-seated failure. Structural data obtained from above the headscarp were too few to obtain a more accurate estimate of structural orientations.

It is possible that the toppling described above extends below the elevation of Creeks B and C. Figure 5.5 is a topographic cross section of the slope just north of the Heather Hill landslide. The cross section also includes the gradient profile of Creek B and the projected position of the back scarp of the Heather Hill slide. This figure illustrates that the creeks are not deeply incised into the slope relative to the Heather Hill landslide. For this reason, structural data from Creeks B and C may be from zones of disturbed rock and not representative of the intact structure.

TOPOGRAPHIC PROFILE SECTION A-A', AND GRADIENT OF CREEK B
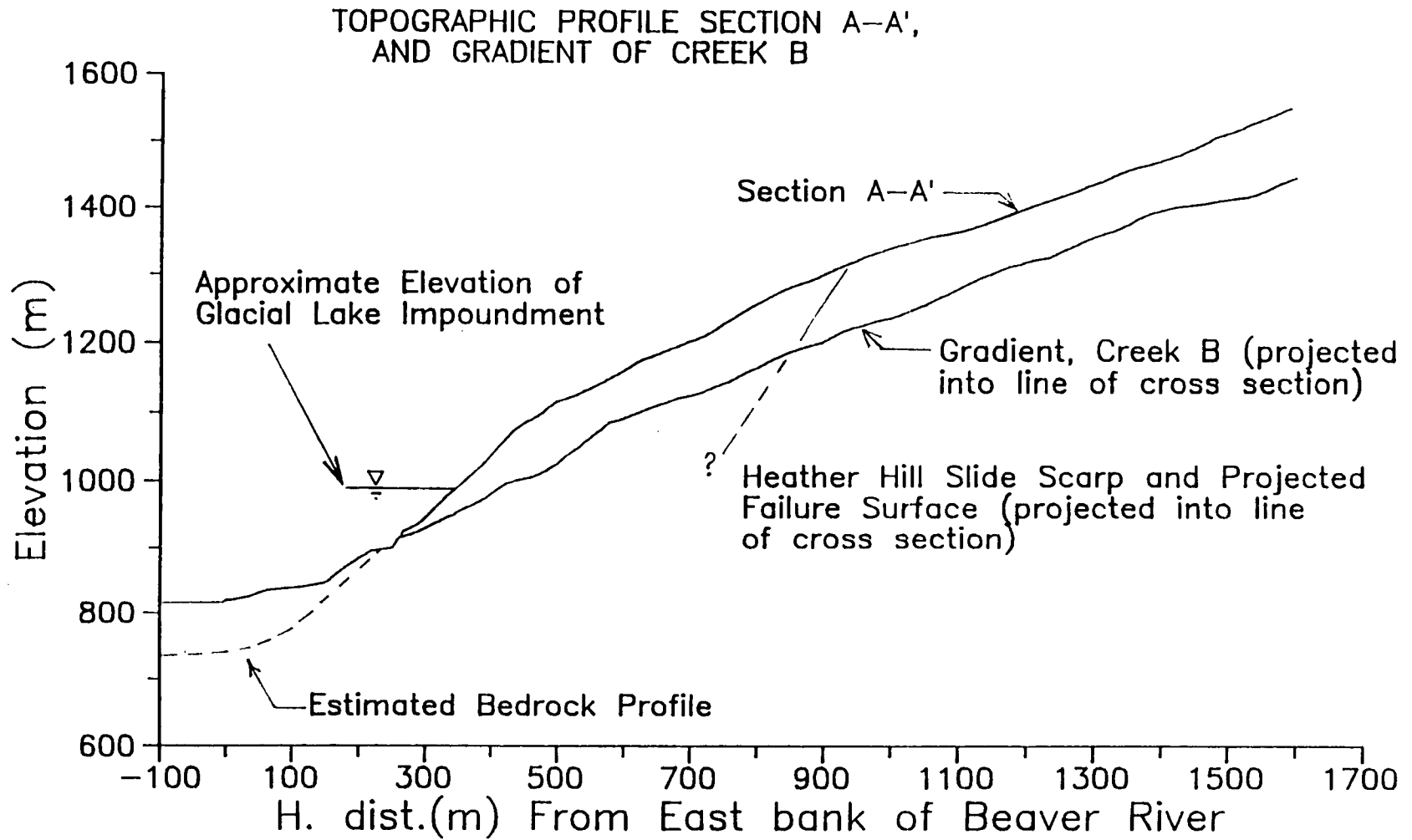
Figure 5.5 Topographic Profile Section A-A'
and Gradient of Creek B

Visible disturbance of the slopes in the study area is greatest in the vicinity of the Heather Hill slide and in the vicinity of Creek B, and decreases towards Creek A. The decreasing disturbance of the slopes towards the north of the study area is supported by the flatter slope profile in the vicinity of Creek A (Fig. 5.6). For these reasons it is believed that the structural data from Creek A are the most representative of the intact rock condition.

TOPOGRAPHIC PROFILE SOUTH OF CREEK A
SECTION B–B'

Approximate Elevation of
Glacial Lake Impoundment

Highway Cut

Elevation (m)

H. dist.(m) From East bank of Beaver River
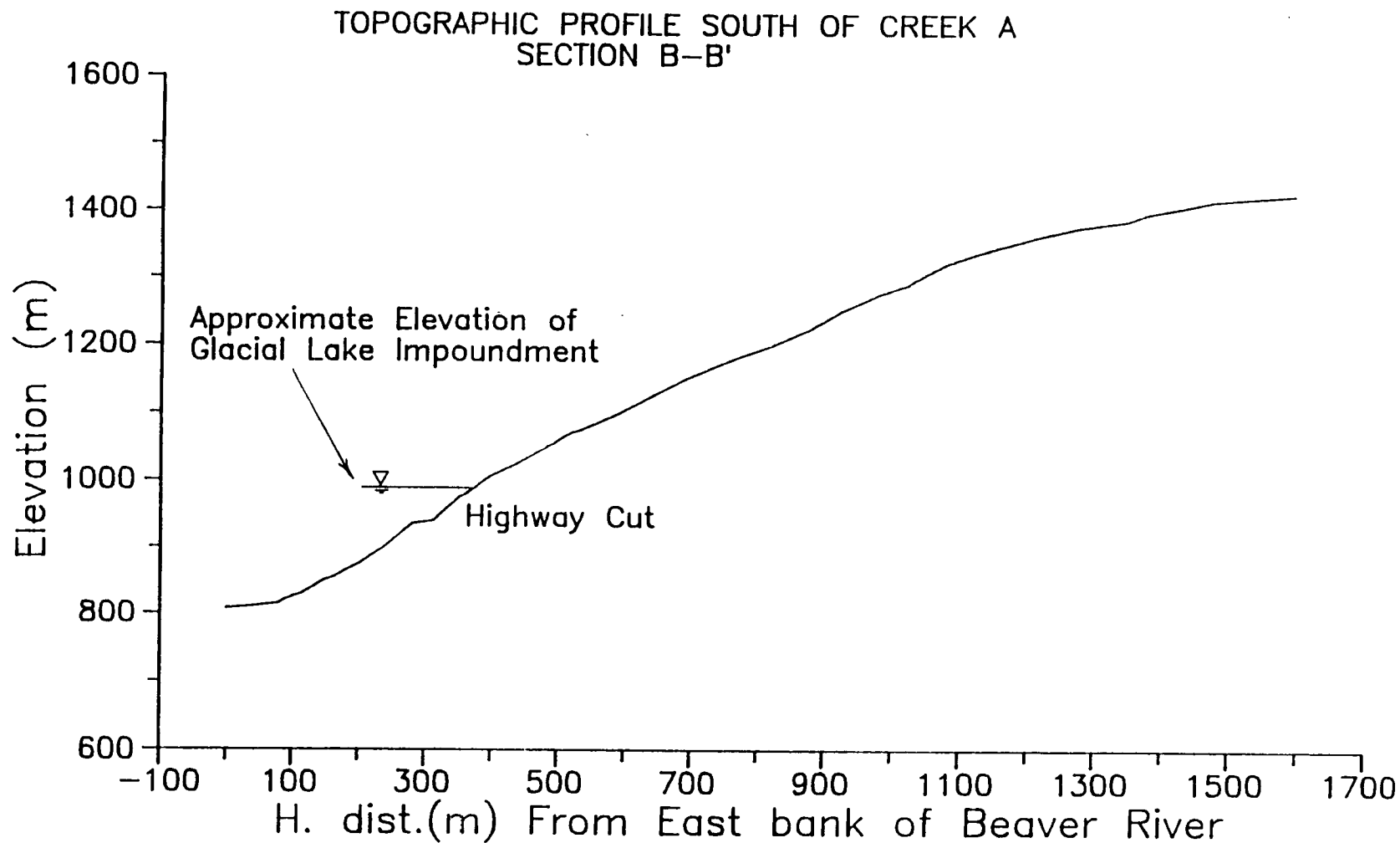
Figure 5.6   Topographic Profile South of Creek A, Section B-B'

6.0 Modelling Heather Hill Landslide Development

6.1 Introduction

The mode of failure of the Heather Hill landslide is examined with UDEC in this chapter. The goals of this analysis are to determine the mode of failure of the slide, and to examine the characteristics of the failure.

There are several factors that make this analysis unique. First, the Heather Hill landslide is a large failure in a natural slope where field evidence indicates toppling is well advanced. Potential toppling failures of this size have never been quantitatively assessed. Second, the lithology of the study area is highly variable and grades from dominantly quartz biotite schist at the base of the slope to dominantly feldspathic grit above the headscarp of the slide. The influence of mixed lithology on toppling development has not been quantitatively assessed.

6.2 Previous Analysis of the Heather Hill Landslide

The only previous modelling on the Heather Hill landslide is by EBA Engineering Consultants Ltd. (1978) who used the Simplified Bishop method of slices to assess the slide as a

106

deep seated rotational failure. The assumed original slope
geometry and slip surface are shown in Figure 6.1. A factor
of safety of 0.64 was obtained for the fully saturated slope.
The rock strength parameters used for this analysis are not
given.

6.3 Characteristics of the UDEC Model

The geometry of the model is simplified from the real site
conditions.

The topographic cross section A-A' (Map 1A) located
immediately north of the slide is used to approximate the
slope profile prior to the landslide. Figure 6.2 illustrates
this profile superimposed on a topographic profile through the
approximate center of the slide scarp. The dashed line in
Figure 6.2 is the assumed pre-slide topography used in the
UDEC model. Note that this topography continues below the
modern floodplain level to the minimum elevation of glacial
excavation estimated in Section 5.2.2.

Figure 6.3 illustrates several features of the UDEC model.
The left (west) boundary of the model is at the center of the
valley, and the symmetry of the valley is invoked to constrain
this boundary from moving horizontally. The base of the model
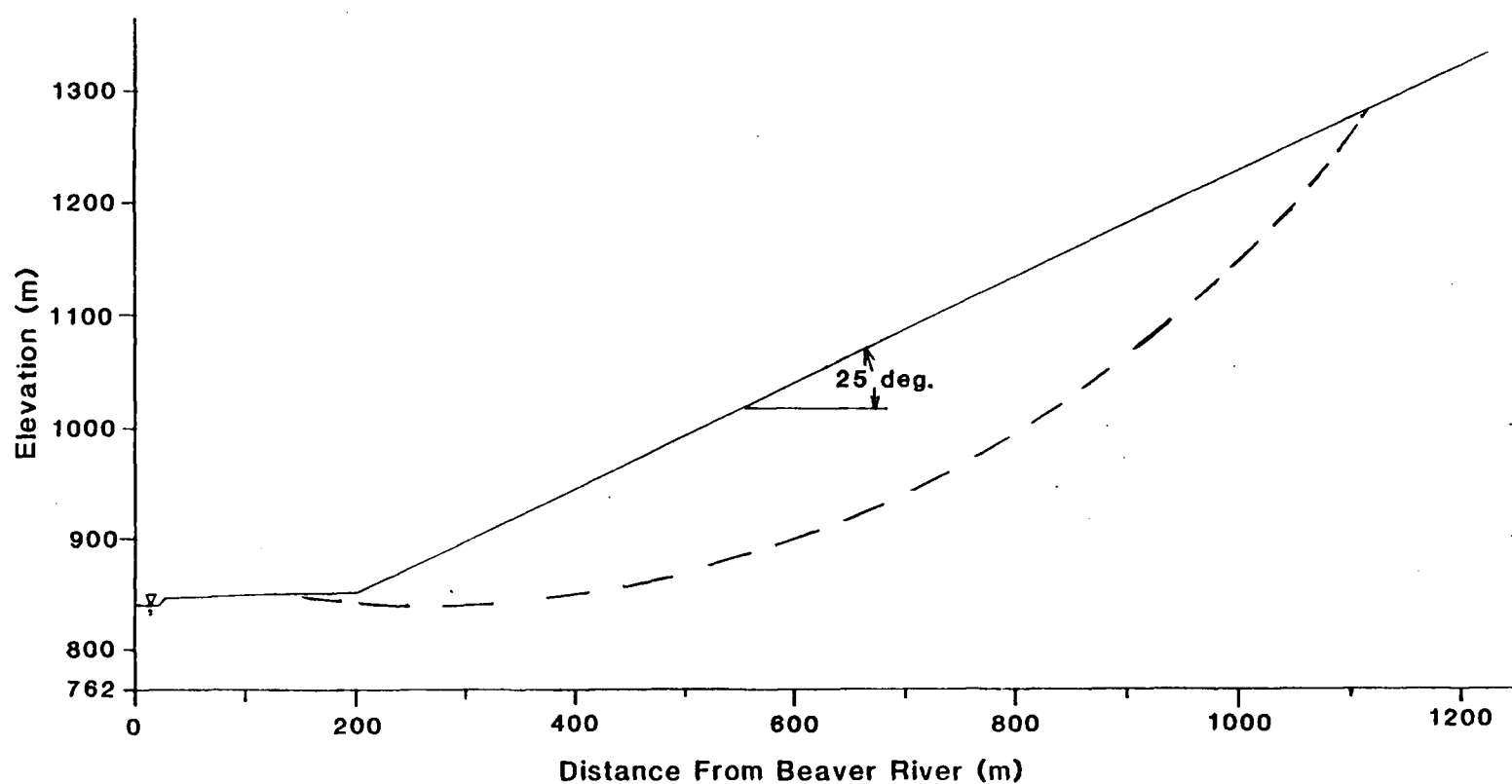
Figure 6.1 Circular Analysis of Heather Hill Landslide;
Assumed Slope Geometry and Failure Surface
(from EBA Engineering Consultants Ltd., 1978)

TOPOGRAPHIC PROFILE SECTIONS A—A'
AND C—C', MAP 1A

Section A—A'

Section C—C'

Assumed Pre—slide Topography
Used in UDEC Model

Elevation (m)

H. dist.(m) From East bank of Beaver River
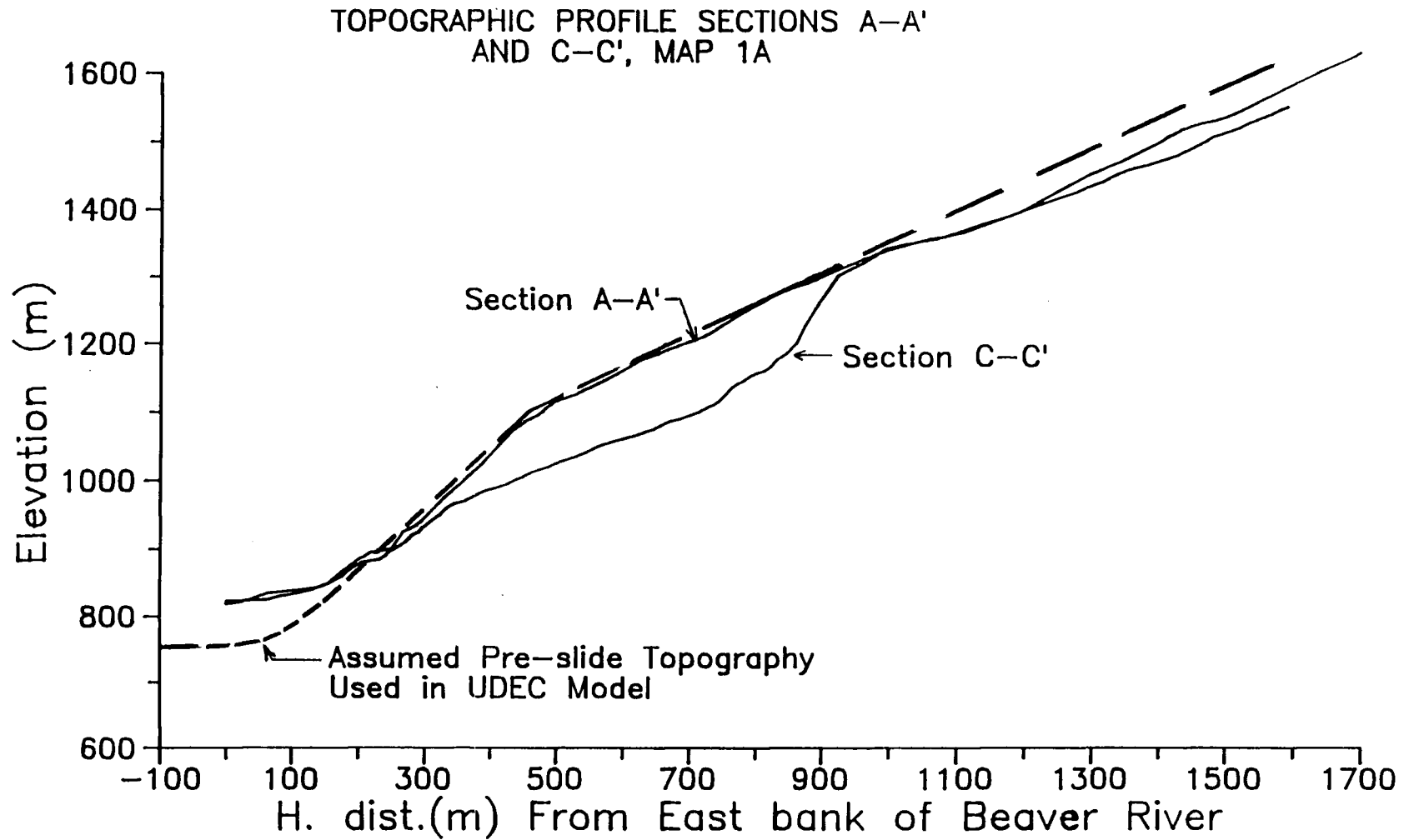
Figure 6.2 Heather Hill: Assumed Pre-Slide Topography

UDEC (Version 1.50)

legend

21/07/1989 17: 46
cycle   0
−1.080E+02 < x <   2.268E+03
−1.838E+03 < y <   5.980E+02

block plot

0   5e   2

Univ. of British Columbia
Dept. of Geological Science

Figure 6.3 Heather Hill: Initial Block Geometry of UDEC
Model

is fixed, and a constant in situ stress at $K_0=0.5$ is applied at the right boundary.

The domain in the model is divided into 65 degree dipping columns. This discontinuity is designed to simulate the combined influence of S0 foliation and S2 cleavage on the rock mass. An inclination of 65 degrees is chosen based on what is believed to be the intact rock structure in the study area (Sec. 5.5.3).

The excavation of the slope in the model is designed to simulate the real glacial excavation of the slope. Initial stresses of $K_0=1.0$ are applied in the domain shown in Figure 6.3 and gravity is applied until the stresses are at equilibrium. The first glacial excavation of the valley is modelled by sequentially removing the blocks that parallel the upper slope face, beginning with the block in the top left corner of the domain. The geometry of the slope at the end of this excavation is shown in Figure 6.4. It is assumed that the slope fails when it is oversteepened by the second glacial excavation. This is simulated by removing the remaining three blocks in Figure 6.4. The stresses in the slope are allowed to come to equilibrium after the excavation of each block.

UDEC (Version 1.50)

legend

21/07/1989 18:05
cycle   0
-1.080E+02 < x <   2.268E+03
-1.838E+03 < y <   5.380E+02

block plot

0   5e 2
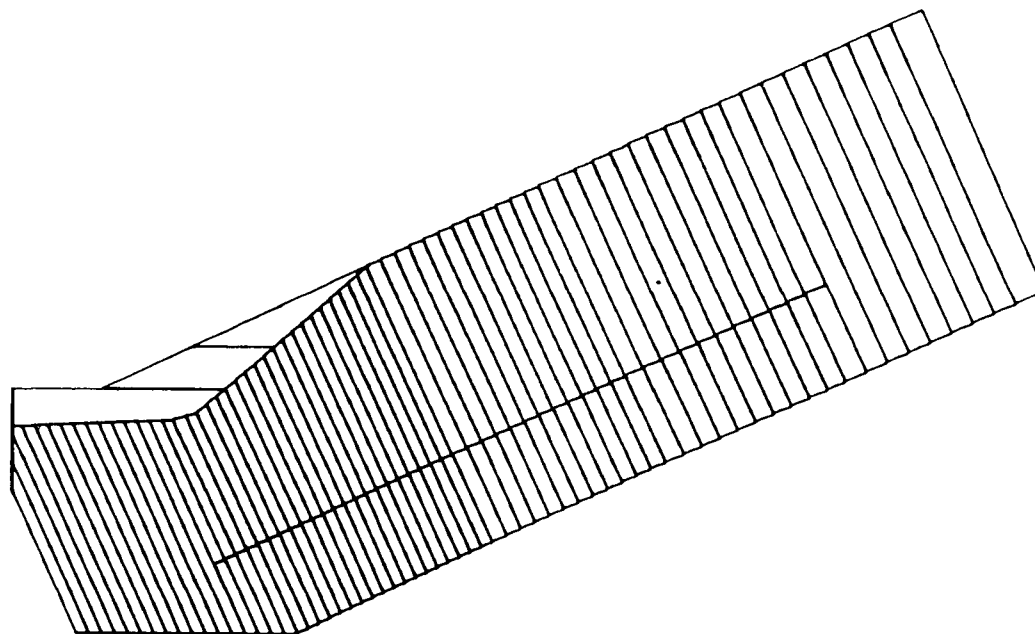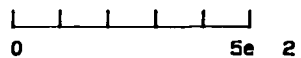
Figure 6.4 Heather Hill: First Glacial Excavation

6.3.1 Pore Pressure

Pore pressures based on a fully saturated slope are included
in the model. Piteau and Associates Ltd. (1982) reports that
the current water table elevation in the west valley slope
close to the entrance to Rogers Pass is near the surface.
When drilling from an elevation of 1040m, Piteau encountered
the water table approximately 15m below the surface at the
contact between surficial materials and bedrock. In addition,
it is considered that the mild climate during downwasting of
the second glaciation may have contributed to high pore
pressures in the slope (Mathewes and Heusser, 1981). For
these reasons, it is reasonable to assume that the water table
in the slope at the end of the second glaciation was as least
as high as it is currently, and may well have been slightly
higher.

6.4 Characterization of Rock Mass

The rock mass in the vicinity of the Heather Hill landslide is
difficult to characterize. The main discontinuity set that
weakens the rock mass is the S0 foliation. These surfaces
divide the rock mass into long thin columns that are
centimeters to several meters thick. The S2 cleavage further
divides the softer pelitic beds, and the harder grit beds are
broken by the J1 and J2 cross joints. At the scale of the

Heather Hill landslide most of these discontinuities are too finely spaced to be explicitly incorporated in a UDEC model.

Although modelling the structure of the study area completely as a discontinuum is not practical, it is essential to incorporate the affect of the discontinuities. This is done by modelling a coarse approximation of the S0 foliation explicitly, and the foliated and jointed "intact" material between the coarse S0 foliations as a continuum with a lower strength than competent rock. A minimum S0 foliation spacing of 25 meters is used in the model. This approximates the minimum separation of obsequent scarps located north of Creek B (Map 1A).

In the vicinity of the Heather Hill landslide the rock changes gradationally from dominantly foliated pelitic rock at the base of the slope to dominantly jointed feldspathic grit above the slide. This change in rock mass is incorporated in the model by allowing the joint and rock mass strength properties, and the S0 foliation spacing to increase approximately linearly from the bottom of the slope to above the headscarp.

The program uses a Mohr-Coulomb failure criterion defined by an internal friction angle, cohesion intercept and tensile strength to characterize the strength of the rock mass. Although these parameters could easily be determined in the laboratory for small, intact rock samples from the study area,

there is no accurate way, short of large scale testing, to determine these parameters for the foliated and jointed in situ rock mass.

There are several indirect methods of assessing the in situ rock mass strength (Hoek and Brown, 1980). These techniques are all empirical and use measurements of characteristics of the rock mass to determine a failure criterion. Many of these failure criteria are qualitative, but some such as the Hoek Brown strength criterion can be used to calculate a failure envelope for the rock mass. Unfortunately, in heavily jointed rock masses this technique still requires a great deal of judgement (Hoek and Brown, 1980). Because of the large uncertainty involved in estimating the rock mass strength parameters empirically, a deterministic analysis based on a single, estimated set of parameters is not attempted.

In this UDEC model, the rock mass strength parameters are determined by back analysis. The procedure is similar to the examples in Chapter 4. Initially, the rock strength parameters are set high enough to ensure that the slope will be stable when fully excavated. Once excavated, the parameters are gradually lowered to determine the point at which the slope becomes unstable. This is discussed further in Section 6.6.

6.5 Evolution of Model

The gradational treatment of the S0 spacing and the rock mass properties was adopted after simpler approximations failed to generate the Heather Hill slide geometry.

Early modelling attempts used a S0 spacing of 25 or 50 meters and one rock type for the entire slope. At a 50 meter spacing, unrealistically weak rock mass and joint properties were required to obtain failure. More realistic properties resulted when a uniform 25 meter spacing was used. However, the geometry of the failure was planar, extending parallel to the upper slope from the toe of the slope to the east boundary of the model.

Changing the rock mass properties from one rock type to a gradational increase in strength up slope resulted in some curvature, but the limit of the model landslide still exceeded the in situ landslide.

This prompted the inclusion of increasing S0 spacing in the model. With this change, the Heather Hill landslide geometry can be approximated using reasonable rock mass properties.

6.6   Results of UDEC Modelling

UDEC is limited to 10 different material properties. One of these materials is used to fix the artificial joint that is created to facilitate block zoning, and the remaining nine are used to simulate the gradational change from foliated pelitic rock at the base of the slope to dominantly feldspathic grit above the headscarp. Figure 6.5 illustrates how the rock strength parameters are assigned to the slope.

Four S0 spacings are used: 25m, 33m, 41m, and 49m. This spacing arbitrarily increases in increments of 8 meters from 25 meters at the base of the slope to 49 meters above the headscarp as illustrated in Figure 6.4.

The analysis begins with the slope excavated to the level of the second glaciation, fully saturated, and stable. Note that the floor of the valley in this analysis is approximately 70 meters below the current floodplain level. From this point the internal friction angle of the rock mass is lowered in small increments until failure develops.

The strength properties of the rock mass at failure are reported in Table 6.1. For simplicity the elastic properties are not reported in this table, but are included in the initial data input file in Appendix 3. In these trials joints
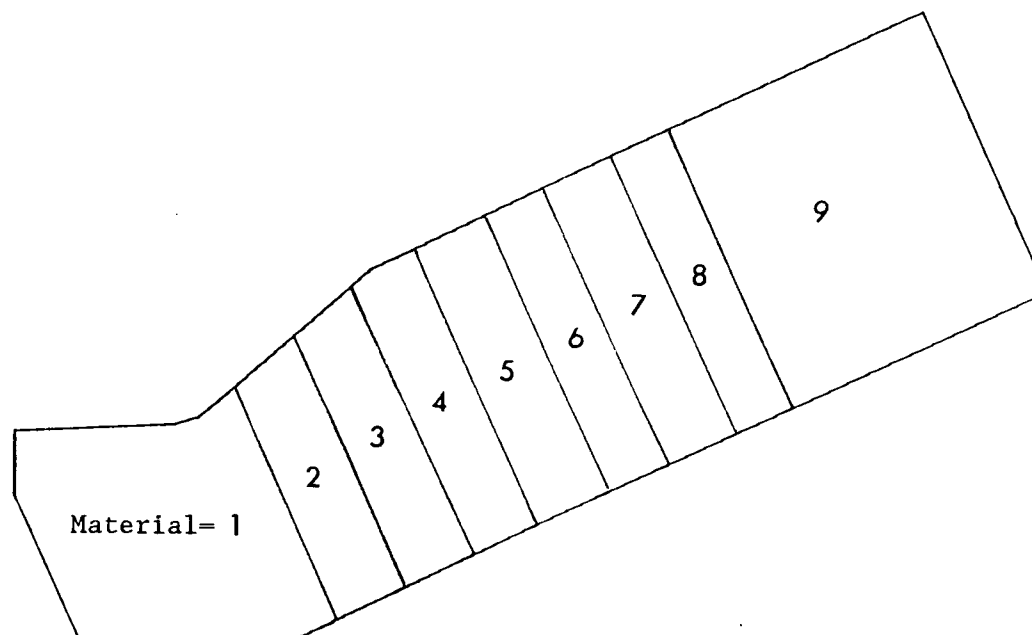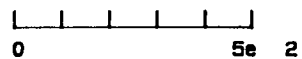
Figure 6.5 Heather Hill UDEC Model: Distribution of Rock Types

are assumed to have no cohesion, tension or dilation, and the rock mass is assumed to have no dilation.

Table 6.1 UDEC Strength Parameters for Heather Hill Model				
	Rock Mass			Joint
Material	Friction Angle (deg.)	Cohesion (MPa)	Tensile Strength (MPa)	Friction Angle (deg.)
1	31.0	.100	.050	22
2	33.0	.150	.075	25
3	35.5	.200	.100	28
4	38.0	.250	.125	31
5	40.5	.300	.150	35
6	43.0	.350	.175	39
7	46.0	.400	.225	44
8	49.0	.450	.250	47
9	52.0	.500	.300	50

The geometry of the failure that results at these strength parameters is shown in Figures 6.6a, and 6.6b. Note that the part of the model depicted in each figure is shown in the top left corner. This is necessary due to the density of the joints and grid points.

Figure 6.6a is a plot of grid point velocities. Note that in the same manner as the Brenda Mine example (Fig. 4.7a), different velocities on either side of an S0 foliation indicate shear is occurring along the foliations, and that velocities attenuate with depth. Both of these features are typical of flexural toppling failure.

UDEC (Version 1.50)

legend

23/07/1989 09:31
cycle 38500
 4.500E+02 < x <   7.500E+02
-8.500E+02 < y < -5.500E+02

block plot

0   5e 1

velocity vectors
      maximum -   4.368E-01

0   2e 0

Univ. of British Columbia
Dept. of Geological Science

Figure 6.6b

Figure 6.6a
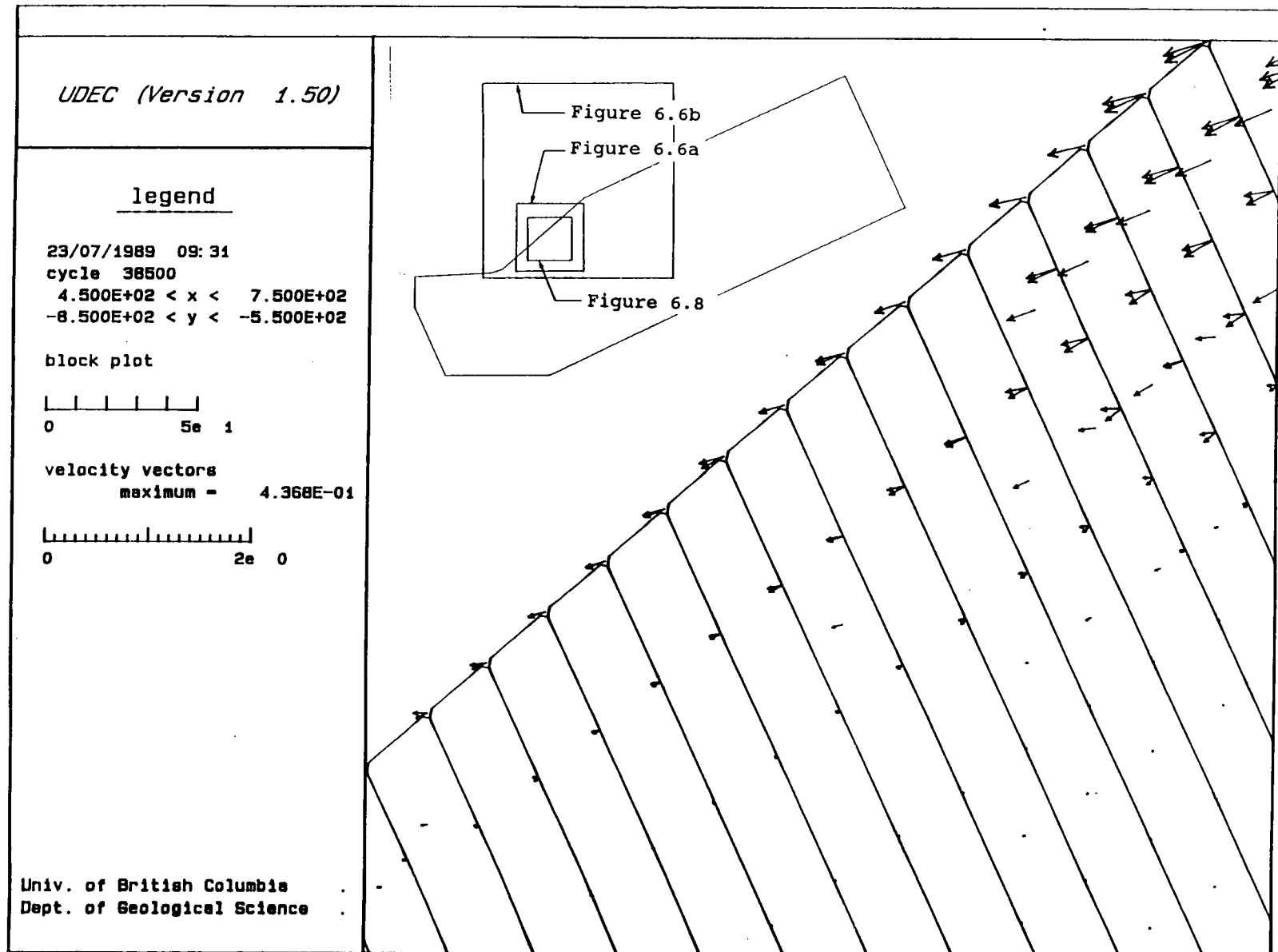
Figure 6.8

Figure 6.6a Heather Hill UDEC Model: Velocities of Grid Points

Figure 6.6b is a contour plot of horizontal displacement and illustrates the geometry of the failure. The shape of the failure surface and the extent of the failure in the UDEC model approximate the observed failure geometry and headscarp location.

There are many combinations of the strength parameters that will cause failure in the model. However, the parameter values reported in Table 6.1 allow a failure to develop in the model that best approximates the observed geometry and extent of the Heather Hill landslide. The variation in the values investigated for this model are listed in Table 6.2. The minimum and maximum values for both material 1 and material 9 are given. The remaining material values range in an approximately linear manner between these two end members.

Table 6.2: Investigated Variation in Parameters				
Material	Range of Values			
	Friction Angle (deg.)	Cohesion (MPa)	Tensile Strength (MPa)	Friction Angle (deg.)
1	30 - 35	.025-.150	.010-.075	22
9	45 - 52	.100-.500	.065-.300	35 - 50

6.7 Limitations of Analysis

The results of the analysis reported in the previous section are limited by the approximations in the model. For example,

UDEC (Version 1.50)

legend

23/07/1989 10:46
cycle 38500
 9.000E+02 < x <   1.150E+03
-8.750E+02 < y < -2.500E+01

block plot

|LLLLLLLLL|LLLLLLLLL|
0   2e 2

    x-disp contours
contour interval=   7.500E-02
number of contours/color=   1
min=-6.750E-01 max=-3.750E-01
-6.750E-01 -6.750E-01
-6.000E-01 -6.000E-01
-5.250E-01 -5.250E-01
-4.500E-01 -4.500E-01
-3.750E-01 -3.750E-01
a: -6.750E-01
f: -3.000E-01

Univ. of British Columbia
Dept. of Geological Science

Figure 6.6b

Figure 6.6a

Figure 6.8

Figure 6.6b Heather Hill UDEC Model: Horizontal Displacement

in this model the SO foliation spacing is varied from 25 to 49 meters. The choice of 25 meters as a minimum spacing of shear surfaces in the slope is supported by the field evidence of obsequent scarps north of Creek B (Map 1A). However the choice of the maximum spacing of 49 meters is arbitrary. If the maximum spacing is altered a different set of rock strength parameters at failure and a different geometry of failure will result. Other approximations in the model include the estimated maximum depth of glacial excavation and the approximation of the rock mass as homogeneous and isotropic between the SO foliations.

The results of the analysis are dependent on the pore pressures in the slope. In reality, the level of the water table in the failing rock would decline as the rock mass becomes increasingly broken and dilated. As the variation of the water table during failure is not known, it is conservatively assumed in this model that pore pressures corresponding to a fully saturated slope apply at all times.

This pore pressure assumption has the effect of propagating the failure. In reality, the combination of a decline in pore pressure and increased joint strength due to joint dilation may cause a failing slope to stabilize. The implications of this possibility for the stability of slopes in the Beaver Valley and for engineering design in these slopes are discussed in Sections 7.2.2 and 7.2.3 respectively.

6.8 Conclusions

6.8.1 Heather Hill Landslide

Due to the approximation of the real geologic conditions discussed in the previous section, a definitive stability analysis is not possible.

Even with these approximations, the UDEC model fails by flexural toppling limiting to a curvilinear failure surface. This model indicates that the most likely mode of failure of the Heather Hill landslide is flexural toppling.

Experience with the UDEC model of the Heather Hill failure indicates the importance of including the up slope increase in rock mass strength due to variation in rock type. It was found in the model that the limit of the failure is related to the gradational change in rock type from foliated pelitic rock at the base of the slope to feldspathic grit above the headscarp of the Heather Hill landslide. This relationship is supported by the overall distribution of landslides in the Beaver Valley (Fig. 5.1). Most of the identified landslides in the valley occur in the Slate division rocks and, with the exception of the large landslide south of the study area, are

roughly limited up slope by the occurrence of the Grit division rocks (Fig. 5.2).

6.8.2   Kinematic Test For Toppling

The kinematic test for toppling potential (Goodman and Bray, 1976; and Sec. 2.4.2) is widely accepted as a conservative means to estimate toppling potential. One of the most interesting conclusions of this chapter is that the geometry of the Heather Hill landslide does not satisfy this test.

For toppling to be possible, the kinematic test requires that the slope face angle (θ) be greater than the sum of the joint friction angle (ϕ) and the inclination from vertical (α) of the back dipping discontinuity set (ie: $\theta \geq \phi + \alpha$) (Fig. 2.2a). When applied to the Heather Hill model discussed in Section 6.6 this test indicates that toppling is not kinematically possible. The test is not satisfied by a margin of 5 degrees at the base of the slope (ie: 42 < 22 + 25) to 15 degrees just below the elevation of the change in slope (ie: 41 < 31 + 25). This is illustrated in Figures 6.7a and 6.7b. There are at least two reasons why this test is not satisfied.

The kinematic test is based on two criteria. For shear on a joint to occur the net stress acting on the joint must be aligned with the slope face and inclined by at least ϕ to the normal of the joint (Sec. 2.4.2). When this test is used to

N

Orientation of Slope

Pole to
S0 Bedding

Pole to S0 Bedding plus
Joint Friction Angle
$(\alpha + \phi) = (25^{O} + 22^{O}) = 47^{O}$
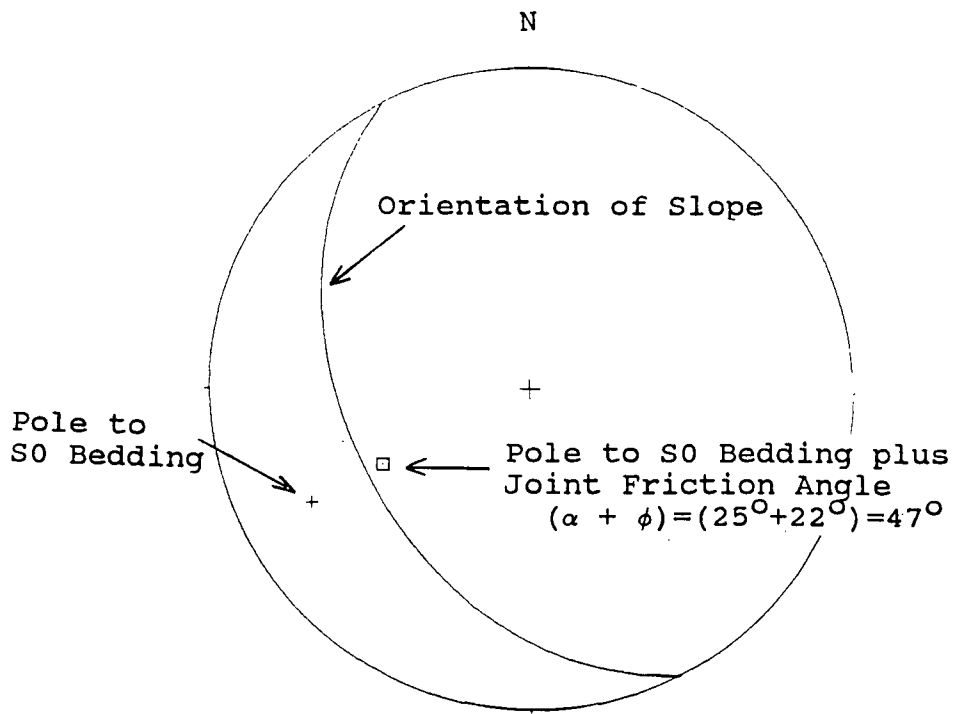
Figure 6.7a   Kinematic Test: Toe of Slope in UDEC Model.

N

Orientation of Slope

Pole to
S0 Bedding

Pole to S0 Bedding plus
Joint Friction Angle
$(\alpha + \phi) = (25^{O} + 31^{O}) = 56^{O}$
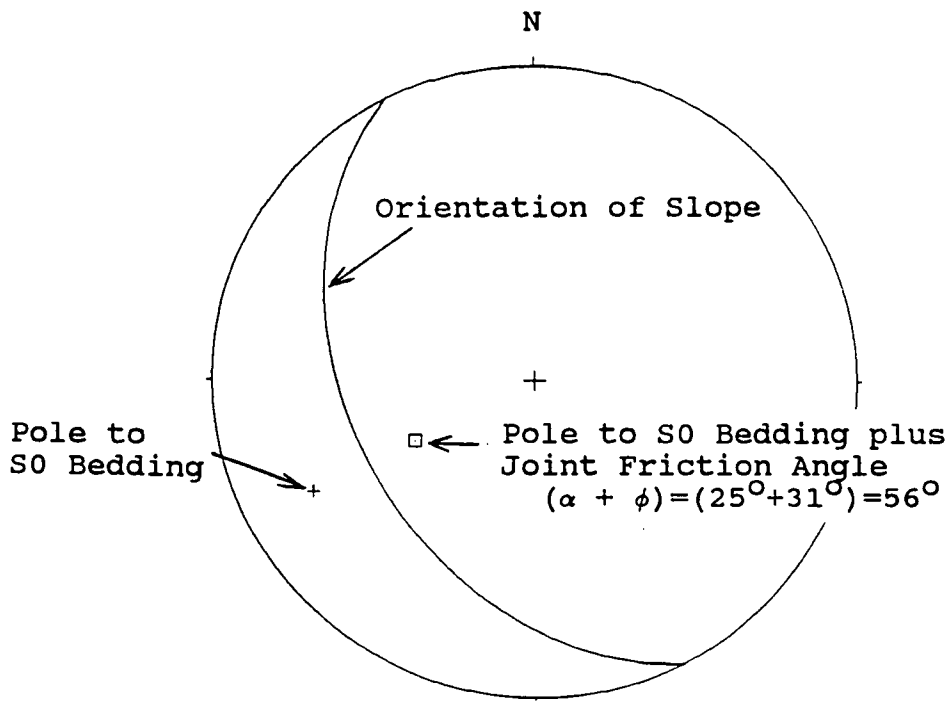
Figure 6.7b   Kinematic Test: Elevation of Change in Slope in
              UDEC Model

assess the toppling potential of a slope, it is assumed that the orientation of the net stress defined by the slope face angle at the surface applies at depth along the joint. This may be a reasonable assumption in small scale slopes, but is not valid in larger slopes.

In larger slopes the principal stress directions along a joint, and hence the net stress direction, change with depth in the slope. Figure 6.8 is taken from the model reported in Section 6.6 at a stage when the slope is stable. This figure is a plot of principal stresses at the grid points in the model and illustrates how the principal stress directions change along the joints. Note that this figure only depicts the portion of the model shown in the top left corner.

Figure 6.9 is a plot of $\tan^{-1}$(shear stress/normal stress) vs. length between A and A' along a joint shown in Figure 6.8. This plot illustrates how the mobilized friction angle on a joint varies with depth in the slope. Note that the mobilized friction angle is lowest near the slope face and increases with depth.

The characteristics of stresses along the joints illustrated in Figures 6.8 and 6.9 indicate that in large slopes, the assumption that net stress on a joint is parallel to the slope face at depth in the slope is not valid. Further, when applied to a kinematic assessment of toppling potential this

UDEC (Version 1.50)

legend

23/07/1989 12:39
cycle 26500
 5.000E+02 < x <   7.000E+02
-8.000E+02 < y < -6.000E+02

block plot

0   5e 1

principal stresses
        maximum =   -1.510E-01
        minimum =   -1.141E+01

0   5e 1

Univ. of British Columbia
Dept. of Geological Science

Figure 6.6b
Figure 6.6a
Figure 6.8

A

A'
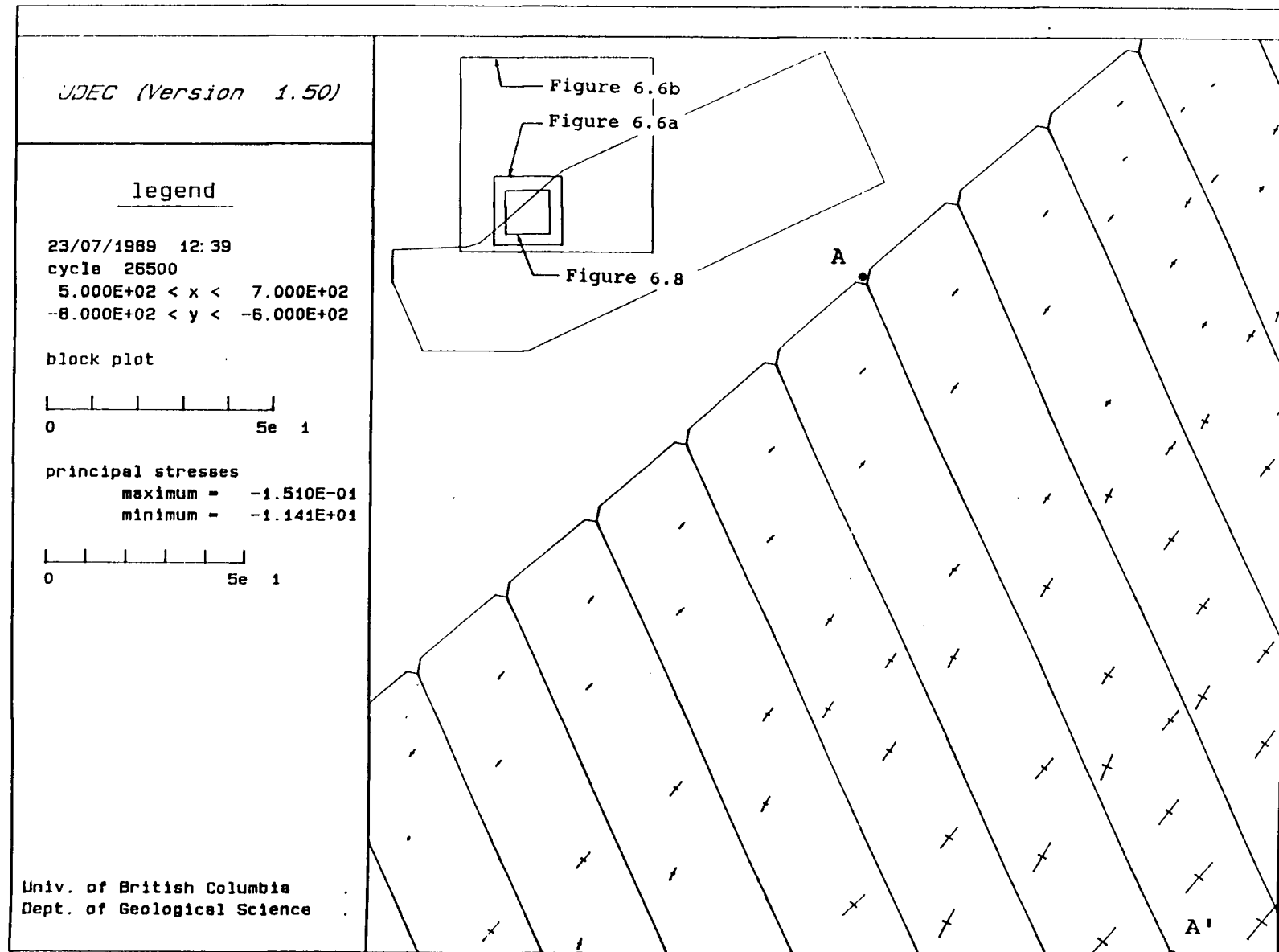
Figure 6.8 Heather Hill UDEC Model: Principle Stresses

Change in Eff. Friction Angle
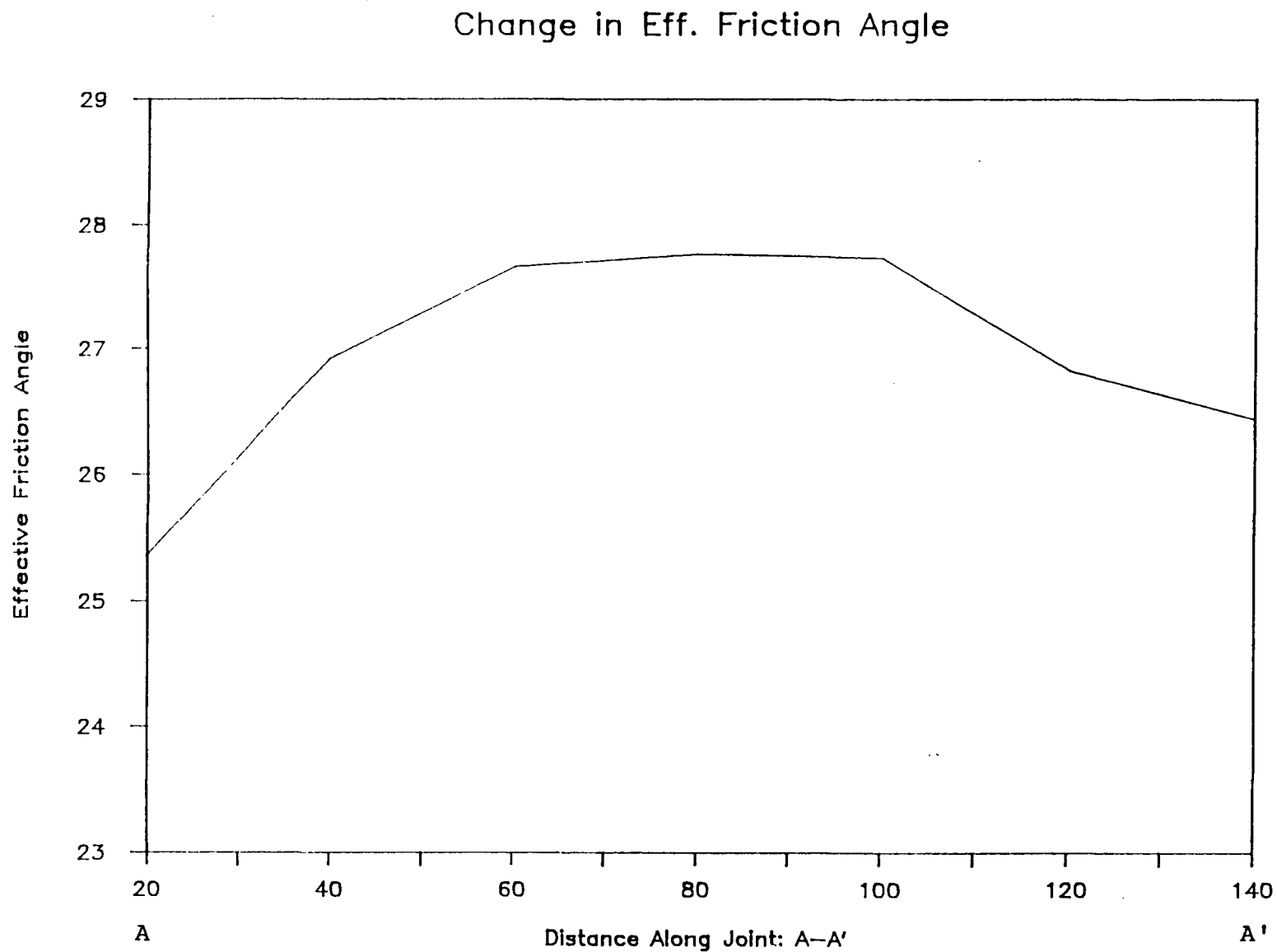
Figure 6.9 Heather Hill UDEC Model: Variation of Effective Friction Angle Along an S0 Foliation

assumption is not conservative. Figure 6.10 is a plot of factor of safety (shear strength/shear stress) along the same joint length as in Figure 6.9. This figure indicates that failure along joints during toppling failure may actually begin at depth, and progresses to the surface as failing sections of a joint transfer their load to adjacent up dip sections.

the UDEC model of the Heather Hill landslide also does not satisfy a second assumption of the kinematic test. It is assumed in the kinematic test that no pore pressures act along the joints. When pore pressures are considered the normal stress (σ_n) is reduced by the magnitude of the pore pressure ($\sigma_n' = \sigma_n - u$), while the shear stress (τ) is not affected. In this situation the failure of the joint occurs when the effective mobilized joint friction angle ($\tan^{-1}$ [shear stress/effective normal stress]) is greater than or equal to the joint friction angle ($\phi_m' \geq \phi$). The net effect of pore pressure is to allow the joint to shear at a lower angle of applied total stress. This is illustrated in Figures 6.11a and 6.11b.

It should be realized that the kinematic test is a test of toppling potential. It is not intended to test the stability of a slope with respect to toppling, it simply indicates if shear on a joint is kinematically possible. Within the limits imposed by the assumptions of the test, it provides a

Factor of Safety Along Joint
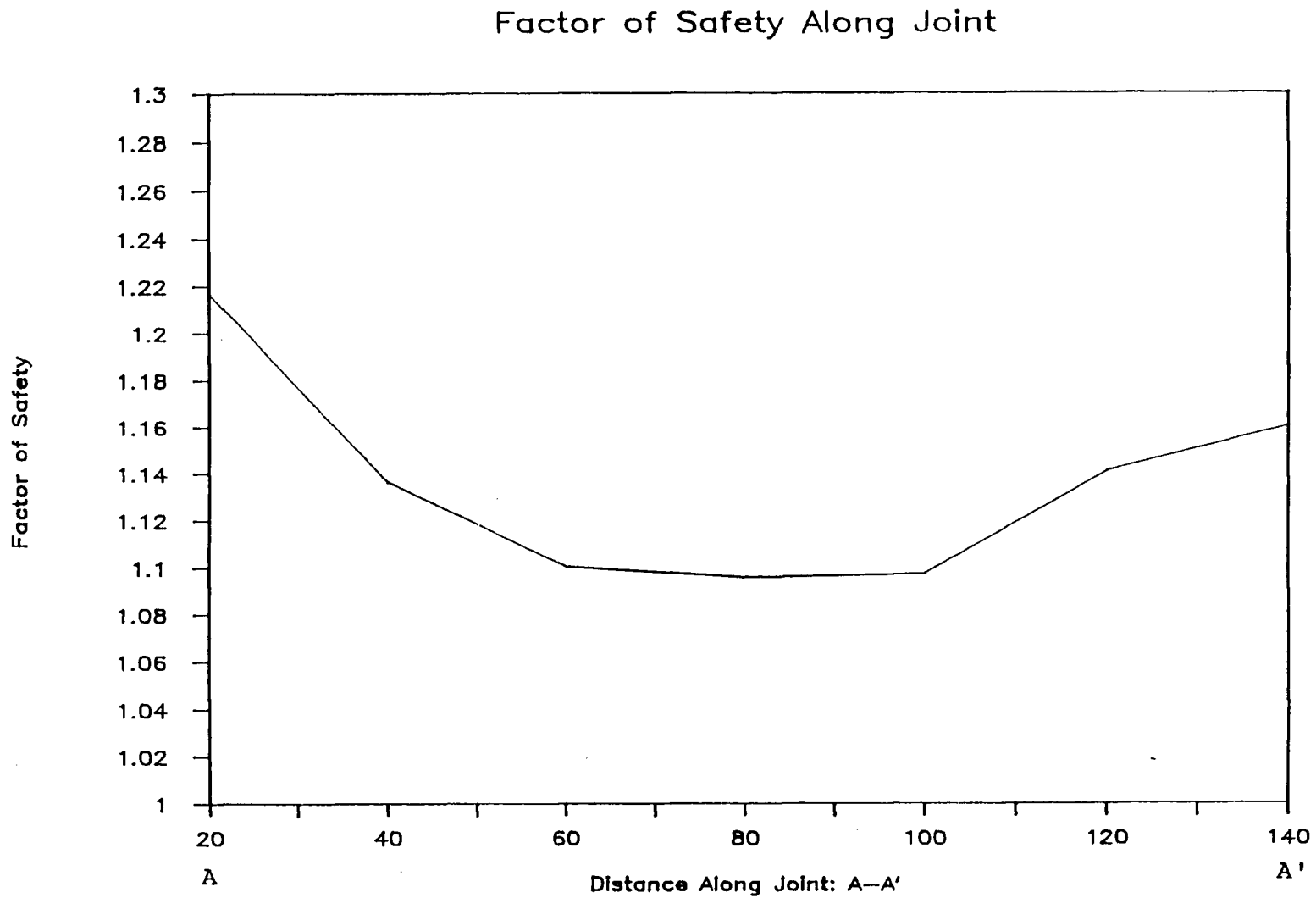
Figure 6.10   Heather Hill UDEC Model: Variation in Factor of
Safety Along S0 Foliation

JOINT

ϕ = Joint Friction Angle

6.11a

σ_N

ϕ_m

At Failure Dry

$\phi_m \geq \phi$

σ_T

τ

ϕ_m = Mobilized Joint Friction Angle

JOINT

ϕ = Joint Friction Angle

6.11b

$\sigma_N' = \sigma_N - u$

u

σ_N

β

At Failure Wet

σ_N'

ϕ_m'

$\beta < \phi$

σ_T

$\phi_m' \geq \phi$

τ

σ_T'

ϕ_m' = Effective Mobilized Joint Friction Angle
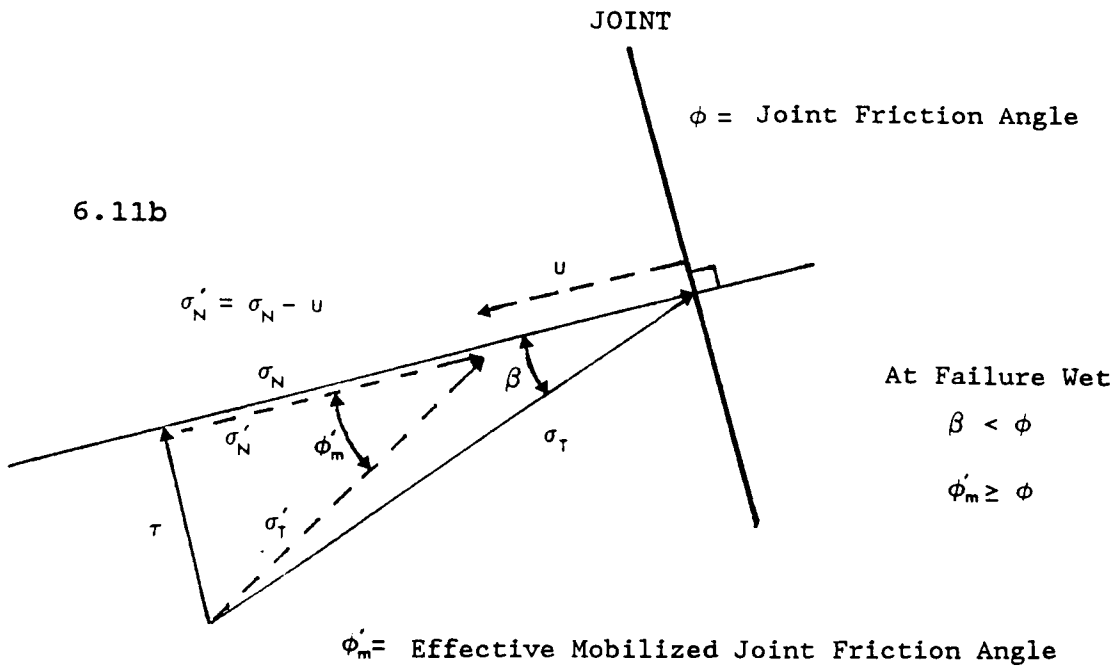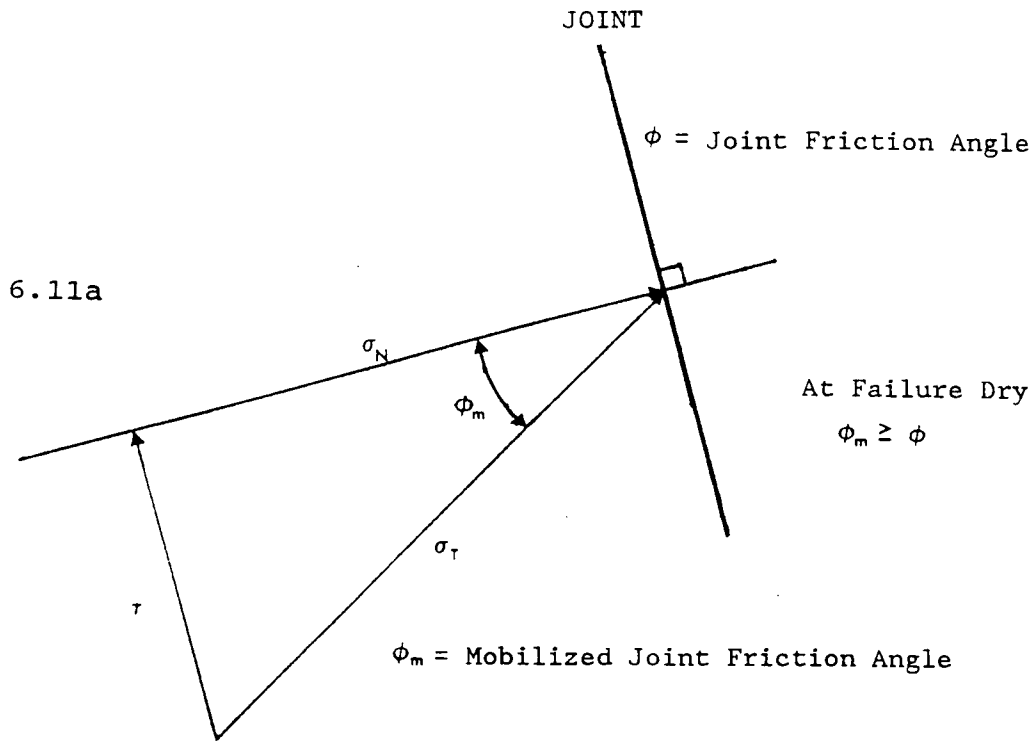
Figure 6.11a) Normal and Shear Stresses on Dry Joint
       6.11b) Effective Normal and Shear Stresses When Pore
               Pressure acts on Joint

132

conservative indication of toppling potential. The above discussion demonstrates that when the assumptions regarding the orientation of total stress and pore pressures along a joint are not satisfied the test is not a conservative estimate of toppling potential.

It is recommended that the kinematic test of toppling potential be qualified. The test should only be applied to small scale drained slopes in which the total stress orientation along the joints is a reasonable approximation of the kinematic test requirements.

7.0 Conclusions and Recommendations

7.1 PART I: Conclusions of Literature Review

Several conclusions result from the literature review on toppling in Chapter 2, and are summarized below.

1. Large scale flexural topples, and the influence of joint dilation, rock material and rock mass strength on toppling, have never been quantitatively assessed.

2. The limit equilibrium technique, finite element method, and distinct element method have all been used to model toppling. The limit equilibrium technique is by far the most popular.

3. The limit equilibrium technique has inherent restrictions however, that make it unsuitable for modelling large scale flexural modes of toppling.

4. Finite element methods overcome the restrictions of the limit equilibrium technique, but have a limited ability to model large deformations in jointed rock mass due to their continuum formulation.

5. The distinct element method overcomes the difficulties with the finite element method. The making and breaking

of joint contacts, large displacements, and rotations of discrete blocks and deformation of the blocks are all easily accommodated.

7.2   PART II: Flexural Toppling: Conclusions of Research

There are several conclusions on flexural toppling that result from the example models in Chapter 4.

1.   The results from the block and flexural toppling examples reported in Chapter 4 confirm that UDEC can simulate all types of topples. These examples also demonstrate that UDEC can be used to back analyze rock mass strength parameters, and determine the shape and location of the final failure surface in flexural toppling.

2.   The geometry of the failure surface formed during flexural toppling failure may be planar or curvilinear. This has never before been quantitatively confirmed.

3.   Two modes of flexural toppling failure appear to be possible: pure flexural toppling, and "graben" toppling. The development of "graben" toppling is largely controlled by the internal friction angle of the rock mass.

4. Pore pressure significantly affects the stability of
   slopes susceptible to flexural toppling.

7.3 PART III: Beaver Valley: Conclusions and
                Recommendations

7.3.1 Heather Hill Study Area

The UDEC model of the Heather Hill failure demonstrates that
the most likely mechanism of failure involves large scale
flexural toppling that limits to a curvilinear failure
surface. Failure begins in the toe of the slope as high
stresses cause failure of the rock mass and shearing on the S0
foliations.

In the study area north of the Heather Hill landslide, field
observations reveal evidence of recent deep-seated movement in
slopes that were initially believed to be stable. Both the
field evidence and the UDEC model of the Heather Hill
landslide indicate that this movement involves flexural
toppling.

Further north in the vicinity of Creek A (Map 1B) the slopes
are believed to be more stable due to the lower slope angle.

The UDEC model of the Heather Hill landslide demonstrates that
the up slope limit of the failure is related to the

gradational change in rock type from foliated pelitic rock at the base of the slope to feldspathic grit above the headscarp of the Heather Hill landslide. This is supported by the distribution of landslides in the Beaver Valley.

The kinematic test for toppling potential proposed by Goodman and Bray (1976) is violated by the Heather Hill landslide model. Consideration of the mechanics of large scale toppling failures indicates that the kinematic test should be qualified. The test should only be applied to small scale drained slopes in which the total stress orientation along the joints is a reasonable approximation of the kinematic test requirements.

7.3.2 Stability of Slopes in Beaver Valley

The evidence of modern movement discovered north of the Heather Hill landslide where no instability was previously suspected raises disturbing questions about the stability of similar slopes throughout the Beaver Valley.

Large toppling failures are generally considered slow failures (de Frietas and Watters, 1973), which accommodate a large degree of deformation prior to collapse and are often self stabilizing (Goodman and Bray, 1976; Nieto, 1987). It has been suggested that toppling failures self stabilize due to

joint dilation which causes a decline in the water table and
an increase in joint strength in the failing rock mass (Bovis,
1982).

It is possible that the slope north of the Heather Hill
landslide and other apparently stable slopes in the Beaver
Valley are locations where toppling is well advanced, or in
the early stages of deep seated toppling failure, and have
undergone some dilation and degradation of rock mass strength.
The implications of this stability condition for engineering
design are discussed in the next section. It is recommended
that slopes in the Beaver Valley that have undergone some
degree of deformation be identified. This can be done by
first categorizing high risk areas of the slopes on the basis
of degree of glacial oversteepening of the toe, rock type, and
proximity to existing landslides. High risk areas can then be
inspected using low level air photographs and on the ground.
Such an assessment can be used to plan more detailed
geotechnical investigations for engineering works.

7.3.3   Engineering Design Implications and
           Recommendations

If the stability of previously disturbed slopes is not
considered during the design and construction of engineering
works, costly design errors or mitigative works may result.
An engineer must consider the effect of an engineered
structure such as a cut or tunnel on the stability of the

whole slope, and, also, how the previous disturbance of the rock mass influences the design.

The impact of an engineering structure on the stability of a previously disturbed slope can be assessed with a UDEC model similar to the one used in Chapter 6. The existing slope can be developed, the structure introduced, and the effect on stability studied.

It is a relatively straight forward exercise to include the rock mass and stress conditions resulting from previous toppling disturbance in the design of surface or sub-surface engineered structures. This can be done by developing a second stability model for the area of interest in the larger model. Due to the smaller area, this model could utilize much more detailed information on the S0 bedding foliation spacing, joint spacing, and rock type variation. This information can be obtained directly from line mapping of the slope. The initial stress conditions for this model can be determined from the larger model of the whole slope, and discontinuities can be assigned strengths based on the degree of deformation of the natural slope.

There are two recommendations that can be made by considering the factors that control the stability of rock slopes in which toppling has occurred. The toe area is critical to the stability of these slopes and it is recommended that major

excavations not be undertaken in this area. In addition, the groundwater flow system should not be altered in a way that would cause increased pore pressures.

7.4 Flexural Toppling: Recommendations for Further Work

7.4.1 Curvilinear Failure Surface in Flexural Topples.

The geometry of the failure surface formed during flexural toppling failure may be planar or curvilinear. It is recommended that further research be done to investigate what factors control the shape of the failure surface. This work should involve sensitivity studies with the strength parameters for the intact rock (internal friction angle, cohesion, and tensile strength), and should be conducted on small (<100m) and large scale slopes.

In both the Brenda Mine and Heather Hill models the failure surface is approximately circular. There may be a relationship between circular failure surfaces in flexural toppling and circular failure surfaces in homogeneous, isotropic rock slopes. It may be possible to develop a relationship that uses accepted nomograms for circular failure potential to assess the stability of flexural topples that limit to a circular failure surface.

7.4.2 Influence of Dilation on Toppling

It is well known that dilation during shear can significantly increase the strength of a joint. Consequently, numerical models that do not include joint dilation will be simulating conservative behaviour (Barton, 1986). It is possible to use UDEC to investigate the influence of different degrees of dilation on the stability of toppling slopes. As the increase in strength of a joint due to dilation is dependent on the confining stress, it is important that such a study be done on both small and large scale slopes.

7.4.3 Influence of Glacial Events on Toppling

Several authors have suggested that slope deformations are initiated either during glacial undercutting of slopes or during glacial retreat (Mollard, 1977; Radbruch-Hall et al., 1976; Tabor, 1971; Terzaghi, 1962). Bovis (1982), Patton and Hendron (1974), and de Frietas and Watters (1973) suggest this specifically in reference to topples. It is possible to use UDEC to model the effect of repeated glacial events on the rock mass and joints of a slope susceptible to toppling. Such an analysis would use the continuously yielding joint model which allows progressive damage and weakening of the joints due to sequences of glacial excavation and cyclic loading.

7.4.4 Mountain Scale Deformation

Sakung is a general term used to describe the gravity deformation of very large slopes. This research has not previously discussed sakung because it is defined as creep on a mountain scale or gravitational sagging (Varnes, 1978). It is believed that many mountain scale movements reported and termed sakung or simply creep deformation in the literature (Tabor, 1971; Nemcok, 1972) may be more accurately described as large scale topples . It may be possible to evaluate the toppling potential and deformation of very large slopes using UDEC.

7.4.5 Application of UDEC to Slope Design

The examples in Chapter 4 and the Heather Hill model demonstrate that UDEC can be used for slope design in a rock mass susceptible to toppling. However, the accuracy of the design is dependent on the accuracy of the rock mass strength parameters used in the model. The best way to determine these parameters is by back analysis of a large number of known toppling failures in similar rock types, which has not yet been done.

It is recommended that UDEC be used to back analyze known flexural toppling failures to develop a volume of case histories characterizing rock mass strength. This information

will allow more accurate engineering design in a rock mass
susceptible to toppling.

7.4.6 Geometric Sensitivity Studies

For each example of toppling in this research, one geometry
was chosen for analysis. A great deal more can be learned
about what controls flexural toppling by varying the geometric
parameters of the slope. This research should be performed on
small and large scale hypothetical slopes utilizing variation
in the slope face angle, column thickness and column
inclination.

REFERENCES

Ashby, J., 1971: Sliding and Toppling Modes of Failure in Model and Jointed Rock Slopes, MSc. thesis, Imperial College, Royal School of Mines, London.

Barton, N.R., 1986: Deformation Phenomena in Jointed Rock. Geotechnique, Vol. 36, No. 2, pp. 147-167.

Bovis, M.J., 1982, Uphill-Facing (Antislope) Scarps in the Coast Mountains, Southwest British Columbia, Geological Society of America Bulletin, v.93, pp. 804--812.

Brown, A., 1982: Toppling Induced Movements in Large, Relatively Flat Rock Slopes: Proc., 23rd U.S. Symposium on Rock Mechanics, Berkeley, California, pp. 1035.

Brown, I., Hittinger, M., and Goodman, R.E., 1980: Finite Element Study of the Nevis Bluff (New Zealand) Rock Slope Failure. Rock Mechanics, Vol. 12, pp. 231-245.

Burman, B.C., 1974: Development of a Numerical Model for Discontinua. Australian Geomechanics Journal, 1974. pp. 1-10.

Burman, B.C., Trollope, D.H., and Philip, M.G., 1975: The Behaviour of Excavated Slopes in Jointed Rock, Australian Geomechanics Journal, 1975, pp.26-31.

Choquet, P., Tanon, D.D.B., 1985: Nomograms for the Assessment of Toppling Failure in Rock Slopes. Proc., 26'th U.S. Symposium on Rock Mechanics, Rapid City, pp. 19-30.

Cundall, P.A., 1971: A Computer Model for Simulating Progressive, Large-Scale Movements in Blocky Rock Systems, Proc. International Symposium on Rock Fractures, Nancy, France, paper II-8.

Cundall, P.A., 1983: Numerical Modeling of Water Flow in Rock Masses., Project PECD 7/9/22, Department of the Environment, United Kingdom.

Cundall, P.A., 1985: A Simple Joint Model That Embodies Continuous Yielding, presented at the 1985 International Symposium on the fundamentals of Rock Joints.

Cundall, P.A, 1987: Distinct Element Models of Rock and Soil Structure, in Analytical and Computational Methods in Engineering Rock Mechanics, pp. 129-163. E.T. Brown, Editor, George Allen and Unwin, London.

Cundall, P.A., and Board, M.P., 1988: A Microcomputer Program for Modeling Large-Strain Plasticity Problems, prepared for: 6'th International Conference on Numerical Methods in Geomechanics, Innsbruck, Austria.

Cundall, P.A. and Hart, R.D., 1984: Analysis of Block Test No. 1 Inelastic Rock Mass Behaviour: Phase 2 - A Characterization of Joint Behavior (Final Report). Itasca Consulting Group, Subcontract SA-957, Rockwell Hanford Operations, Richland, Washington, March 1984.

Cundall, P.A., and Lemos, J.V., 1988: Numerical Simulation of Fault Instabilities with the Continuously-Yielding Joint Model, Second International Symposium of Rock bursts and Seismicity in Mines, University of Minnesota, June, 1988.

Cundall, P.A., Marti, J., Beresford, P.J., Last, N.C. and Asgian, M.I., 1978: Computer Modelling of Jointed Rock Masses, U.S. Army Engineer Waterways Experiment Station, Technical Report No. N-78-4, 399p.

Cundall, P.A., and Marti, J., 1979: Some new Developments in Discrete Numerical Methods for Dynamic Modelling of Jointed Rock Masses, Proc. of the Rapid Excavation and Tunnelling Conference, Atlanta, Georgia.

Cundall, P.A., Voegele, M., Fairhurst, C., 1977: Computerized Design of Rock Slopes using Interactive Graphics for the Input and Output of Geometrical Data, Proc. 16'th Symposium on Rock Mechanics, Univ. of Minnesota, Minneapolis. pp. 5-14.

de Frietas, M.H., and Watters, R.J., 1973: Some Field Examples of Toppling Failure, Geotechnique, Vol 23, no. 4, pp. 495-514.

Duncan, J.M., and Goodman, R.E., 1968: Finite Element Analyses of Slopes in Jointed Rock, Contract Report S-68-3, U.S. Army Eng. Waterways Exper. Station, Corps of Engineers, Vicksburg, Miss., 271 pp.

EBA Engineering Consultants Ltd. 1976: CPR - Rogers Pass, Geotechnical Evaluation of Alternate Routes, Report to Canadian Pacific Railways, July 1976.

EBA Engineering Consultants Ltd. 1978: Heather Hill Landslide, Glacier National Park. Report to Parks Canada, File 36-0267, Feb., 1978.

Evans, S.G., 1987: Surface Displacements and Massive Toppling on the Northeast Ridge of Mount Currie, British Columbia, Current Research, Part A, Geological Survey of Canada, Paper 87-1A, pp. 181-189.

Evans, R., Valliappan, S., McGuckin, D., and Raja Sekar, H.L., 1981: Stability Analysis of a Rock Slope Against Toppling Failure. Proc., 3rd International Symposium on Weak Rock, Tokyo., pp. 665-670.

Goodman, R.E., and Bray, J.W., 1976: Toppling of Rock Slopes, Proc. of ASCE Specialty Conference, Rock Engineering for Foundations and Slopes, Vol. 2, Boulder, Colorado, pp. 201-234.

Goodman, R.E., and Dubois, J., 1971: Duplication of Dilitant Behaviour in the Analysis of Jointed Rocks. U.S. Army, Corps of Engineers, Rept., Omaha.

Goodman, R.E., Taylor, R.L., Brekke, T.L., 1968: A Model for the Mechanics of Jointed Rock. Journal of the Soil Mechanics and Foundation Division, ASCE, May, 1968, SM 3, pp. 637-658.

Hittinger, M., 1978: Numerical Analysis of Toppling Failures in Jointed Rock: Ph.D thesis, University of California, Berkeley.

Hocking, G., 1978: Analysis of Toppling-Sliding Mechanisms for Rock Slopes: Proc., 19'th Symposium on Rock Mechanics, pp. 288.

Hoek, E., and Brown, E.T., 1980: Underground Excavations in Rock, The Institute of Mining and Metallurgy, London.

Hoek, E., and Bray, J., 1977: Rock Slope Engineering (2nd edition), The Institute of Mining and Metallurgy, London.

Hofmann, H., 1972: Kinematische Modellstudien zum Boschungsproblem in regelmassig geklüfteten Medien. Veroffentlichungen des Institutes für Bodenmechanik und Felsmechanik, Karlsruhe, Heft 54.

Hofman, K. von, 1973: Modellversuche zur Hangeltektonic. Geol. Rdsch. 62, No. 1, pp.16-29.

Holmes, G., and Jarvis, J.J., 1985: Large Scale Toppling Within a Sackung type Deformation at Ben Attow, Scotland, Quarterly Journal of Engineering Geology, London, Vol 18, pp. 287-289.

Hunt R.E., 1986: Geotechnical Engineering Analysis and Evaluation. McGraw Hill Inc., 1986, p.134.

Ishida, T., Chigira, M., and Hibino, S., 1987: Application of the Distinct Element Method for Analysis of Toppling Observed on a Fissured Rock Slope, Rock Mechanics and Rock Engineering 20, pp. 277-283.

Itasca, 1989: Universal Distinct Element Code: Manual, Version ICG1.5, Itasca Consulting Group, Inc., Minneapolis, Minnesota.

Kalkani, E.C., 1977: Two Dimensional Finite Element Analysis for the Design of Rock Slopes. 16'th Symposium on Rock Mechanics, University of Minnesota, Minneapolis, U.S.A., pp. 15-24.

Kalkani, E.C., and Piteau, D.R., 1976: Finite Element Analysis of Toppling Failure at Hell's Gate Bluffs, British Columbia. Bull. assoc. Eng. Geol., 13, pp. 315-327.

Kuykendall, L., 1975: Kinematic Study of Toppling Failure Mode and Practical Aspects of Using the Base Friction Modelling Machine. Internal Report, University of California, Berkeley, Department of Civil Engineering.

Ladanyi, B., and Archambault, G., 1969: Simulation of Shear Behaviour of a Jointed Rock Mass. 11'th Symposium on Rock Mechanics, Berkeley, California, pp. 105-125.

Lemos J.V., and Brady B.H.G., 1983: Stress Distribution in a Jointed and Fractured Medium, 24'th U.S. Symposium on Rock Mechanics, June, 1983, pp. 53-59.

Lemos, J.V., Hart, R.D., and Cundall, P.A., 1985: A Generalized Distinct Element Program for Modelling Jointed Rock Mass, Proc. Int. Symp. on Fundamentals of Rock Joints, Bjorkliden, Sweden, pp. 335-343.

Lorig, L.J., 1984: A Hybrid Computational Model for Excavation and Support Design in Jointed Media, Ph.D. Thesis, University of Minnesota, 1984.

Mathewes, R.W., and Heusser, L.E., 1981: A 12,000 Year Palynological Record of Temperature and Precipitaion Trends in Southwestern British Columbia. Canadian Journal of Botany, Vol. 59, pp. 707-710.

Mollard, J.D., 1977: Regional Landslide Types in Canada, in Reviews in Engineering Geology, Vol. 3: Landslides. Boulder, Colorado, Geological society of America. pp. 29-56.

Muller, L., 1968: New considerations on the Vajont Slide, Felsmechanik und Ingenieurgeologie, Vol. 6, no. 1, pp. 1-91.

Nemcock, A., 1972: Gravitational Slope Deformation in High Mountains. Proceedings, 24'th International Geological Congress, Sec. 1, pp. 132-141.

147

Nieto A.S., 1987: Influence of Geological Details on the
    Field Behavior of Soils and Rocks: Some Case Histories,
    in R.B. Peck Symposium Volume: The Art and Science of
    Geotechnical Engineering at the Dawning of the Twenty-
    First Century. W.T. Hall, Editor, Prentice-Hall Inc.,
    Englewood Cliffs, New Jersey.

Otter, J.R.H., Cassell, A.C., Hobbs, R.E., 1966: Dynamic
    Relaxation, Proc. Inst. of Civil Eng., Vol. 35, Dec.,
    1966, pp. 633-656.

Patton, F.D. and Hendron A.J., 1974: Mass Movements - General
    Report, Theme V. 2nd International Congress of
    Engineering Geology, Sao Paulo, pp. 1-57.

Patton, F.D., 1966: Multiple Modes of Shear Failure in Rock
    and Related Materials. Ph.D thesis, University of
    Illinois at Urbana.

Piteau and Associates Ltd., 1988: Preliminary Geotechnical
    Assessment of South Wall Slope Stability Problems.
    unpublished report to Brenda Mines Ltd., Oct. 6, 1988

Piteau and Associates Ltd., 1982: Engineering Geology and
    Rock Mechanics Assessments for Estimating Support
    Requirements for the Proposed Rogers Pass Short Tunnel.
    Report to CPR. Project 81-340, March 1982

Piteau, D.R., and Martin, D.C., 1981: Mechanics of Rock Slope
    Failure. 3rd Int. Conference on Stability in Surface
    Mining, C.O. Brawner ed., pp. 113.

Piteau, D.R., Stewart, A.F., and Martin, D.C., 1981: Design
    Examples of Open pit Slopes Susceptible to Toppling.
    Proc. Third International Conference on Stability in
    Surface Mining, Soc. of Min. Eng. of AIME, Vancouver, pp.
    679-712.

Poulton, T.P., and Simony, P.S. 1980: Stratigraphy,
    sedimentology, and regional correlation of the Horsethief
    Creek Group (Hadrynian, Late Precambrian) in the northern
    Purcell and Selkirk Mountains, British Columbia. Canadian
    Journal of Earth Sciences v.17, pp. 1708-1724.

Pritchard M.A., Savigny K.W., and Evans S.G., 1988: Deep-
    Seated Slope Movements in the Beaver River Valley,
    Glacier National Park, B.C.. Geological Survey of Canada,
    Open File 2011.

Radbruch-Hall, D.H., Varnes, D.J., and Savage, W.Z., 1976:
    Gravitational Spreading of Steep-Sided Ridges ("sakung")
    in Western United States. Int. Assoc. of Eng. Geology,
    Bull. No. 14, pp. 23-35.

Rapp, P.A. 1987: Rock Toppling and Massive Slope Instability in the Beaver Valley, British Columbia., unpub. B.A.Sc thesis, University of British Columbia, Vanc., B.C.

Rickard M.J. 1961: A note on cleavages in crenulated rocks. Geol. Mag., v.98 no.4, pp. 324-332.

Sagaseta C., 1986: On the Modes of Instability of a Rigid Block on an Inclined Plane, Rock Mechanics and Rock Engineering 19, pp. 261-266.

Simony, P.S., and Wind, G. 1970: Structure of the Dogtooth Range and adjacent portions of the Rocky Mountain Trench. in Structures of the Canadian Cordillera. Geological Association of Canada, Special Paper 6, pp. 41-51.

Soto, C., 1974, A Comparative Study of Slope Modelling Techniques for Fractured Ground, MSc. thesis, Imperial College, Royal School of Mines, London.

Tabor, R.W., 1971, Origin of Ridge-Top Depressions by Large-Scale Creep in the Olympic Mountains, Washington. Geological Society of America Bulletin, v.82, pp. 1811-1822.

Teme S.C., and West T.R., 1983: Some Secondary Toppling Failure Mechanisms in Discontinuous Rock Slopes, 24'th U.S. Symposium on Rock Mechanics, June, 1983.

Terzaghi, K., 1962: Stability of Steep Slopes on Hard Unweathered rock. Geotechnique, Vol. 12, pp. 251-270.

Thurber Consultants Ltd., 1983a: Rogers Pass Revision, Volume 1: Geology, Geomorphology and Hydrology. Report to CP Rail Special Projects, File 17-6-58

Thurber Consultants Ltd., 1983b: Rogers Pass Revision, Volume 5: Beaver Valley Grade 1982 Route Investigation, Part 3. Report to CP Rail Special Projects, File 17-6-58

Thurber Consultants Ltd. 1979: Assessment of Griffith Landslides for Proposed Rogers Pass Grade Revision, Mile 72.2 to 73.1 Mountain Subdivision, Report to CP Rail Special Projects. File 17-6-31, December, 1979.

VanBuskirk, C.D., 1987: Reassessment of the Griffith Landslide, Rogers Pass, British Columbia. unpub. B.A.Sc. thesis, University of British Columbia, Vanc., B.C.

Varnes, D.J., 1978: Slope Movements Types and Processes, in Landslides, Analysis and Control, Transport Research Board Special Report 176, Schuster R.L. and Raymond J.K., editors, National Academy of Sciences, Washington, D.C.

Wheeler, J.O. 1963: Rogers Pass map area, British Columbia and Alberta (82N W1/2). Geological Survey of Canada, Paper 62-32.

Williams J.R., and Mustoe, G.W, 1987: Modal Methods for the Analysis of Discrete Systems, Computers and Geotechnics, 4, pp.1-19.

Whyte, R.J., 1973, A Study of Progressive Hanging Wall Caving at Chambishi Coppermine in Zambia Using the Base Friction Model Concept, M.Sc. thesis, Imperial college, Royal School of Mines, London.

Wyllie, D.C., 1980: Toppling Rock Slope Failures; Examples of Analysis and Stabilization. Rock Mechanics, Vol. 13, pp. 89-98.

Zanbak C., 1983: Design Charts for Rock Slopes Susceptible to Toppling, Journal of Geotechnical Engineering, ASCE, V.109, pp. 1039-1061.

APPENDIX 1

UDEC Input Data Files for:

-- Goodman and Bray Block Topple, Section 4.2
-- Base Friction Model, Section 4.3.1
-- Brenda Mine Model, Section 4.4

```
**Goodman and Bray Block Topple**
START
ROUND .1
BLOCK -8.66025 -97.5 56.02241 0.46634 131.0641 4.9706 131.0641
-97.5
SAVE GB1
*CRACK FOLIATION FOR BLOCKS 10-16
CRACK      82.10254 -34.7057 61.60254 0.801270
CRACK      90.26279 -28.8397 72.76279 1.471143
CRACK      98.42304 -22.9737 83.92304 2.141016
CRACK      106.5833 -17.1076 95.08330 2.810889
CRACK      114.7435 -11.2416 106.2435 3.480762
CRACK      122.9038 -5.37564 117.4038 4.150635
CRACK      131.0640 0.490381 128.5640 4.820508
*CRACK FOLIATION FOR BLOCKS 1-10
CRACK            0     -92.5      -2.5 -88.1698
CRACK      8.660254     -87.5 3.660254 -78.8397
CRACK      16.82050 -81.6339 9.820508 -69.5096
CRACK      24.98076 -75.7679 15.98076 -60.1794
CRACK      33.14101 -69.9019 22.14101 -50.8493
CRACK      41.30127 -64.0358 28.30127 -41.5192
CRACK      49.46152 -58.1698 34.46152 -32.1891
CRACK      57.62177 -52.3038 40.62177 -22.8589
CRACK      65.78203 -46.4378 46.78203 -13.5288
CRACK      73.94228 -40.5717 52.94228 -4.19872
SAVE GB2
*CRACK BASE OF BLOCKS
CRACK            0     -92.5 8.660254     -87.5
CRACK      8.160254 -86.6339 16.82050 -81.6339
CRACK      16.32050 -80.7679 24.98076 -75.7679
CRACK      24.48076 -74.9019 33.14101 -69.9019
CRACK      32.64101 -69.0358 41.30127 -64.0358
CRACK      40.80127 -63.1698 49.46152 -58.1698
CRACK      48.96152 -57.3038 57.62177 -52.3038
CRACK      57.12177 -51.4378 65.78203 -46.4378
CRACK      65.28203 -45.5717 73.94228 -40.5717
CRACK      73.44228 -39.7057 82.10254 -34.7057
CRACK      81.60254 -33.8397 90.26279 -28.8397
CRACK      89.76279 -27.9737 98.42304 -22.9737
CRACK      97.92304 -22.1076 106.5833 -17.1076
CRACK      106.0833 -16.2416 114.7435 -11.2416
CRACK      114.2435 -10.3756 122.9038 -5.37564
CRACK      122.4038 -4.50961 131.0640 0.490381
SAVE GB3
* CRACK OFF TOP OF BLOCKS
CRACK      6.160254 -83.1698      -2.5 -88.1698
CRACK      12.32050 -73.8397 3.660254 -78.8397
CRACK      18.48076 -64.5096 9.820508 -69.5096
CRACK      24.64101 -55.1794 15.98076 -60.1794
CRACK      30.80127 -45.8493 22.14101 -50.8493
CRACK      36.96152 -36.5192 28.30127 -41.5192
```

```
CRACK        43.12177  -27.1891  34.46152  -32.1891
CRACK        49.28203  -17.8589  40.62177  -22.8589
CRACK        55.44228  -8.52885  46.78203  -13.5288
CRACK        61.60254  0.801270  52.94228  -4.19872
CRACK        72.76279  1.471143  64.10254  -3.52885
CRACK        83.92304  2.141016  75.26279  -2.85898
CRACK        95.08330  2.810889  86.42304  -2.18911
CRACK        106.2435  3.480762  97.58330  -1.51923
CRACK        117.4038  4.150635  108.7435  -0.84936
CRACK        128.5640  4.820508  119.9038  -0.17949
SAVE GB4
*DELETE SMALL BLOCKS LEFT ON SLOPE
DEL 0,133 -100,10 26
**CRACK BASE BLOCK
CRACK -8.660254,-97.5 0,-92.5
SAVE GB5
**PROPERTIES FOR MATERIAL 1 (AREA CONTACT):CONS=1, JCONS=2
PROP MAT=1 DENS=.0025484 BULK=26974 G=25554 JKN=25000
PROP MAT=1 JKS=25000 JCOH=0 JTEN=0 JDIL=0 JFRIC=.80
SAVE GB6
**ASSIGN MATERIAL NUMBER, CONSTITUTIVE LAW
CHANGE MAT=1 CONS=1 JCONS=2
SAVE GB7
**SET BOUNDARY CONDITIONS: FIX BOTTOM AND END BLOCK
FIX 60 100 -80 -40
FIX -10 0 -100 -90
*SET HISTORIES
HIST XVEL 52,-4 YVEL 52,-4 XDIS 52,-4 YDIS 52,-4 XVEL 96 -2.5
HIST YVEL 96 -2.5 XDIS 96 -2.5 YDIS 96 -2.5
HIST DAMP
**APPLY GRAVITY TO BLOCKS
GRAVITY 0 -9.81
SAVE GB8
FRAC=.1
DAMP AUTO
CYCLE=0
SAVE GB9
cycle=5000
save gb10
del -10 0 -100 -90
gravity 0 -9.81
save gb10a
STOP
```

```
**DATA FILE FOR KUK. FIG 4-13 **FDEF BLOCKS*
**100 times larger than base friction modeL
*********************************
START
ROUND .3
**CREATE CENTER AND SUPPORT BLOCKS**
BLOCK 0,0 76.2,0 76.2,-36.48 0,-36.48
CRACK -1,-30.48 77.2,-30.48
CRACK 73.15,1 73.15,-30.5
CRACK 3.048,0 3.048,-30.5
SAVE F1
**FIX VELOCITIES OF BOUNDARY SUPPORT BLOCKS**
FIX 0,76.2 -36.5,-30.5
FIX 73.2,76 -30.5,0
FIX 0 3.0 -30,0
**CREATE CENTER BLOCK PROPERTIES**
PROP MAT=1 DEN=.0026 BULK=10500 G=5700 COH=.15 FRIC=1
JKN=15000
+ JKS=10000
PROP MAT=1 TENS=.1 JCOH=0 JTENS=0 JFRIC=.81 DIL=0
PROP MAT=3 DEN=.0026 BULK=10000 G=10000 JKS=10000 JKN=15000
+ JFRIC=.81
PROP MAT=3 FRIC=1 COH=1 TENS=.1 DIL=0
**CREATE JOINTS**
JREGION 1.5,0 73.15,0 73.15,-30.5 4,-30.5
JSET -60,0 80,0 0,0 5.08,0 21.33,-30.48
**CRACK FOR LATER EXCAVATION**
CRACK 21.33,-30.48 28.017,.978
**ASSIGN BLOCK AND JOINT PROPERTIES TO FDEF ZONE AND SUPPORT**
CHANGE 3.046,73.16 -30.5,0 MAT=1 Cons=3 JCons=2 JMat=1
GENER REG 21.33,-30.5 27.8,0 73.1,0 73.1,-30.5 QUAD 2.2
GENER REG 21.33,-30.5 27.8,0 73.1,0 73.1,-30.5 EDGE 3.6
GENER REG 3.048,0 27,0 21,-30 3.048,-30 EDGE 10
**STIFFEN SUPPORT BLOCKS ALLOWING MAT=1 JOINT ON BOUNDARIES**
CHANGE 0,77 -36,-29 MAT=3 JMAT=1 CONS=1
CHANGE 0,4.0 -30.5,0 MAT=3 JMAT=1 CONS=1
CHANGE 72 77 -30,0 MAT=3 JMAT=1 CONS=1
**ASSIGN HISTORIES ON FACE AT TOP BOTTOM AND MIDDLE**
HIST XVEL 27.8,-1.5 YVEL 27.8,-1.5 XDIS 27.8,-1.5 YDIS 27.8,-
1.5
HIST XVEL 21.35,-30.47 YVEL 21.35,-30.47 XDIS 21.35,-30.47
HIST YDIS 21.35,-30.47 DAMP TYPE 9
HIST XVEL 24.49,-15.63 YVEL 24.49 -15.63 XDIS 24.49 -15.63
HIST YDIS 24.49 -15.63
HIST TYPE 1
**CONSOLIDATE CENTER BLOCKS**
INSITU 3,73 -30.5 0 STR 0,0,0 YGRAD .0265, 0, .0265
GRAVITY 0,-9.81
FRAC=.2
DAMP AUTO
save F2
CYC 0
```

```
SAVE F2
CYC 2000
SAVE F3
**EXCAVATE SLOPE**
DEL 0,21.33 -30.48,0
DEL 21.33 27.80 -20 0
**RESET RECORDS
RESET DISP HIST JDISP TIME ROTA
**RE-ASSIGN HISTORIES ON FACE AT TOP MIDDLE AND BOTTOM**
HIST XVEL 29,-2 YVEL 29,-2 XDIS 29,-2 YDIS 29,-2
HIST XVEL 21.35,-30.47 YVEL 21.35,-30.47 XDIS 21.35,-30.47
HIST YDIS 21.35,-30.47 DAMP TYPE 9
HIST XVEL 24.49,-15.63 YVEL 24.49 -15.63 XDIS 24.49 -15.63
HIST YDIS 24.49 -15.63
HIST TYPE 1
frac=.2
**APPLY GRAVITY TO SLOPE**
gravity 0 -9.81
HIST NCYC 50
SAVE F4
STOP
**(From this point reduce strength of rock and joints to
failure)
```

```
**DATA FILE FOR BRENDA MINES SLOPE, **FDEF BLOCKS*
************************************
START
ROUND 1.
**CREATE CENTER AND SUPPORT BLOCKS**
BLOCK 0,0  800,0  800,-300  0,-300
**BENCH FACE CRACKS
CRACK      440.000       0.000  459.0498  -30.4798
CRACK      470.480     -30.480  489.5298  -60.9593
CRACK      500.960     -60.960  520.0099  -91.4389
CRACK      531.440     -91.439  550.4900 -121.918
CRACK      561.919    -121.919  580.9701 -152.398
CRACK      592.399    -152.399  611.4502 -182.877
CRACK      622.879    -182.879  641.9303 -213.357
**BENCH LEVEL CRACKS
CRACK    459.0498  -30.4798    800.000    -30.480
CRACK    489.5298  -60.9593    800.000    -60.960
CRACK    520.0099  -91.4389    800.000    -91.439
CRACK    550.4900 -121.918     800.000   -121.919
CRACK    580.9701 -152.398     800.000   -152.399
CRACK    611.4502 -182.877     800.000   -182.879
CRACK    641.9303 -213.357     800.000   -213.357
**CREATE CENTER BLOCK PROPERTIES**
PROP MAT=1 DEN=.0027 BULK=33333 G=20000 COH=.15 FRIC=.70
+ JKN=40000 JKS=20000
PROP MAT=1 TENS=.21 JCOH=0 JTENS=0 JFRIC=.466 DIL=0
PROP JMAT=2 JKN=40000 JKS=20000 JCOH=3 JTENS=5 JFRIC=.84
**CRACK TO DIVIDE FDEF ZONES**
CRACK 0,-150 626.653,-300
**CREATE JOINT SET**
JREGION 0,0 800,0 800,-300 0,-300
JSET 80,0 400,0 0,0 27.43,0 641.9303,-213.357
SAVE BR1
**ASSIGN BLOCK AND JOINT PROPERTIES TO FDEF ZONES*
CHANGE MAT=1 Cons=3 JCons=2 JMat=1
**BASE BLOCK
GENER REG 0,-300 0,-150 626.6,-299 626.6,-301 EDGE 90
**TOE REGION
GENER REG 641.9,-213.3 800,-213.3 800,-300 626.6,-300 EDGE 60
**MATERIAL TO BE EXCAVATED CLOSE TO FACE
GENER REG 440,0 500,0 800,-213.4 641.9,-213.4 EDGE 60
**MATERIAL TO BE EXCAVATED FAR FROM FACE
GENER REG 500,-1 500,1 800,0 800,-213.358 EDGE 90
**MAIN SLOPE
GENER REG 216.8,-188.2 250,0 641.9,-213.3 633.4,-261.67 EDGE
32
GENER REG 0,0 250,0 216.8,-188.2 0,-150 EDGE 90
**FIX ARTIFICIAL CRACK AND EXCAVATION LEVEL CRACKS**
CHANGE ANGLE -15,1 JMAT=2
**ASSIGN HISTORIES ON FACE AT TOP MIDDLE AND BOTTOM**
**TOP OF BENCH 1
HIST XVEL 440.000,0.000 YVEL 440,0 XDIS 440,0 YDIS 440,0
```

```
**TOP OF BENCH 2
HIST XVEL 470.48,-30.48 YVEL 470.48,-30.48
HIST XDIS 470.48,-30.48 YDIS 470.48,-30.48
**TOP OF BENCH 3
HIST XVEL 500.96,-60.96 YVEL 500.96,-60.96
HIST XDIS 500.96,-60.96 YDIS 500.96,-60.96
**TOP OF BENCH 4
HIST XVEL 531.44,-91.44 YVEL 531.44,-91.44
HIST XDIS 531.44,-91.44 YDIS 531.44,-91.44
**TOP OF BENCH 5
HIST XVEL 561.92,-121.92 YVEL 561.92,-121.92
HIST XDIS 561.92,-121.92 YDIS 561.92,-121.92
**TOP OF BENCH 6
HIST XVEL 592.40 -152.40 YVEL 592.40,-152.40
HIST XDIS 592.40 -152.40 YDIS 592.40,-152.40
**TOP OF BENCH 7
HIST XVEL 622.88 -182.88 YVEL 622.88,-182.88
HIST XDIS 622.88 -182.88 YDIS 622.88,-182.88
**BASE OF SLOPE
HIST XVEL 641.9,-213.4 YVEL 641.9,-213.4
HIST XDIS 641.9,-213.4 YDIS 641.9,-213.4
HIST DAMP TYPE 9
**ASSIGN BOUNDARY CONDITIONS**
BOUND 0,800 -301,-299 YVEL=0
BOUND -1,1 -300,0 XVEL=0
BOUND 799,801 -300,0 XVEL=0
**CONSOLIDATE STABLE PROBLEM**
GRAVITY 0,-9.81
FRAC=.1
DAMP AUTO
save BR2
CYC 0
SAVE BR3
CYC 7500
SAVE BR4
**EXCAVATE FIRST TWO BENCHES
DEL 440,800 -60,0 AREA=1000
**APPLY GRAVITY TO SLOPE**
CYC 5000
SAVE BR5
**EXCAVATE NEXT TWO BENCHES
DEL 440,800 -121,0 AREA=1000
CYC 5000
SAVE BR6
DEL 440,800 -183,0 AREA=1000
CYC 5000
SAVE BR7
DEL 440,800 -213,0 AREA=1000
CYC 5000
SAVE BR8
STOP
**(Continue by lowering joint friction angle to failure)
```
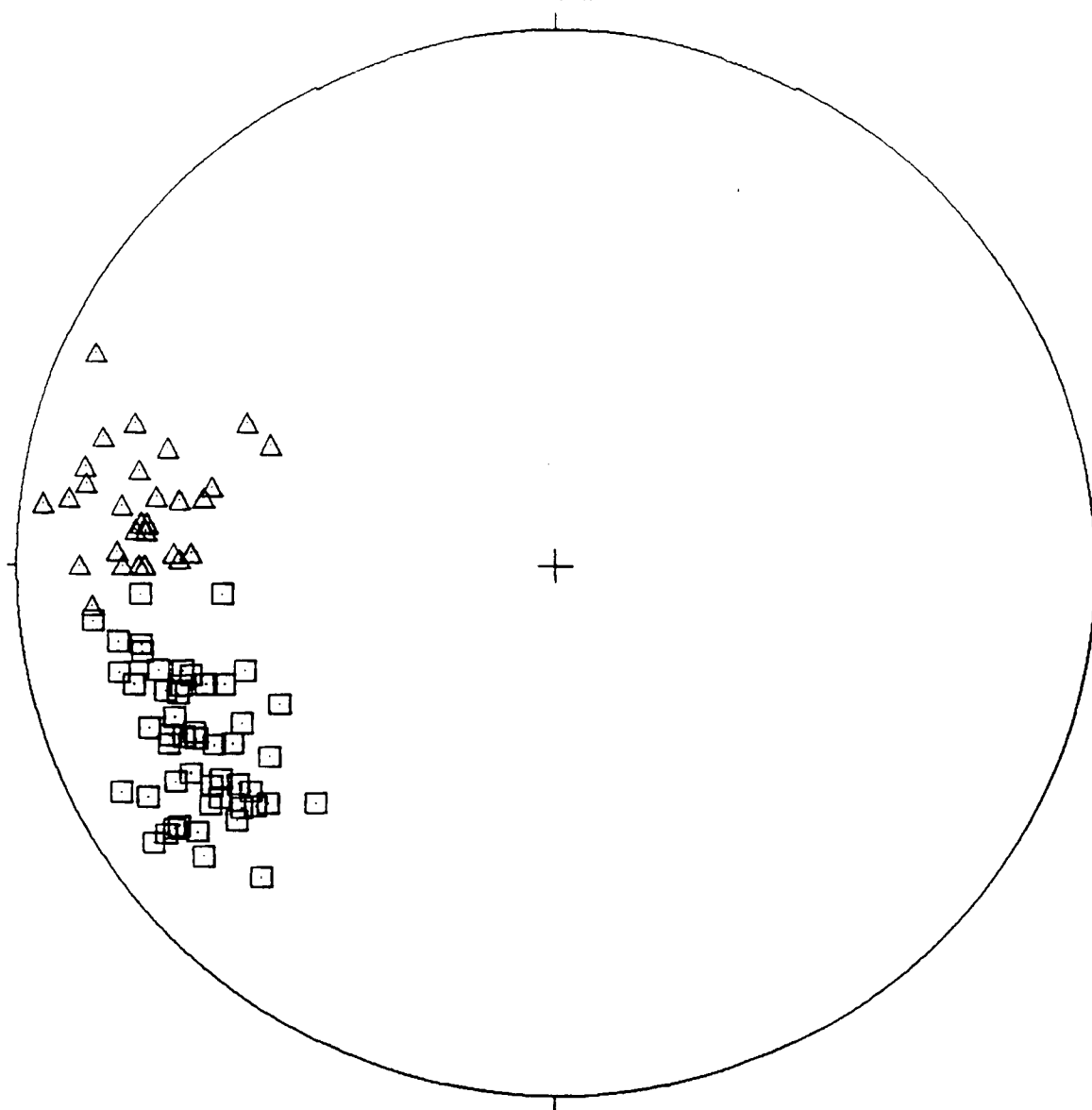
APPENDIX 2

Structural Data from Heather Hill Study Area

The stereographic projections contained in this appendix are equal area projections (Schmidt net), and were processed using software available in the Geology Department at UBC.
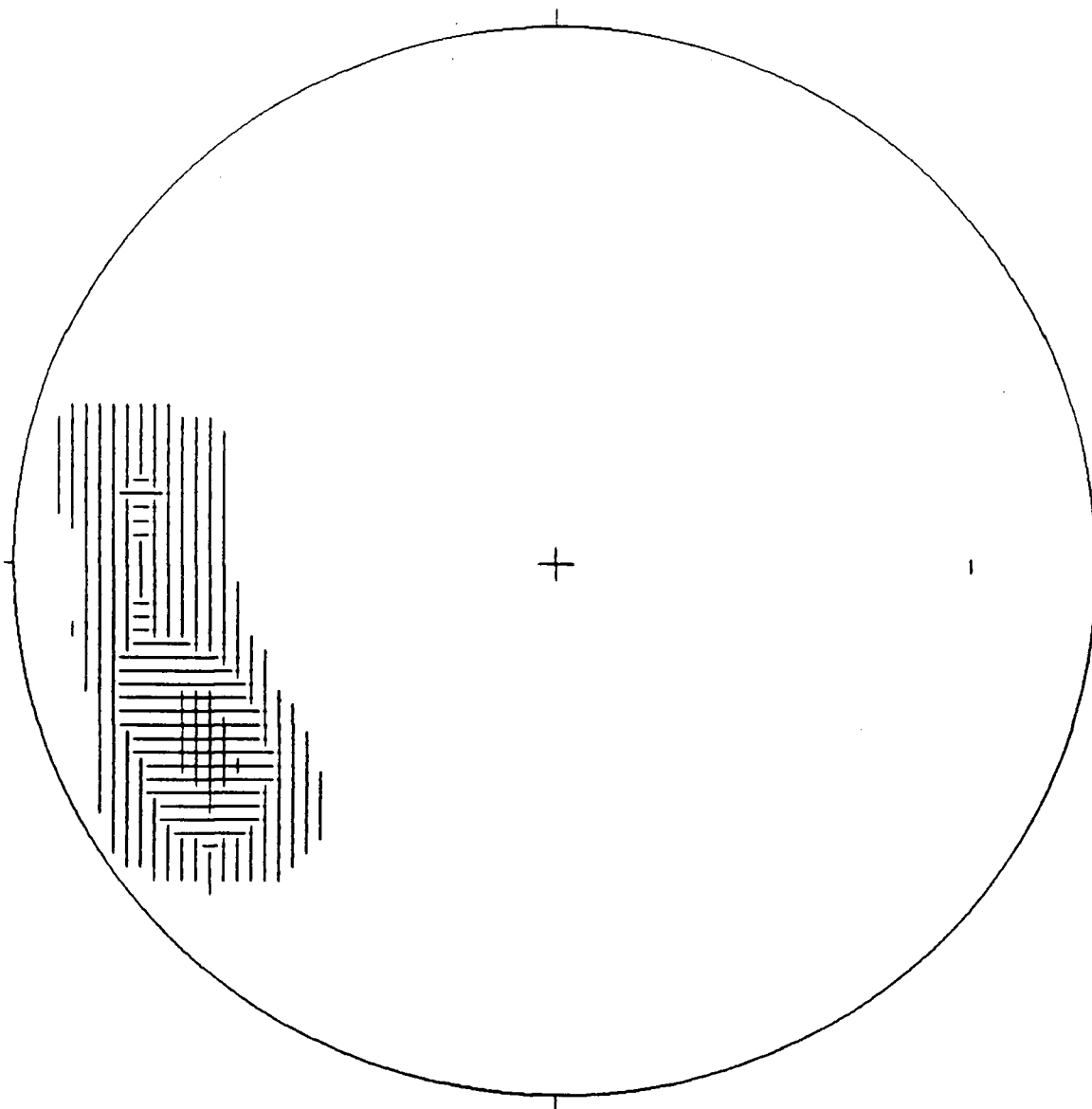
CREEK A S0 BEDDING AND S2 CLEAVAGE
North

EQUAL AREA PROJECTION   Symbol

S0 Bedding Foliation, Creek A   30 Points   □
FOLIATIONS, LOWER PART CRKA, SEPT 23,1988   22 Points   □
CRENULATION CLEAVAGES IN CREEK "A"   17 Points   △
CREN., CLEAVAGE, LOWER PART CRKA, SEPT 23, 1988 12 Points   △

                                                 81 Points Total

CREEK A SO BEDDING AND S2 CLEAVAGE: CONTOUR PLOT
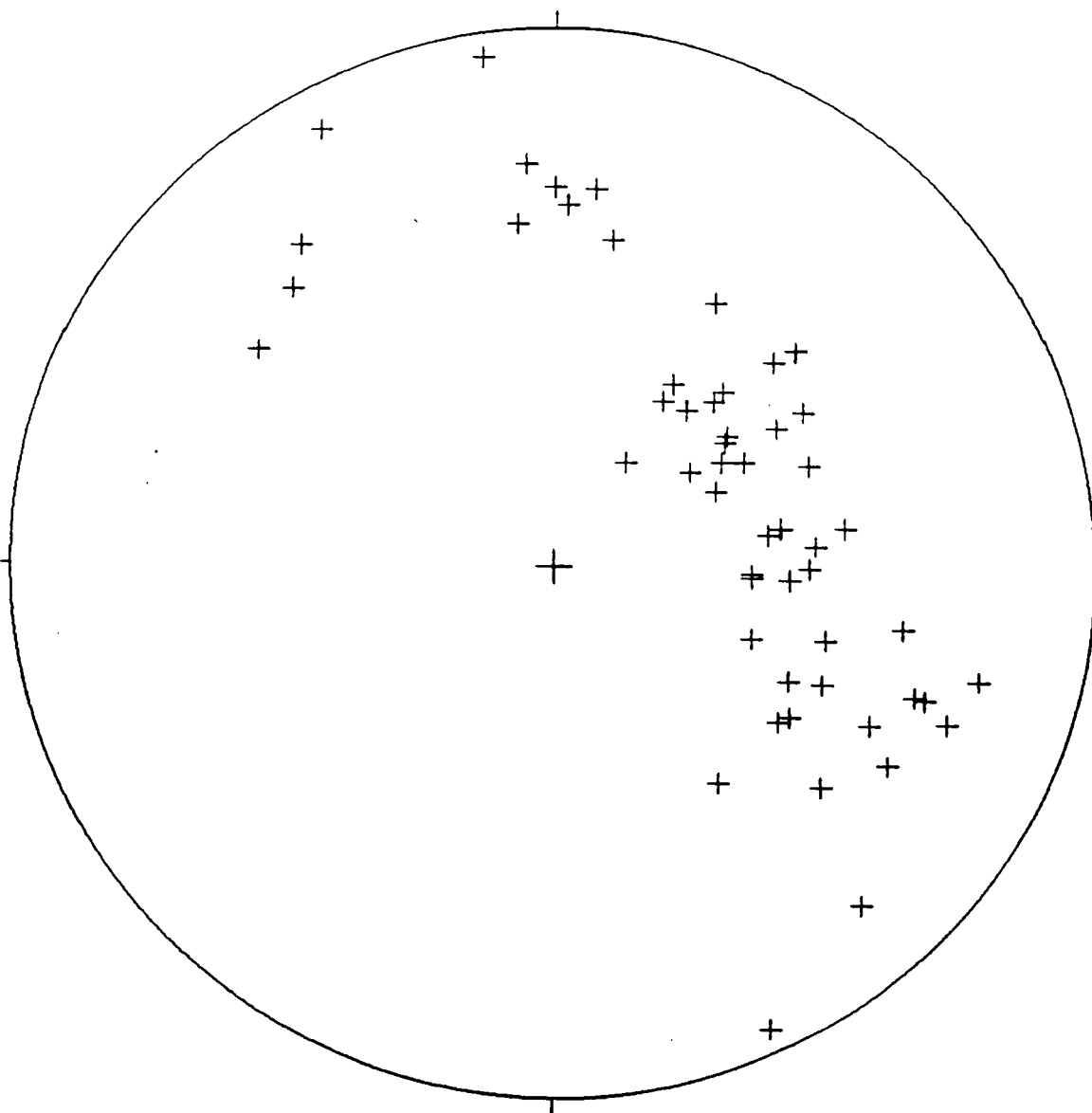North

81 Points

LEGEND (for first 9 intervals)

⊞	1- 7	▨	36- 42	
⊟	8- 14	▧	43- 49	
⊞	15- 21	▨	50- 56	
⊞	22- 28	■	57- 63	
⊞	29- 35			

Contour Method: Schmidt (1925)
Counting Area: 0.010
Contour Interval: 7% Points per 1% Area
Maximum Contour: 21

NOTE: Contour Patterns Repeat Every 9 Intervals
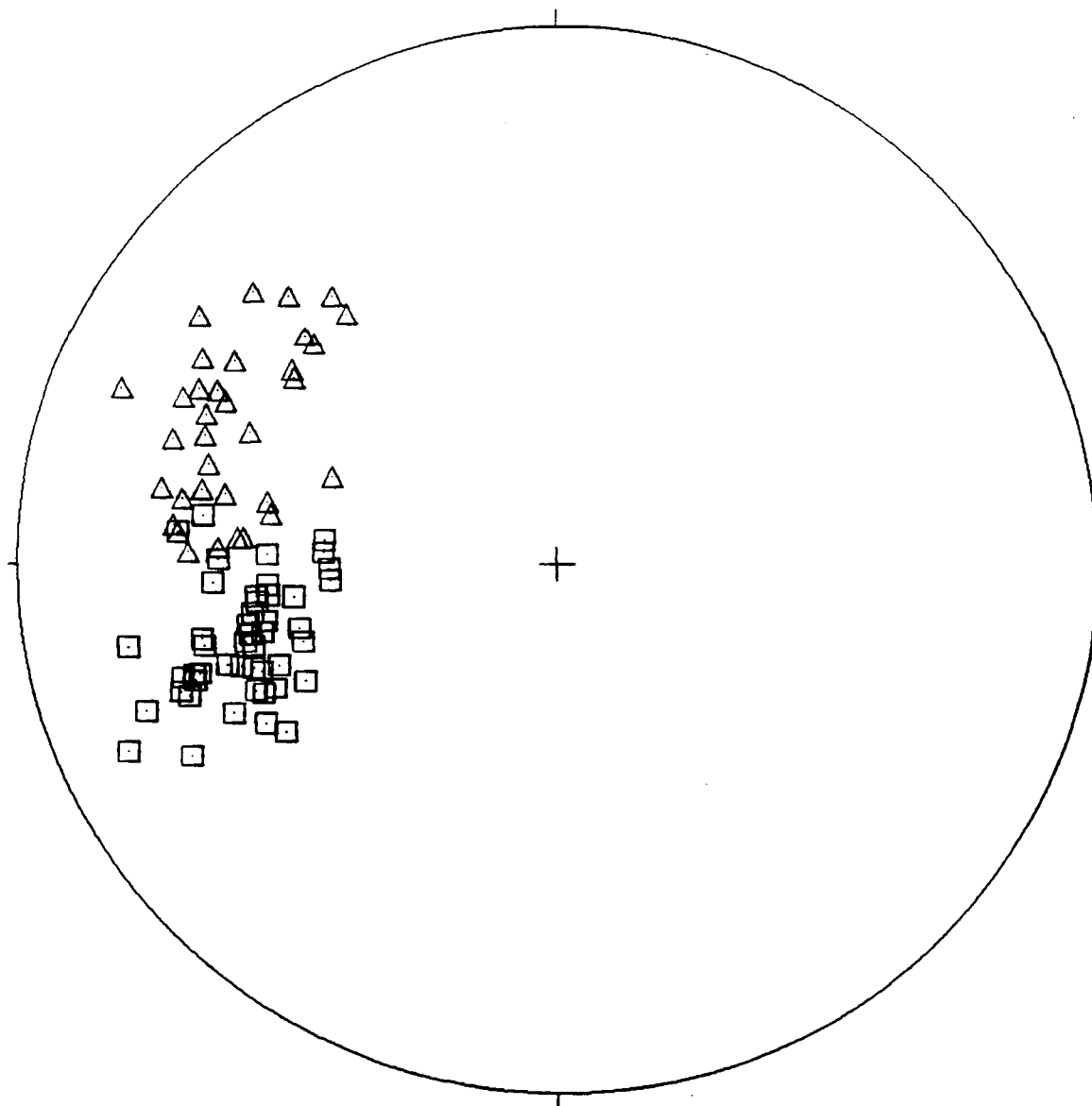
CREEK A: JOINT PLOT
North

EQUAL AREA PROJECTION

Joint Readings, Creek A, Aug. 4,5 1988
Joint Readings, Creek A, Sept. 23

	Symbol
21 Points	+
33 Points	+
54 Points Total	

CREEK B BEDDING AND S2 CLEAVAGE
North

EQUAL AREA PROJECTION   Symbol

SO Bedding Foliation, Creek B   34 Points   □
SO Bedding Foliation, Creek B, Sept. 11,12 1988   14 Points   □
S2 Cleavage Foliation, Creek B   30 Points   △
S2 Cleavage Foliation, Creek B, Sept. 1988   6 Points   △
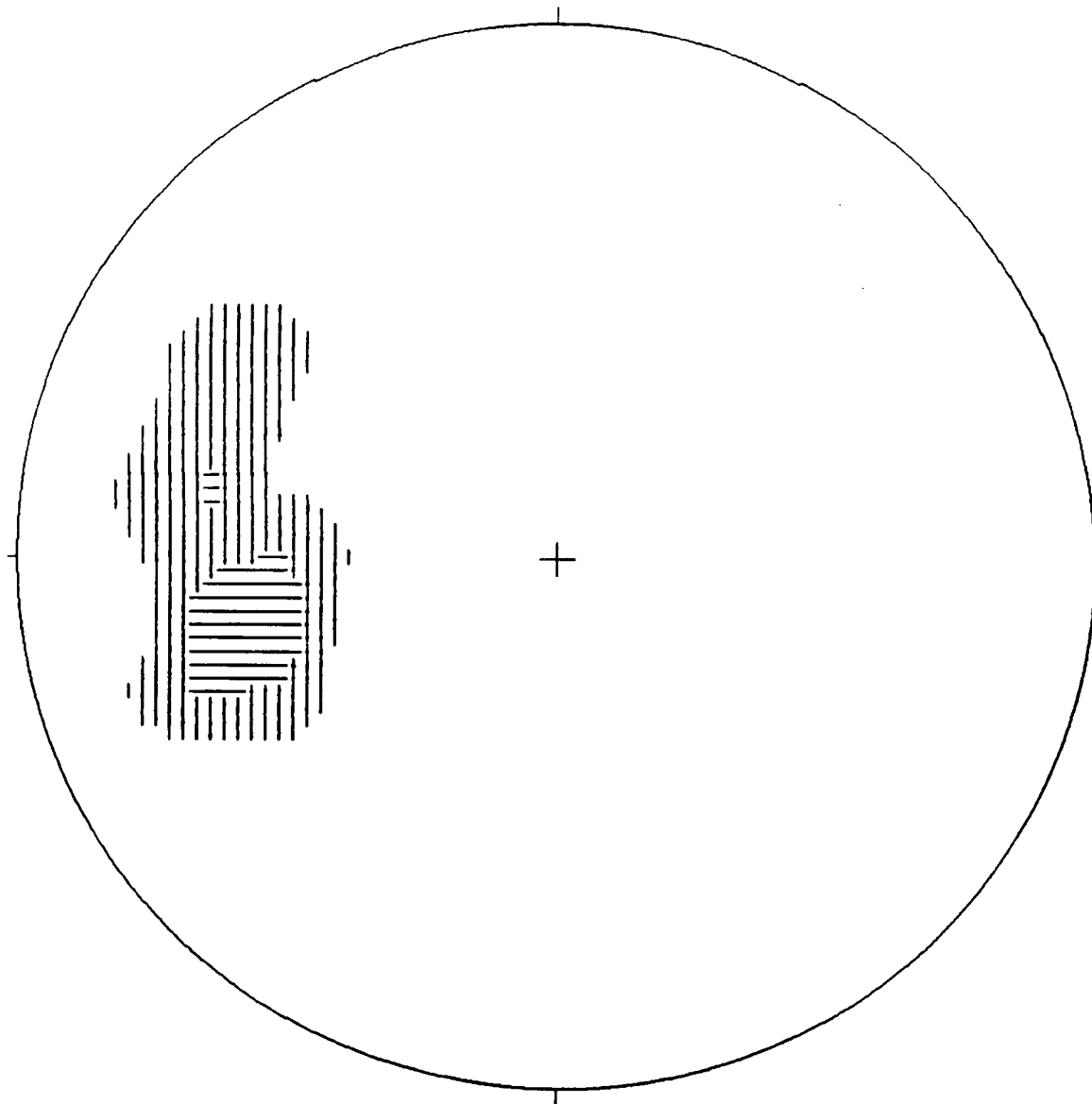
                                                             84 Points Total

CREEK B S0 BEDDING AND S2 CLEAVAGE: CONTOUR PLOT
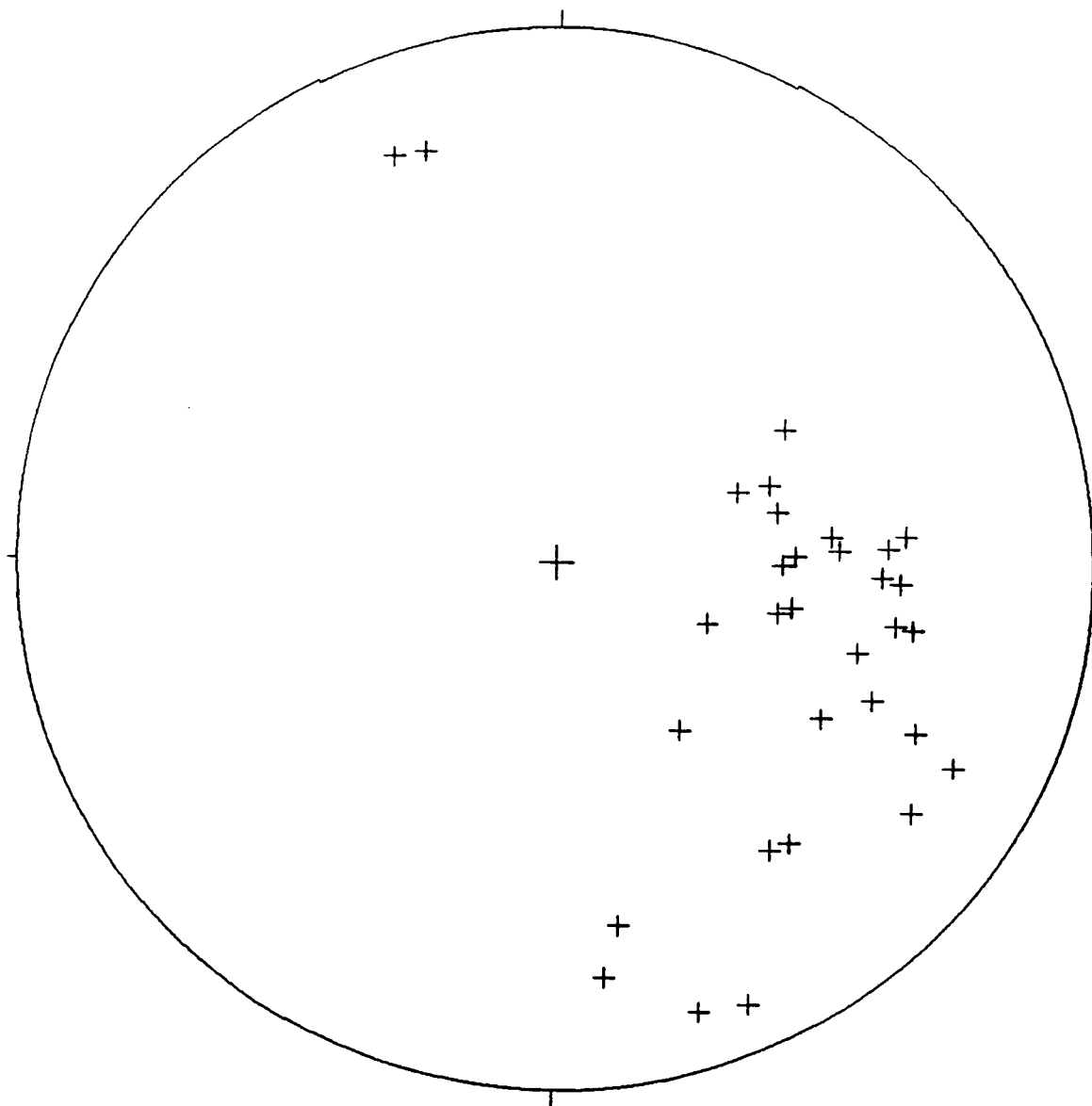North

84 Points

LEGEND (for first 9 intervals)
⊞	1- 9	▨ 46- 54
⊟	10- 18	▨ 55- 63
⊞	19- 27	▨ 64- 72
⊞	28- 36	■ 73- 81
⊞	37- 45	

Contour Method: Schmidt (1925)
Counting Area: 0.010
Contour Interval: 9% Points per 1% Area
Maximum Contour: 18

NOTE: Contour Patterns Repeat Every 9 Intervals
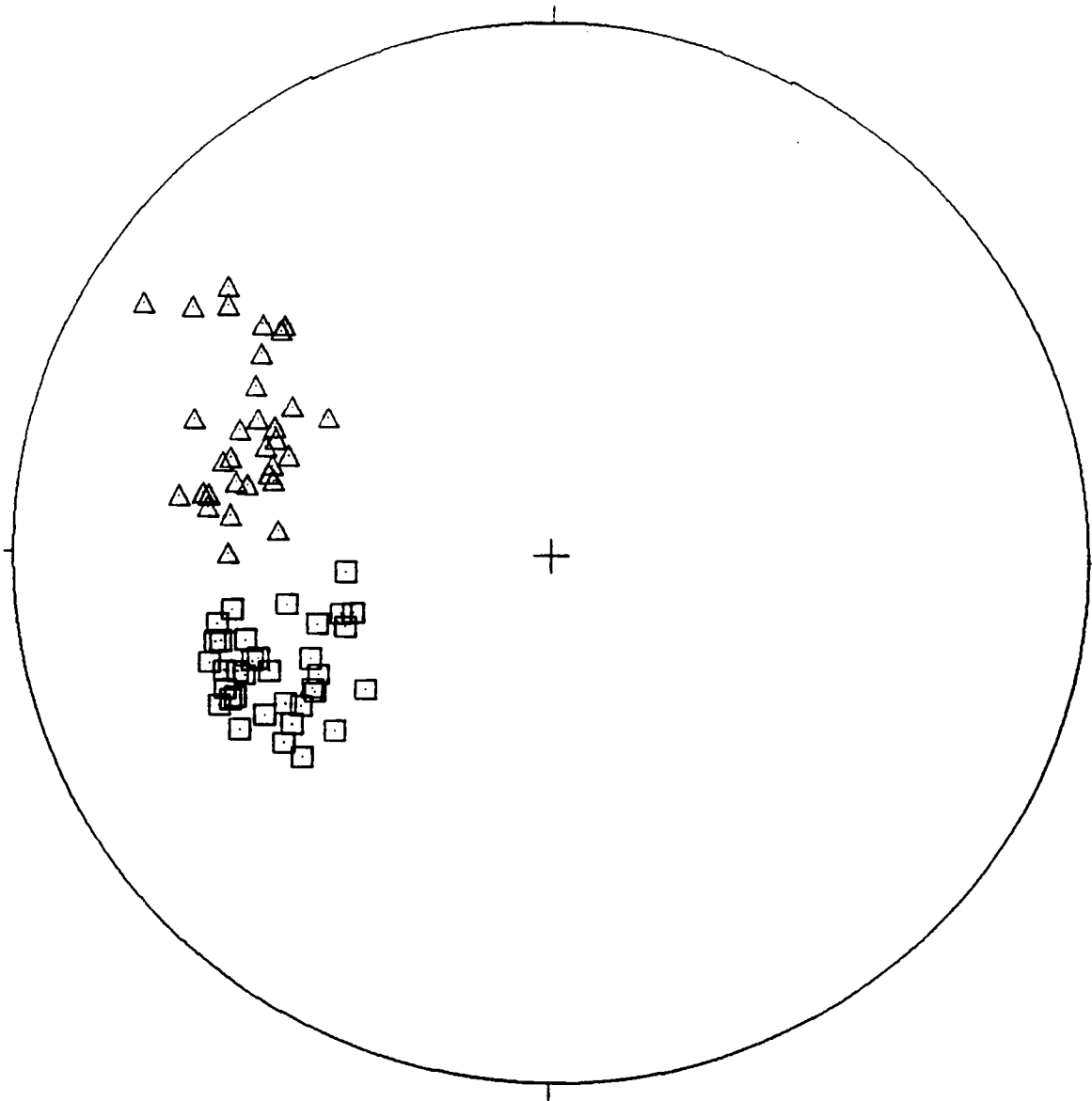
CREEK B: JOINT PLOT
North

EQUAL AREA PROJECTION

Joint Measurements in Creek B
Joint Measurements in Creek B, Sept. 23, 1988

Symbol
------
31 Points   +
1 Points   +

32 Points Total

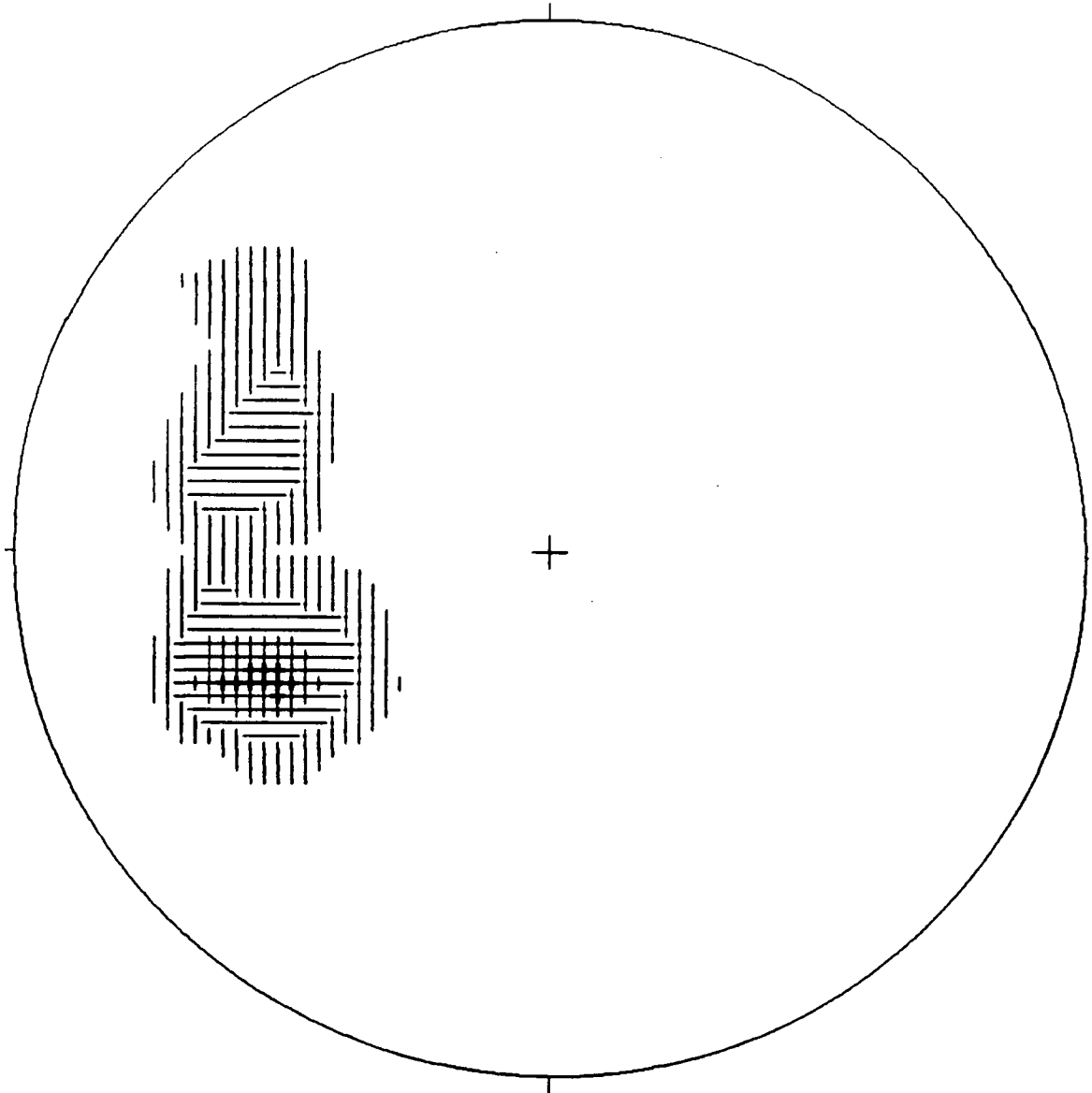CREEK C SO BEDDING AND S2 CLEAVAGE
North

EQUAL AREA PROJECTION

SO Bedding Foliation Creek C
S2 Cleavage Foliation, Creek C

Symbol
------

38 Points   □
32 Points   Δ

70 Points Total

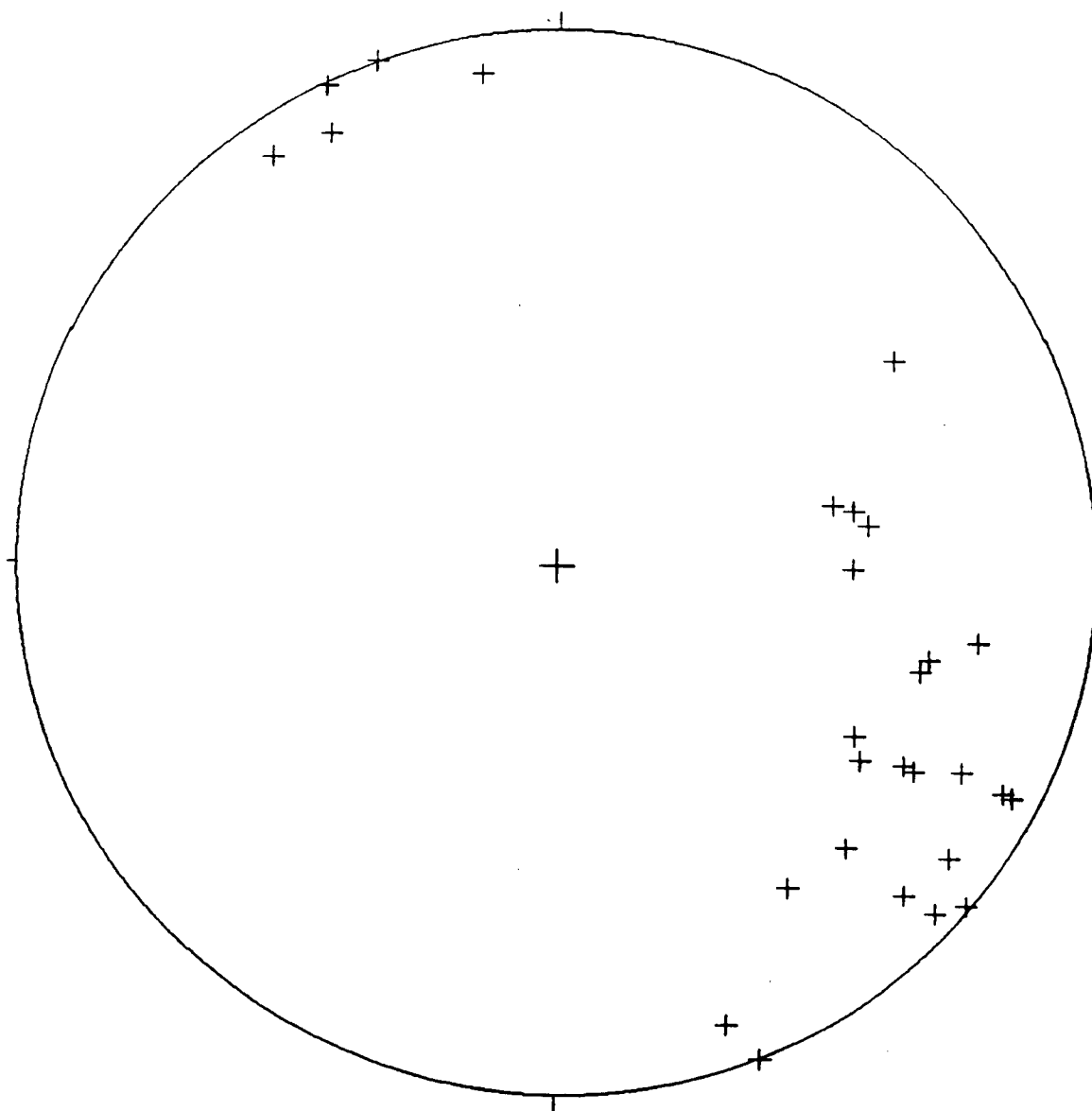CREEK C S0 BEDDING AND S2 CLEAVAGE: CONTOUR PLOT
North

70 Points

⊞	1- 6	◩	31- 36
⊟	7- 12	▨	37- 42
⊞	13- 18	▩	43- 48
⊞	19- 24	■	49- 54
⊞	25- 30		

Contour Method: Schmidt (1925)
Counting Area: 0.010
Contour Interval: 6% Points per 1% Area
Maximum Contour: 24

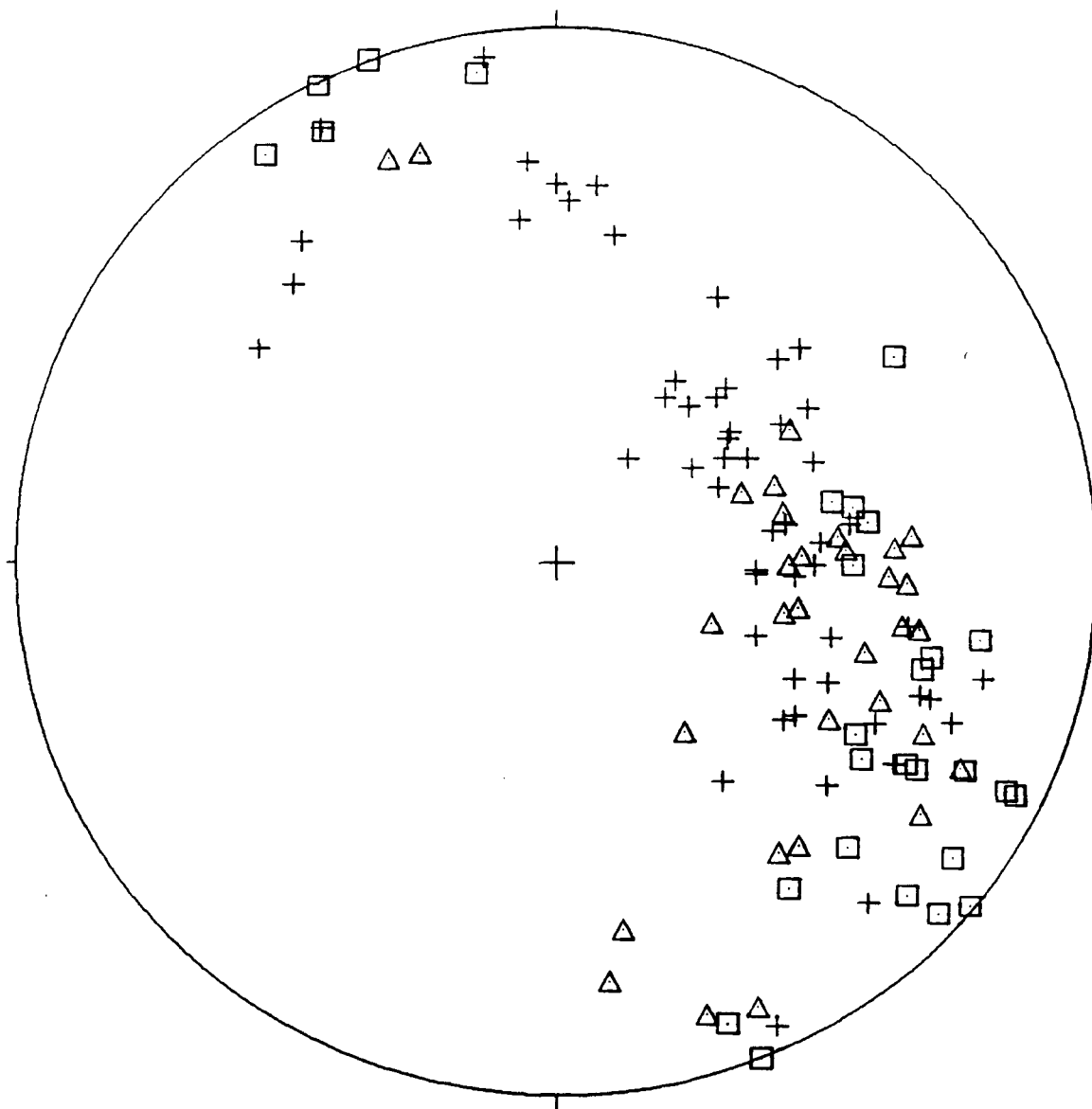NOTE: Contour Patterns Repeat Every 9 Intervals

Joint Orientations, Creek C
North

EQUAL AREA PROJECTION

Joint Orientations, Creek C

Symbol
------

29 Points   +

29 Points Total
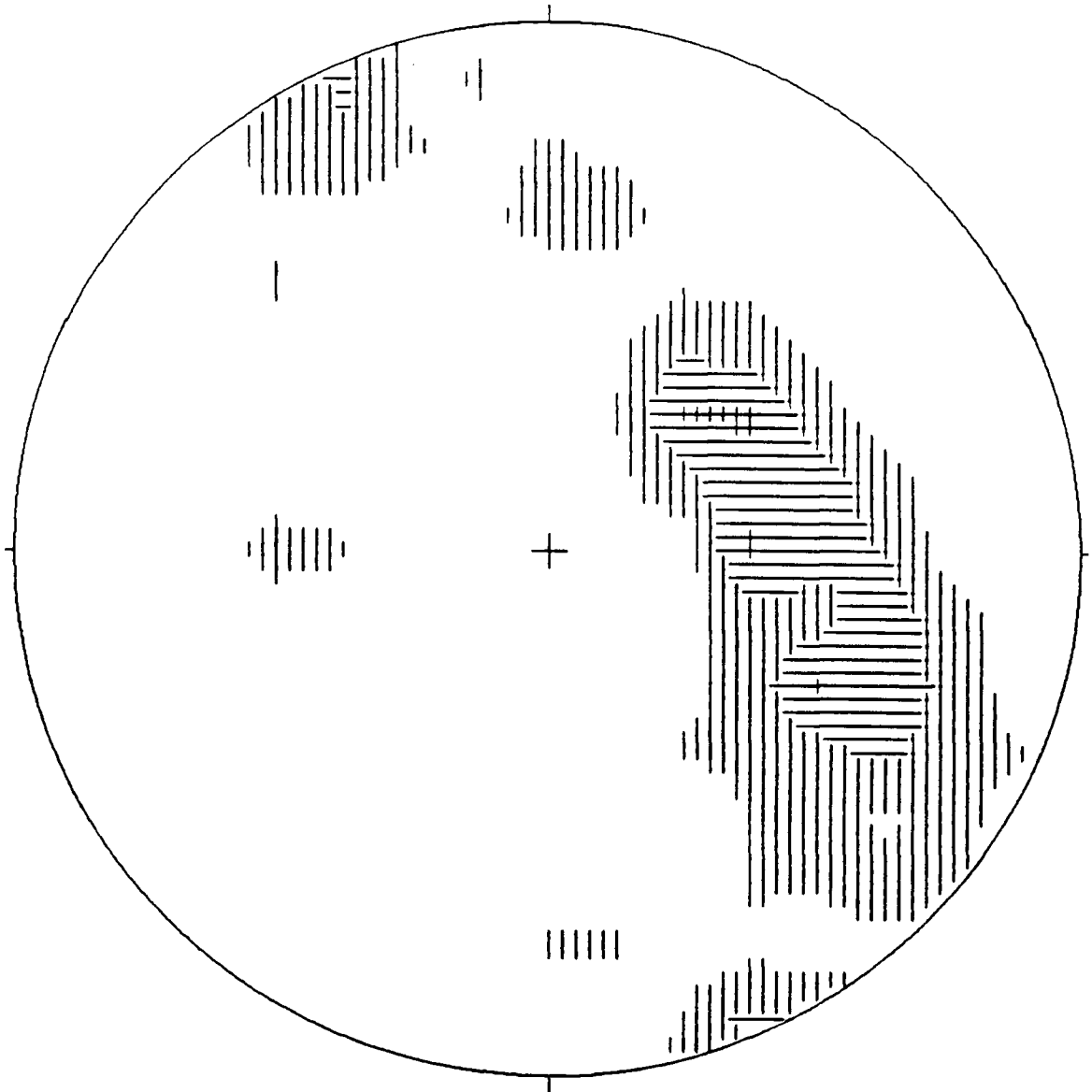
JOINT PLOT FOR CREEK A, B, AND C
North

EQUAL AREA PROJECTION

		Symbol
Joint Readings, Creek A, Aug. 4,5 1988	21 Points	+
Joint Readings, Creek A, Sept. 23	33 Points	+
Joint Measurements in Creek B	31 Points	Δ
Joint Measurements in Creek B, Sept. 23, 1988	1 Points	Δ
Joint Orientations, Creek C	29 Points	□

115 Points Total

COUNTOUR PLOT OF POLES TO ALL JOINTS
North

115 Points

LEGEND (for first 9 intervals)

	1- 3		16- 18
	4- 6		19- 21
	7- 9		22- 24
	10- 12		25- 27
	13- 15		

Contour Method: Schmidt (1925)
Counting Area: 0.010
Contour Interval: 3% Points per 1% Area
Maximum Contour: 9

NOTE: Contour Patterns Repeat Every 9 Intervals

SCARP TRAVERSE S0 BEDDING AND S2 CLEAVAGE
North
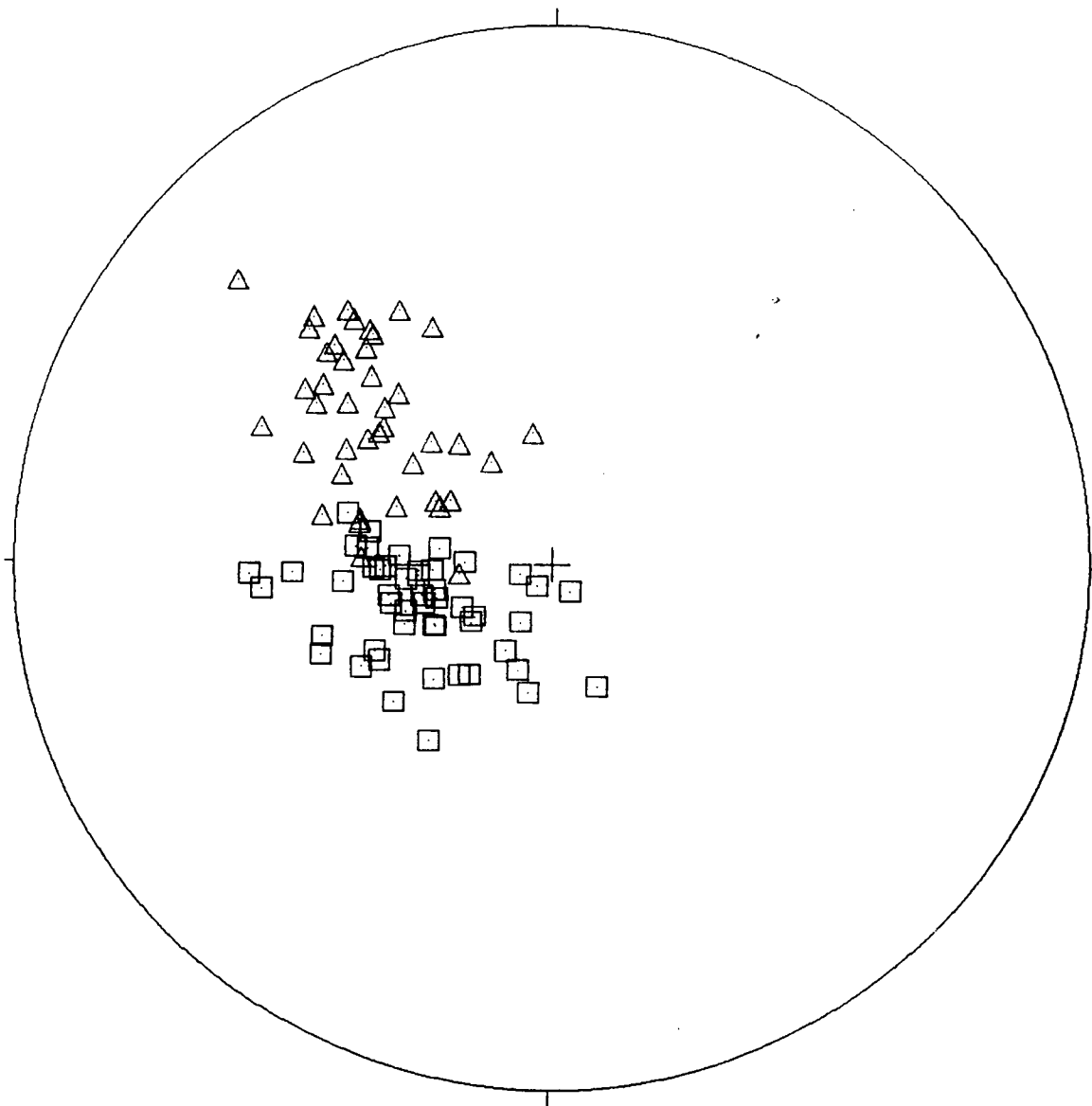
EQUAL AREA PROJECTION   Symbol

S0 BEDDING FOLIATION, SCARP, AUG. 10,11,13   54 Points   □
S0 BEDDING FOLIATION UP SCARP FROM STA.137, AUG 11   4 Points   □
S2 CRENULATION CLEAVAGE, SCARP, AUG. 10,11,13   41 Points   △
S2 CRENULATION CLEAVAGE UP SCARP FROM STA. 137   3 Points   △
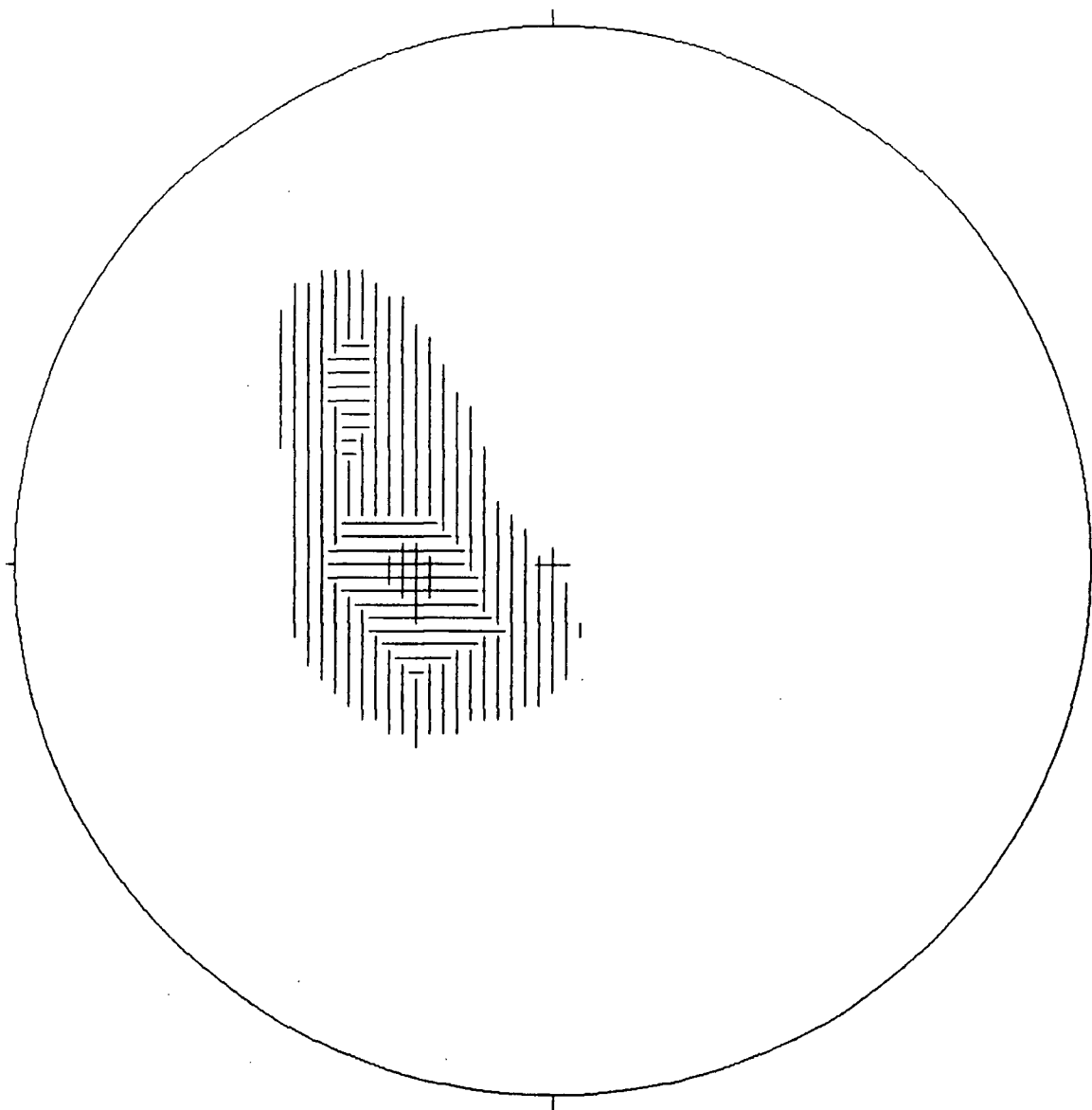
                                                           102 Points Total

SCARP TRAV. SO BEDDING, S2 CLEAVAGE: CONTOUR PLOT
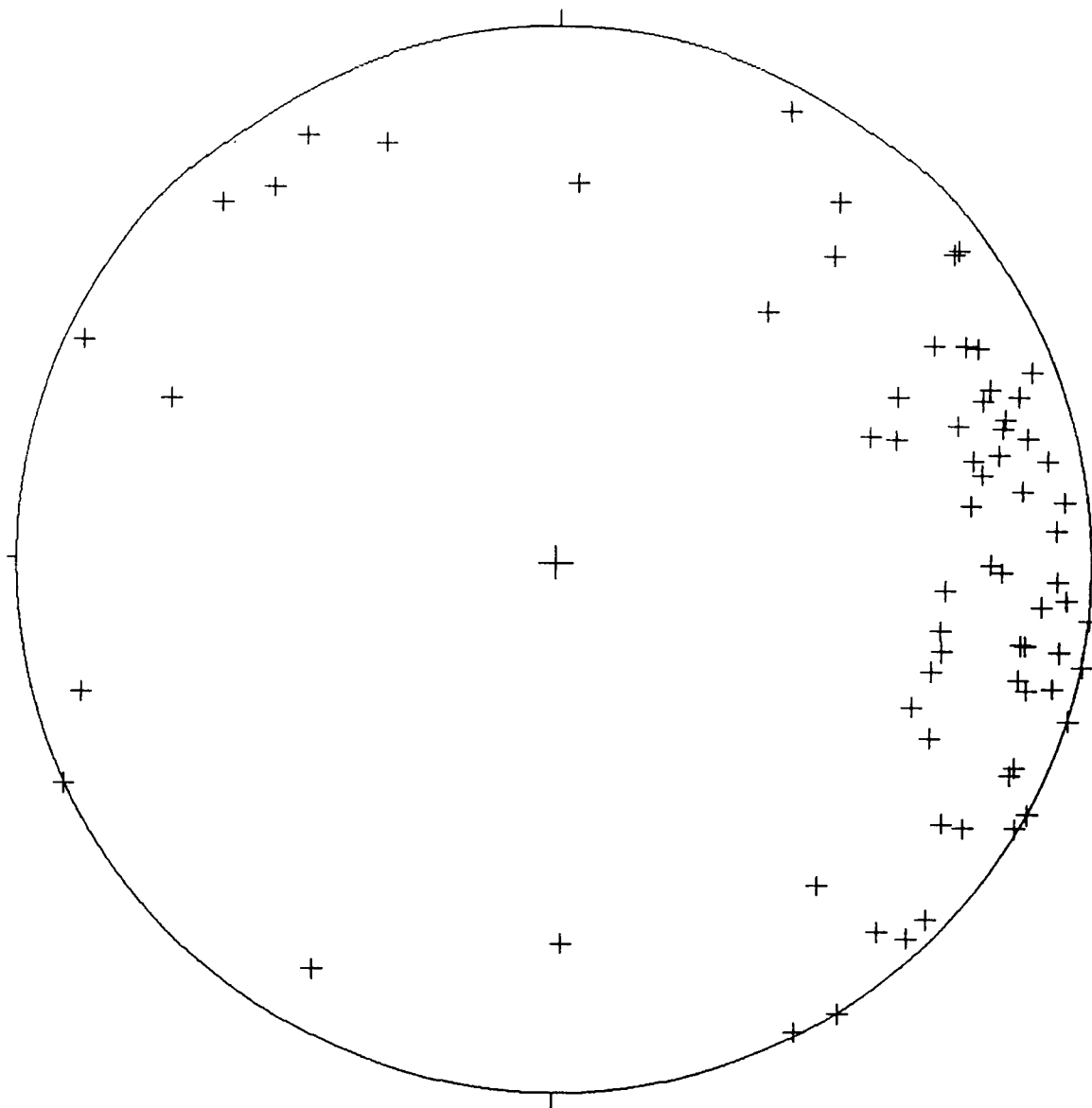
North

95 Points

LEGEND (for first 9 intervals)

⊞	1- 7	▨	36- 42
⊟	8- 14	▨	43- 49
⊞	15- 21	▨	50- 56
⊞	22- 28	■	57- 63
⊞	29- 35		

Contour Method: Schmidt (1925)
Counting Area: 0.010
Contour Interval: 7% Points per 1% Area
Maximum Contour: 21

NOTE: Contour Patterns Repeat Every 9 Intervals

JOINTS ON SCARP TRAVERSE, AUGUST 10, 11, 13, 1988
North

EQUAL AREA PROJECTION
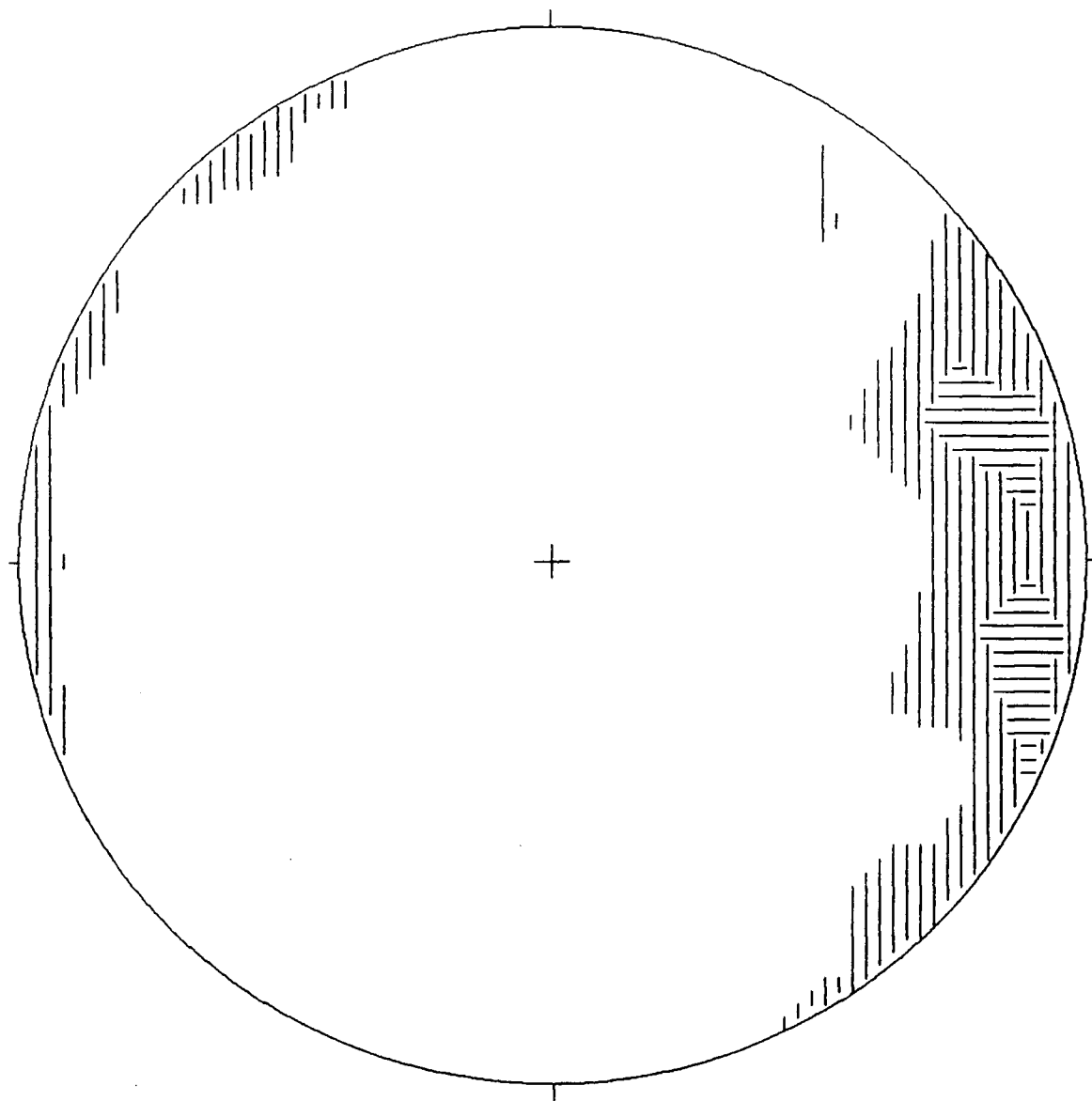
JOINTS ON SCARP TRAVERSE, AUGUST 10, 11, 13, 1988   71 Points

Symbol

+

71 Points Total

JOINTS ON SCARP TRAVERSE, AUGUST 10, 11, 13, 1988
North

71 Points

174

APPENDIX 3

Data Input File for UDEC Model of Heather Hill Landslide.

```
**DATA FILE FOR HEATHER HILL BASE **FDEF BLOCKS*
**New Data Deck, with changing spacing
**PRIMARY DISCONTINUITY DIP 65 DEG., PURE FLEXURE
**GRADATIONAL ROCK PROPERTIES
**********************************
START
ROUND 2.0
**CREATE CENTER AND SUPPORT BLOCKS**
BLOCK 0,0 2160,0 2160,-1300 0,-1300
**CRACK OFF CORNERS
CRACK 1890,20 2170,-600
CRACK 2200,-560 580,-1310
**FINAL SLOPE PROFILE CRACKS
CRACK  0,-870 340,-855
CRACK  340,-855 390,-840
CRACK  390,-840 450,-790
CRACK  450,-790 750,-530
CRACK  750,-530 1895,0
**FIRST LEVEL GLACIAL EXCAVATION CRACK AND VALLEY BOTTOM
CRACK  0,-790 450,-790
CRACK 350,-700 565,-700
CRACK  190,-790 750,-530
**INITIAL EXCAVATION LEVEL CRACKS
CRACK 0 -200 500,0
CRACK 0 -400 900 0
CRACK 0 -600 1300 0
CRACK 0 -750 1600 0
**DELETE CORNERS
DEL 1900,2200 -600,0
DEL 1400,2200 -1300,-900
*************
**CREATE INITIAL GRADATIONAL ROCK PROPERTIES**
**MAT=1**
PROP MAT=1 DEN=.0027 BULK=9500 G=8700 COH=.100 FRIC=.649
PROP MAT=1 JKN=1200 JKS=600
PROP MAT=1 TENS=.050 JCOH=0 JTENS=0 JFRIC=.404 JDIL=0
**MAT=2**
PROP MAT=2 DEN=.00269 BULK=9650 G=9100 JKS=1275 JKN=2550 JFRIC=.466
PROP MAT=2 FRIC=.687 COH=.150 TENS=.075 DIL=0 JTENS=0 JDIL=0 JCOH=0
**MAT=3**
PROP MAT=3 DEN=.00268 BULK=9800 G=9400 JKS=1800 JKN=3600 JFRIC=.532
PROP MAT=3 FRIC=.726 COH=.200 TENS=.100 DIL=0 JTENS=0 JDIL=0 JCOH=0
**MAT=4**
PROP MAT=4 DEN=.00267 BULK=9950 G=9750 JKS=2400 JKN=4800 JFRIC=.601
PROP MAT=4 FRIC=.781 COH=.250 TENS=.125 DIL=0 JTENS=0 JDIL=0 JCOH=0
**MAT=5**
PROP MAT=5 DEN=.00266 BULK=10100 G=10100 JKS=3000 JKN=6000
PROP MAT=5 JFRIC=.700
PROP MAT=5 FRIC=.854 COH=.300 TENS=.150 DIL=0 JTENS=0 JDIL=0 JCOH=0
**MAT=6**
PROP MAT=6 DEN=.00265 BULK=10250 G=10450 JKS=3600 JKN=7200
PROP MAT=6 JFRIC=.810
PROP MAT=6 FRIC=.933 COH=.350 TENS=.175 DIL=0 JTENS=0 JDIL=0 JCOH=0
```

```
**MAT=7**
PROP MAT=7 DEN=.00264 BULK=10400 G=10800 JKS=4200 JKN=8400
PROP MAT=7 JFRIC=.965 JCOH=0
PROP MAT=7 FRIC=1.036 COH=.400 TENS=.200 DIL=0 JTENS=0 JDIL=0
**MAT=8**
PROP MAT=8 DEN=.00263 BULK=10550 G=11150 JKS=4800 JKN=9600
PROP MAT=8 JFRIC=1.072 JCOH=0
PROP MAT=8 FRIC=1.150 COH=.450 TENS=.225 DIL=0 JTENS=0 JDIL=0
**MAT=9**
PROP MAT=9 DEN=.00262 BULK=10700 G=11500 JKS=5400 JKN=10800
PROP MAT=9 JFRIC=1.192 JCOH=0
PROP MAT=9 FRIC=1.280 COH=.500 TENS=.250 DIL=0 JTENS=0 JDIL=0
**************************
**CREATE PROPERTIES TO FIX LOWER BOUND CRACK**
PROP JMAT=10 JKN=1200 JKS=600 JFRIC=1. JCOH=1 JTEN=.3
*************
**CREATE PRIMARY JOINT SET**
JREGION 0,-1300 0,-870 390,-840 600,-1300
JSET -65,0 700,0 0,0 25,0 0,-1300
JREGION 600,-1300 390,-840 750,-530 1016,-1110
JSET -65,0 700,0 0,0 25,0 0,-1300
JREGION 1016,-1110 750,-530 1111,-363 1375 -944.4
JSET -65,0 720,0 0,0 33,0 1015,-1110
JREGION 1375,-944.4 1111,-363 1483.3,-191.2 1747.2,-772.2
JSET -65,0 700,0 0,0 41,0 1374,-944
JREGION 1747.2,-772.2 1483.3,-191.2 1870,-10 2137,-590
JSET -65,0 700,0 0,0 49,0 1746,-773
***************
**GENERATE FDEF ZONES**
**CREATE ARTIFICIAL CRACK TO FACILITATE ZONING
CRACK 419,-1162 1719,-561
**AREA OF INTEREST ZONING
GENER REG 432,-1151 298,-854 720,-555 886,-942 EDGE 50
GENER REG 886,-942 720,-555 1434.5,-214 1694,-796 EDGE 50
**MAIN SLOPE
GENER REG 600,-1300 0,-1300 0,-870 390,-840 EDGE 100
GENER REG 390,-840 750,-530 1015,-1110 600,-1300 EDGE 100
GENER REG 750,-530 1895,0 2160,-580 1015,-1110 EDGE 100
**MATERIAL TO BE EXCAVATED FROM FACE
GENER REG 0,0 1500,0 350,-840 0,-840 EDGE 300
**ASSIGN A MATERIAL AND CONSTIT. REL'NS TO DOMAIN*
CHANGE MAT=5 Cons=3 JCons=2 JMat=5
**************************
**ASSIGN GRADATIONAL INCREASE IN STRENGTH UPSLOPE**
CHANGE REG 0,-870 472,-773 689,-1250 0,-1400 MAT=1 JMAT=1
CHANGE REG 472,-773 588,-675 831,-1190 689,-1250 MAT=2 JMAT=2
CHANGE REG 588,-675 709,-568 965,-1130 831,-1190 MAT=3 JMAT=3
CHANGE REG 709,-568 838,-493 1100,-1060 965,-1130 MAT=4 JMAT=4
CHANGE REG 838,-493 965,-425 1243,-996 1100,-1060 MAT=5 JMAT=5
CHANGE REG 965,-425 1100,-364 1378,-935 1243,-996 MAT=6 JMAT=6
CHANGE REG 1100,-364 1250,-297 1513,-876 1378,-935 MAT=7 JMAT=7
CHANGE REG 1250,-297 1385,-236 1648,-816 1513,-876 MAT=8 JMAT=8
CHANGE REG 1385,-236 1895,0 2160,-580 1648,-816 MAT=9 JMAT=9
```

```
**FIX ARTIFICIAL CRACK
CHANGE ANGLE 10 35 JMAT=10
*CHANGE REG 419,-1170 419,-1150 1710,-557 1710,-577 JMAT=10
*****************
**DELETE BOTTOM LEFT CORNER (2 BLOCKS)
DEL 0 75 -1300 -1150
**ASSIGN BOUNDARY CONDITIONS**
BOUND CORNER 524 135 STR 0,0,0 YGRAD .01325, 0, .0265
BOUND CORNER 135 2928 XVEL=0 YVEL=0
BOUND CORNER 3132 24  XVEL=0
**ASSIGN HISTORIES ON UPPER FINAL SLOPE**
HIST XVEL 1500,-200  YVEL 1500,-200 XDIS 1500,-200 YDIS 1500,-200
**UPPER SLOPE IN SLIDE
HIST XVEL 1050,-400 YVEL 1050,-400
HIST XDIS 1050,-400 YDIS 1050,-400
**TRIM LINE
HIST XVEL 750,-550 YVEL 750,-550
HIST XDIS 750,-550 YVEL 750,-550
**GLACIER MID HEIGHT
HIST XVEL 550,-720 YVEL 550,-720
HIST XDIS 550,-720 YDIS 550,-720
**TOE OF SLOPE
HIST XVEL 360,-860 YVEL 360,-860
HIST XDIS 360,-860 YDIS 360,-860
HIST DAMP TYPE 9
**SET INITIAL STRESSES, Ko=1
INSITU 0 2200 -1300 0 STR 0,0,0 YGRAD .0265, 0, .0265
**CONSOLIDATE STABLE PROBLEM**
GRAVITY 0,-9.81
FRAC=.5
DAMP AUTO
SAVE HN265S.2
CYC 0
SAVE HN265S.3
STOP
**********
**********
**CONTINUE WITH EXCAVATION**
REST HN265S.3
CYC 1000
SAVE HN265S.4
CYC 3000
SAVE HN265S.4
DEL 0 250 -150 0
RESET DISP JDISP ROTA TIME
RESET HIST
**ASSIGN HISTORIES ON UPPER FINAL SLOPE**
HIST XVEL 1500,-200  YVEL 1500,-200 XDIS 1500,-200 YDIS 1500,-200
**UPPER SLOPE IN SLIDE
HIST XVEL 1050,-400 YVEL 1050,-400
HIST XDIS 1050,-400 YDIS 1050,-400
**TRIM LINE
HIST XVEL 750,-550 YVEL 750,-550
HIST XDIS 750,-550 YVEL 750,-550 .
```

```
**GLACIER MID HEIGHT
HIST XVEL 550,-720 YVEL 550,-720
HIST XDIS 550,-720 YDIS 550,-720
**TOE OF SLOPE
HIST XVEL 360,-860 YVEL 360,-860
HIST XDIS 360,-860 YDIS 360,-860
HIST DAMP TYPE 13
***********
HIST NCYC 75
FRAC=.5
CYC 2000
SAVE HN265S.5
DEL 0 500 -200 0
CYC 2000
SAVE HN265S.5
DEL 0 650 -350 0
CYC 2500
SAVE HN265S.5
DEL 0 800 -450 0
CYC 2500
SAVE HN265S.5
DEL 0 1100 -500 0
CYC 3000
SAVE HN265S.5
*****************
***ADD WATER TABLE
PFIX REG 0,-870 390,-840 600,-1300 0,-1300 P=-8.7 X=0 Y=-.01
PFIX REG 390,-840 750,-530 1015,-1110 600,-1300 P=-11.76 X=.00861
+Y=-.01
PFIX REG 750,-530 1895,0 2160,-580 1015,-1110 P=-8.77 X=.00463
+ Y=-.01
*********
CYC 2500
SAVE HN265SW.6
DEL 0 500 -700 0
CYC 2000
SAVE HN265SW.6
DEL 0 600 -800 0
CYC 2000
DEL 0 400 -870 0
CYC 3500
SAVE HN265SW.7
STOP
```